| **Titre:** Title: | Development of Polylactide-Clay Nanocomposites for Food Packaging Applications |
|---|---|
| **Auteur:** Author: | Naqi Najafi Chaloupli |
| **Date:** | 2011 |
| **Type:** | Mémoire ou thèse / Dissertation or Thesis |
| **Référence:** Citation: | Najafi Chaloupli, N. (2011). Development of Polylactide-Clay Nanocomposites for Food Packaging Applications [Master's thesis, École Polytechnique de Montréal]. PolyPublie. https://publications.polymtl.ca/672/ |

## Document en libre accès dans PolyPublie
Open Access document in PolyPublie

| **URL de PolyPublie:** PolyPublie URL: | https://publications.polymtl.ca/672/ |
|---|---|
| **Directeurs de recherche:** Advisors: | Marie-Claude Heuzey, & Pierre Carreau |
| **Programme:** Program: | Génie chimique |

UNIVERSITÉ DE MONTRÉAL

DEVELOPMENT OF POLYLACTIDE-CLAY NANOCOMPOSITES FOR
FOOD PACKAGING APPLICATIONS

NAQI NAJAFI CHALOUPI
DÉPARTEMENT DE GÉNIE CHIMIQUE
ÉCOLE POLYTECHNIQUE DE MONTRÉAL

UNIVERSITÉ DE MONTRÉAL


ÉCOLE POLYTECHNIQUE DE MONTRÉAL


Ce mémoire intitulée:


DEVELOPMENT OF POLYLACTIDE-CLAY NANOCOMPOSITES FOR
FOOD PACKAGING APPLICATIONS


présenté par: NAJAFI  CHALOUPI. Naqi

en vue de l'obtention du diplôme de: Maîtrise ès Sciences Appliquées
a été dûment accepté par le jury d'examen constitué de:


M. THERRIAULT Daniel, Ph.D., président

Mme HEUZEY Marie-Claude, Ph.D., membre et directrice de recherche

M. CARREAU Pierre, Ph.D., membre et codirecteur de recherche

Mme CHAPLEAU Nathalie, Ph.D., membre

# DEDICATION

This dissertation is dedicated to my lovely wife, Faezeh, whose love and support have always carried me through and to my father and mother, who have supported me spiritually and materially since I was born

# ACKNOWLEDGEMENT

This dissertation would not have been possible without the help and support of multitude people.

First and foremost, I would like to express my sincere appreciation to my supervisors, Professor Marie-Claude Heuzey and Professor Pierre J. Carreau, who guided me into the world of science and technology. They always supported me very well in my research with availability, patience and encouragement.

My especial thanks are dedicated to Professor Paula Wood-Adams for her valuable insight, continues guidance, and encouragement during the past one year.

I would like to convey my heartfelt appreciation to my colleagues, friends specially *Ms. Mélina Hamdine* and *Ms. Weawkamol Leelapornpisit* and Amir Hossein Maani for their sympathies, supports and great help in this work.

***And finally, my special gratitude to my wife and parents for their supports and their loves.***

# RÉSUMÉ

L'acide polylactique, abrégé PLA, est un polymère biodégradable, provenant de sources renouvelables, avec une structure semi-cristalline ou amorphe. Bien que ces caractéristiques fassent du PLA un candidat approprié à l'emballage alimentaire, il y a cependant quelques problématiques importantes qui devraient être surmontées comme la faible stabilité thermique, la résistance mécanique faible et des propriétés barrière au gaz limitées. En s'appuyant sur les résultats énoncés dans la littérature, l'ajout de charges (argiles) de taille nanométrique peut améliorer les propriétés mécaniques et barrières de manière significative à condition qu'elles soient bien dispersées dans la matrice et forment une structure exfoliée. D'autre part, ce travail montre que l'incorporation d'argile organique modifiée dans le PLA augmente la vitesse de dégradation et alors, diminue manifestement la stabilité thermique des nanocomposites obtenus. Donc, le contrôle de la dégradation thermique du PLA est un autre défi dans le développement des nanocomposites PLA/argile**.**

Dans la première partie du projet de maîtrise, des nanocomposites PLA/argile contenant différents allongeurs de chaîne ont été préparés. Le polycarbodiimide (PCDI), le tris (nonylphenyl) phosphite (TNPP) et le Joncryl ® ADR 4368 ont été utilisés comme allongeurs de chaîne dans ce travail. L'effet de l'incorporation des allongeurs de chaîne sur le contrôle de la dégradation thermique, sur les propriétés rhéologiques et thermo-physiques et sur la structure moléculaire a été examiné. Les résultats ont révélé que l'incorporation de PCDI (2 % en poids), TNPP (1 % en poids), ou Joncryl (1 % en poids) avait un profond effet sur la dégradation. De telles concentrations ont non seulement stabilisé la viscosité et le module avec le temps, mais ont aussi augmenté leurs valeurs. Le mécanisme de stabilisation est fort probablement l'extension des chaînes. L'extension des chaînes a conduit à la formation de chaînes linéaires plus longues dans les nanocomposites à base de PCDI et de TNPP, et à une structure de longues chaînes ramifiées (LCB) dans les nanocomposites à base de Joncryl. L'analyse thermogravimétrique (TGA) a révélé que l'ajout d'argile dans le PLA a diminué sa stabilité thermique, tandis qu'une augmentation de la température de début de dégradation a été observée après l'incorporation des allongeurs de chaîne. Le Joncryl est finalement l'allongeur de chaîne le plus efficace dans les conditions de mise en forme parmi ceux utilisés dans cette étude.

Dans la deuxième partie du projet, des nanocomposites à base de Joncryl ont été préparés en utilisant différentes stratégies. L'effet de l'allongeur de chaîne et des conditions de mise en forme sur le degré de dispersion de l'argile, sur les propriétés barrières et mécaniques des nanocomposites obtenus ont été examinés. Les nanocomposites à base de Joncryl ont été préparés selon cinq stratégies différentes et comparées à un nanocomposite de référence. L'incorporation de 2 % en poids de Cloisite®30B (nano argile) et de 1 % en poids de Joncryl dans la matrice de PLA a conduit à une réduction significative de la perméabilité à l'oxygène et à l'amélioration des propriétés mécaniques comme le module en traction, l'allongement à la rupture et la ténacité des nanocomposites de PLA préparés selon la deuxième stratégie basée sur un mélange-maître de PLA/argile.

# ABSTRACT

Poly (lactic acid), abbreviated PLA, is a biodegradable polymer, made from renewable sources, with either a semi-crystalline or amorphous structure. Although these features make PLA an appropriate candidate for food packaging there are, however, some important issues that should be overcome such as poor thermal stability, low mechanical resistance, and limited gas barrier properties. Based on results reported in the literature, the addition of nano-sized fillers (clays) can efficiently improve the mechanical and barrier properties provided that they are well dispersed in the matrix and form an exfoliated structure. On the other hand, this work shows that the incorporation of organically modified clay into PLA enhances the rate of degradation and hence markedly decreases the thermal stability of the resulting nanocomposites. Therefore, control of PLA thermal degradation is another challenge in developing PLA-clay nanocomposites.

In the first step of this Master's project, PLA-clay nanocomposites containing different chain extenders were prepared. Polycarbodiimide (PCDI), tris (nonylphenyl) phosphite (TNPP), and Joncryl ®ADR 4368 were used as chain extenders in this work. The effect of incorporating chain extenders on controlling the thermal degradation, the rheological and thermo-physical properties and the molecular structure has been investigated. The results revealed that the incorporation of PCDI (2 wt. %), TNPP (1 wt. %), or Joncryl (1 wt. %) had a profound effect on controlling the degradation. Such concentrations not only stabilized the viscosity and modulus with time but also increased their magnitudes in some cases. The mechanism of stabilization is most likely chain extension. The chain extension led to the formation of longer linear chains in the PCDI and TNPP based nanocomposites, and to a long chain branched (LCB) structure in Joncryl-based nanocomposites. Thermal gravimetric analysis (TGA) revealed that the addition of clay into PLA decreased its thermal stability, whereas an increase in the temperature for the onset of degradation was observed after the incorporation of the chain extenders. Joncryl was found as the most efficient chain extender under processing conditions among the ones used in this study.

In the second part of this project, Joncryl-based nanocomposites were prepared using different strategies. The effect of chain extender and processing conditions on the degree of clay dispersion, mechanical, and barrier properties of the resulting nanocomposites were investigated.

The Joncryl-based nanocomposites were prepared using five different strategies, and compared to a benchmark nanocomposite. Incorporating 2 wt. % Cloisite®30B (nanoclay) and 1 wt. % Joncryl into the PLA matrix led to a significant reduction in oxygen permeability and improvement of the mechanical properties such as tensile modulus, strain at break and toughness of PLA nanocomposites prepared by the second strategy based on the master batch of PLA/clay.

# TABLE OF CONTENT

# LIST OF TABLES

# LIST OF FIGURES

# CHAPITRE 1

# INTRODUCTION

## Introduction

Polylactide (PLA) is a rigid thermoplastic polyester with a semicrystalline or completely amorphous structure depending on the stereopurity of the polymer backbone. PLA has gained a considerable interest due to its bioresorbability, biodegradability, and biocompatibility. Furthermore, its ability to be crystallized under stress, thermally crystallized, filled, and copolymerized, turn it into a polymer with a wide range of applications. The principal drawbacks of such a biodegradable polymer in terms of industrials application like food packaging are its poor thermal resistance, low mechanical and limited gas barrier properties. These drawbacks could be overcome by improving the thermomechanical properties through copolymerization, blending, and filling techniques. However, the use of fillers appears to be the most attractive approach because of lower cost. There are different approaches for the preparation of PLA nanocomposites: *in-situ* polymerization, solution intercalation, and melt intercalation. Since melt intercalation provides more advantages as compared to others, this technique has been used as a standard method to develop polymer-layer silicate nanocomposites.

Depending on the specific interactions between the polymeric matrix and the clay, different structures such as intercalated and exfoliated may be obtained. The clay layers may be well dispersed provided that a strong interaction can be developed between the clay and the polymeric matrix. Moreover, an increase in clay-PLA interactions can influence the mechanical properties.

The lack of thermal stability of PLA at high temperature is another main problem. It has been found that hydrolysis, random main-chain scission reaction, oxidative reaction, and transesterification are the main undesirable reactions, strongly affecting the physical and mechanical properties of PLA.

The main objective of this Master's project is to develop PLA-clay nanocomposites, where control of PLA thermal degradation is achieved using chain extenders. Specific objectives are aimed at determining the influence of chain extenders on clay dispersion, and mechanical and barrier properties of the final extruded products.

The organization of this Master's thesis is as follows: Chapter 2 provides a literature review on the PLA and PLA nanocomposites covering the following subjects: the methods used to

synthesize PLA, the preparation of PLA nanocomposites, the effect of clay on the mechanical and barrier properties of the resulting nanocomposites and the degradation mechanisms of PLA.

The objectives of this work are presented in Chapter 3. Chapter 4 briefly explains the organization of the two papers reported in this thesis (Chapters 5 and 6).

In Chapter 5, the effect of different chain extenders on controlling the degradation of the PLA nanocomposites, the molecular structure and thermo-physical properties is investigated using rheometry, thermogravimetric analysis (TGA), FT-IR spectroscopy, and gel permeation chromatography (GPC). The morphological, mechanical, and barrier properties of PLA and Joncryl-based nanocomposites prepared by different strategies are discussed in Chapter 6. In Chapter 7, a general discussion includes a full review regarding the most important factors affecting the preparation and properties of the resulting PLA nanocomposites. Finally, Chapter 8 summarizes the most important conclusions of this thesis and outlines some recommendations for future work in this field.

# CHAPITRE 2

# LITERATURE REVIEW

# Literature Review

## 2.1  Biodegradable Polymers

A huge volume of produced plastics have been consumed in the packaging industry since the last decade of the twentieth century. The substitution of plastics for other alternative materials in the packaging industry reduces the cost of packaging while meeting convenience, safety, softness, good aesthetic qualities, lightness, and transparency (Ray, 2005). Recently, 41% of such plastics have been consumed in packaging applications among which 47% are being used for packaging foodstuffs (Fomin, 2001). These plastics are usually fabricated from polyolefins such as: Polypropylene (PP), Polystyrene (PS), Polyethylene terephthalate (PET) and Polyethylene (PE) that are fully petrochemical-based materials.

PP can be used for hot-fill liquids due to its high distortion temperature. PS is generally utilized in protective packaging, food service packaging, bottles, and food containers.

PET is a transparent, tough polymer with an excellent barrier to oxygen, water, and carbon dioxide. Moreover, its high impact and tensile strength makes it ideal for using in beverage bottles like soft drinks, water, juices, sport drinks and alcoholic beverages. However, as most polymers traditionally used in packaging, the manufacture of PET starts from raw materials derived from petroleum refining (Amano, 2004). Using this durable polymer for disposable items leads to serious ecological problems.

Polyethylene (PE) is another common polymer used in lightweight packaging. PE is available in many different grades (linear low density, low density, high density) with a wide range of performance characteristics. Low density polyethylene (LDPE) is predominately used in film applications due to its toughness, flexibility and relative transparency, while high density polyethylene (HDPE) is employed to make different types of bottles. Furthermore, its relative good barrier properties and good chemical resistance make HDPE well-suited for packaging products with a short shelf life such as milk (Patel, 2008). Polyethylene is a non-biodegradable polymer, and harms the plant life when it is disposed in the soil since the toxic substances of polyethylene get blocked among the soil particles.

Using such petrochemical-based polymers, which are generally not degradable, in the field of disposable items leads to a fast growth of plastic wastes and thus pollution of the environment. To keep the environment free from such plastic wastes different approaches have been found. The first one is the disposing of the plastic wastes in a landfill site. The use of landfill sites is not the best solution, since the society is quickly developing and thus there is a limitation for such sites. Furthermore, burial of waste materials only partly solves the problem for a short term and postpones it upon new generations (Ray, 2005). A better proposed solution is to re-use these materials. The reutilization can be done through incineration of these materials, leading to heat generation that could be used to produce hot water and electricity, or recycling. The incineration of waste materials generates carbon dioxide and, occasionally, toxic by-products, resulting in global warming and global pollution, respectively. On the other hand, although recycling could in some way solve the problem, however, expensive costs should be expended for further processing such as the removal of plastic wastes, separation based on plastic type, washing, drying, grinding. In spite of this, the quality of the recycled materials is poor in comparison with the original ones (Ray, 2005).

Therefore, the exponential growth of plastic wastes and nonexistence of an appropriate solution have incited a search for alternative materials that are environmentally benign. Hence, many attempts have been made to substitute the petrochemical-based plastics by the biodegradable ones (Alexandre, 2000; Ray, 2005; Siracusa, 2008; Yang, 2007).

Biodegradable polymers are being employed increasingly in mass-production applications such as packaging, paper coating, fibers, films, and for other disposable materials (Theinsathid, 2009). Additionally, biocompatibility and biodegradability of such biopolymers make them favor for biomedical applications such as resorbable surgical sutures, implants, and controlled drug delivery devices (Soppimath, 2001; Theinsathid, 2009).

### 2.1.1 Definition and Categories of Biodegradable Polymers

The biodegradability, defined as the degree to which microbes use organic compounds, is directly correlated to the chemical structure of materials. Indeed, the microbes could attack the polymer chains and degrade the chemical bond or link in the chemical structure, leading to mineralization

(Siracusa, 2008). To biodegrade such polymers, some specific conditions in terms of pH, moisture, presence of oxygen and some metals are needed.

Biodegradable polymers can be produced from various sources; some of them are made from natural sources like corn, wood and cellulose, while some others are derived from petroleum like aliphatic polyester (Ray, 2005). Furthermore, there are some biopolymers made from a mixing source of bio and petroleum like poly(ether urethane)[1] (Ligadas, 2007).

However nowadays, an increasing attention has been paid to biodegradable and biocompatible polymers originating from renewable source such as polylactic acid (PLA) and polyglycolic acid (PGA). The life cycle of such materials is schematically illustrated in Fig. 2-1. Among the renewable source-based biodegradable plastics, PLA has attracted the most attention since it is thermoplastic, biocompatible, bioresorbable, biodegradable, while having good processability and transparency after processing (Garlotta, 2001; Krikorian, 2003; Ray, 2003a).
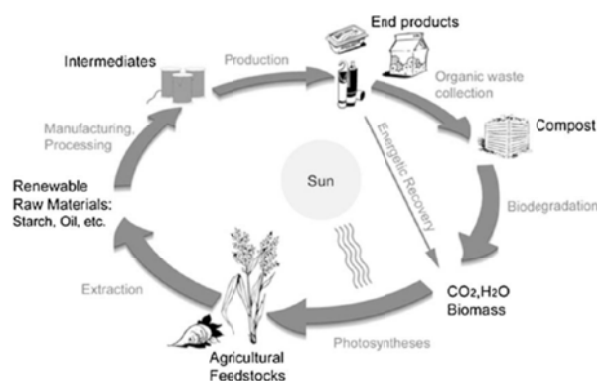


Figure 2-1:  Life cycle of renewable source biopolymers (Ray, 2005)

## 2.2  Polylactic Acid

### 2.2.1  Polylactic Acid Synthesis

Polylactic acid (PLA) is a linear, aliphatic thermoplastic polyester that can be in either the semicrystalline or completely amorphous state depending on the stereopurity of the polymer

---

1 - The polyol segment of polyurethanes may be prepared using biomaterials.

backbone (Lima, 2008). According to stereochemical structure, PLA can be categorized into L-lactic acid (PLLA), and D-lactic acid (PDLA), among which PLLA is the natural and most common form and PDLA is usually incorporated into PLLA stereo-structure to optimize the crystallization kinetics for specific fabrication and application (Amar, 2005). PLA can be produced by direct polycondensation of lactic acid (Achmad, 2009; Nagahata, 2007 ; Wang, 2009) or *ring-opening* polymerization of a cyclic dimer of lactic acid called lactide in the presence of a catalyst such as tin (II) octoate (Hrkach, 1995; Kim, 1992). These two synthesis approaches are briefly explained in the following sections.

### 2.2.1.1 **Polycondensation Polymerization**

Direct polycondensation (DP) is an approach of polymerization where the end groups of monomers, oligomers or polymers reacts with each other, leading to forming polymer having relatively low molecular weight. For the sake of reducing the financial cost, polycondensation of PLA can be conducted in the absence of catalyst, solvent, and initiator (Achmad, 2009). This process can be performed by distilling-out water from 90 % aqueous solution of lactic acid at high temperatures and reduced pressure. During the process, the temperature is gradually raised up to target point, while the pressure continuously decreases. The pressure reduction occurring during polymerization leads to further distilling-out water from the reactor, with the result that the condensation reaction of lactic acid is accelerated and forms the viscous lactic acid oligomers. The synthesis of PLA through direct polycondensation is schematically shown in Fig. 2-2.
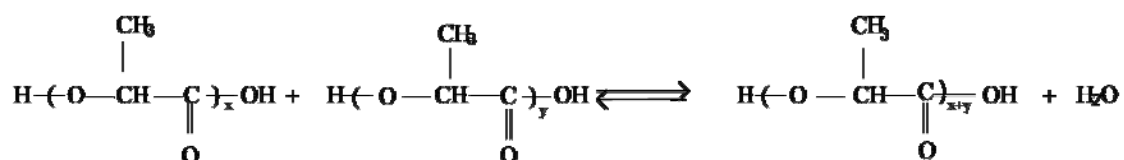


Figure 2-2: Polycondensation polymerization process of polylactic acid (Amar, 2005).

Since polycondensation is an equilibrium reaction, eliminating the trace amounts of water in the last stages of polymerization is difficult, hence low molecular weight polymer chains are obtained (Amar, 2005). Accordingly, it can be concluded that direct polycondensation is an

appropriate approach to synthesize low molecular weight PLA with high biodegradation rate which are good candidate for drug delivery purposes (Bamford, 1976; Hyon, 1997).

### 2.2.1.2 *Ring-opening Polymerization (ROP)*

Since the ultimate molecular weight obtained by direct polycondensation is restricted, ring-opening polymerization of PLA has gained most interest. Ring-opening polymerization is a type of addition polymerization, where the terminal end of polymer acts as a reactive center. In *ROP*, cyclic monomers attach together by ionic propagation to form longer polymer chains. The treatment of some cyclic compounds with catalyst results in a cleavage of the rings followed by polymerization that produces high molecular weight polymer chains. In this approach, a cyclic lactide (dimer) is synthesized from lactic acid, and the ring-opening polymerization is carried out using the lactide monomer.

A continuous process of PLA production by a new technology developed by Cargill Dow LLC has decreased its production cost and enlarged its range of applications. In addition to economic advantages resulting from PLA synthesis in the melt rather than solution state, the substantial environmental benefits arising from the absence of solvent is also considered in this approach. The solvent-free synthesis of PLA is depicted in Fig. 2-3.
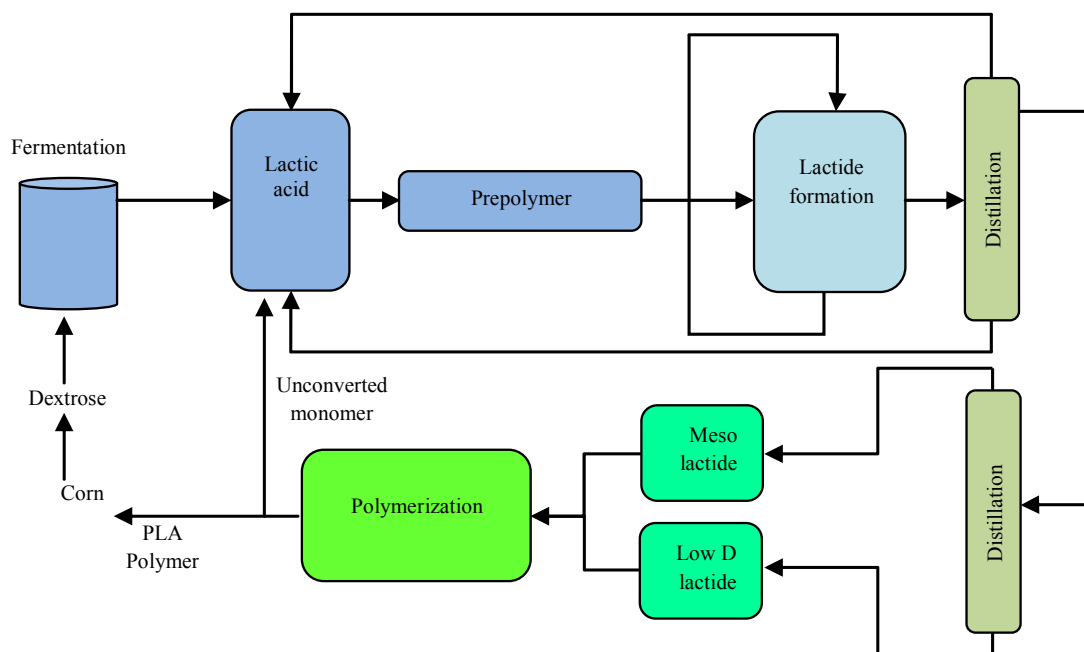


Figure 2-3: Solvent-free process of preparing polylactic acid (Amar, 2005).

The lactic acid obtained from fermentation of plant substances is used as a feed to synthesize PLA. Then, a continuous condensation reaction of aqueous lactic acid is carried out in order to provide the PLA prepolymer having a low molecular weight. This mechanism is illustrated in Fig. 2-4 (Amar, 2005; Drumright, 2000; Ndreopoulos, 1999).

A catalyst (tin (II) octoate) is incorporated into the polymerization system to convert such low $M_w$ oligomers into a mixture of lactide stereoisomer, leading to an increase in the rate and selectivity of the intramolecular cyclization reaction. The resulting molten lactide mixture is then distilled and purified by vacuum distillation. The ring-opening lactide polymerization in the melt leads to high $M_w$ PLA at the end of this process. After the polymerization is complete, the remaining monomer is removed from the polymer by vacuum and recycled to the lactic acid vessel located at the beginning of the process (Amar, 2005; Drumright, 2000; Hyon, 1997; Schwach, 1997).
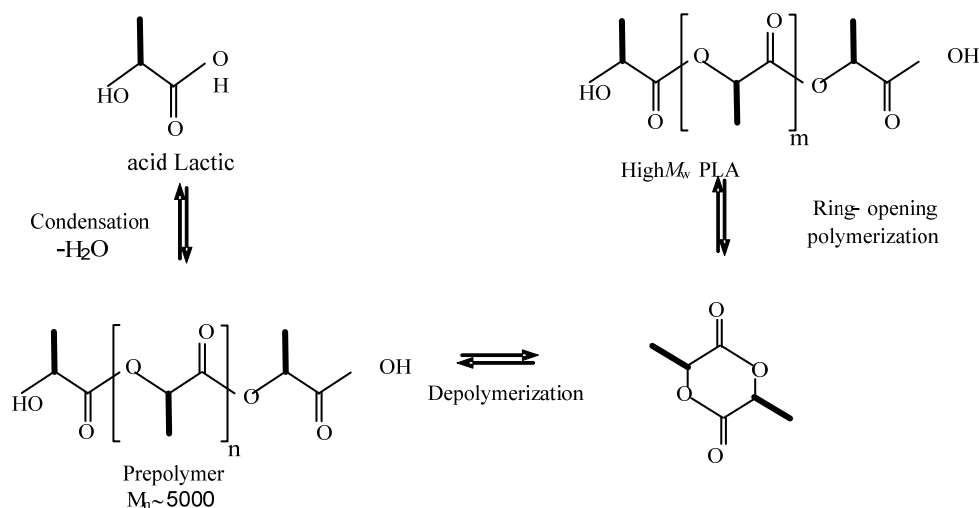


Figure 2-4: PLA production via prepolymer and lactide (Amar, 2005).

Ring-opening polymerization is carried out in the presence of a catalyst. Numerous catalyst systems have been so far developed for the ROP such as complex of aluminum, zinc, tin, and lanthanide. Among them, tin compound, especially tin (II) bis-2-ethylhexanoic acid (tin-octoate) is usually preferred for the bulk polymerization of lactide due to their solubility in molten lactide,

high catalytic activity, low rate of racemization, and high reaction rate. Moreover, a high molecular weight polymer chains can be synthesized under relatively mild polymerization conditions as such if a catalyst is used (Amar, 2005; Drumright, 2000; Schwach, 1997).

Fig.2-5 illustrates the polymerization process of lactide with the aid of a tin-octoate catalyst. As shown, the ring of lactide is opened by the catalyst and the hydroxyl groups are located at both ends (Amar, 2005).
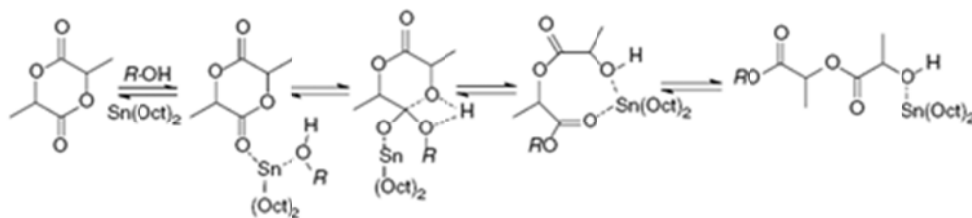


Figure 2-5: Generalized coordination–insertion chain growth mechanism of lactide to PLA (Amar, 2005).

It was also indicated that the octoate ion could not initiate alone the polymerization, and hence an alcohol should be incorporated as a co-initiator (Amar, 2005; Drumright, 2000). The properties of the resulting PLA differ depending on the conditions which are used for the synthesis. Several factors strongly affecting the properties are co-initiator concentration and type, catalyst concentration, monomer/ initiator ratio, polymerization temperature, and time of polymerization (Mehta, 2005). For instance, the rate of polymerization may be promoted by the loading of an hydroxyl initiator such as butanol, for which a low $M_w$ PLA is obtained as a large amount of catalyst is used (Amar, 2005).

The viscosity average molecular weight of an L-lactide polymer and monomer conversion is shown in Fig.2-6 as a function of catalyst concentration. Polymerization process was carried out at 130 ºC for 72 h (Hyon, 1997). As illustrated, the largest molecular weight as well as the highest degree of conversion was found when 0.05 %wt of catalyst is added, indicating the existence of an optimal concentration of catalyst (Drumright, 2000; Hyon, 1997).
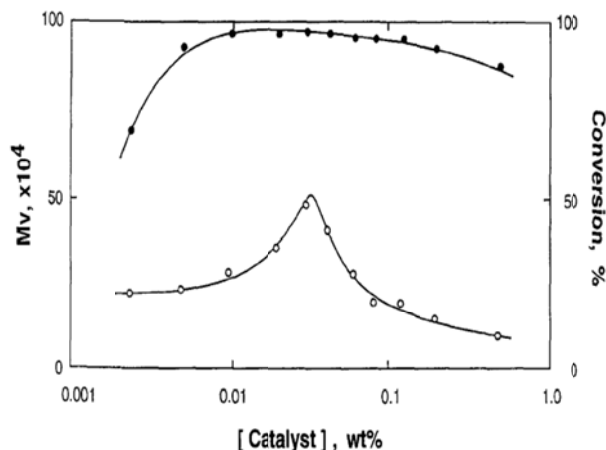
Figure 2-6: Effect of catalyst concentration on molecular weight of polylactic acid and monomer conversion for bulk polymerization of lactide,○ molecular weight,● monomer conversion (Hyon, 1997)

Processing time and temperature are other critical parameters affecting the molecular weight and the monomer conversion. Figs. 2-7 and 2-8 illustrate the molecular weight and monomer conversion as a function of time over a polymerization temperature range 120 ºC to 220 ºC, respectively (Drumright, 2000).
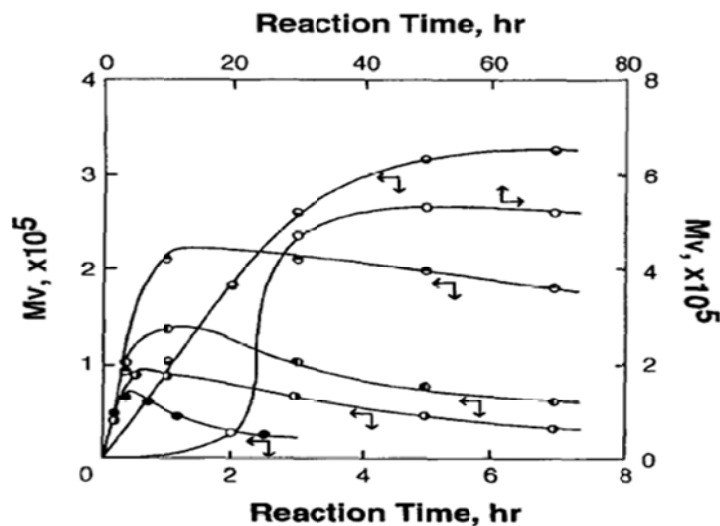


Figure 2-7: Effect of reaction time and temperature on the molecular weight of polylactic acid for bulk polymerization (catalyst concentration is 0.05% wt )○ 120 °C ●140 °C ◖160 °C ◐80 °C ◑00 °C ●220 °C (Hyon, 1997).
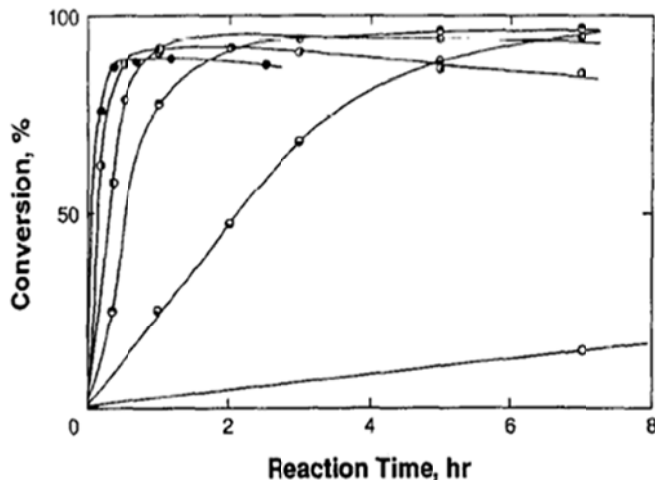
Figure 2-8: Dependence of monomer conversion on reaction time for bulk polymerization at different temperature (catalyst concentration is 0.05% wt)  ○20 °C  ◕40 °C  ◑60 °C  100 °C  200 °C ●220 °C (Hyon, 1997).

As shown, in the early stage of polymerization, the molecular weight as well as monomer conversion gradually increases with reaction time, followed by a reduction, leading to the existence of an optimal reaction time. Such a trend is more pronounced at higher temperature (Drumright, 2000; Hyon, 1997).

## 2.3   Degradation Mechanisms of PLA

### 2.3.1  Thermal Degradation of PLA

Thermal instability of PLA at high temperatures such as those encountered in the extrusion process has been broadly investigated (Amar, 2005; Fan, 2004; Kopinke, 1997; Li, 1999; Lucas, 2008; Nicolae, 2008; Nostrum, 2004). Numerous researches reveal that degradative reactions can occur during processing of PLA and lead to a molecular weight reduction. These side reactions include hydrolysis, random main-chain scission, depolymerization, oxidative reaction and transesterification (Amar, 2005; Fan, 2004; Gupta, 1982; Kopinke, 1997; Li, 1999; Lucas, 2008; Nostrum, 2004; Signori, 2009). Furthermore, the thermal stability of PLA is strongly affected by the nature of its reactive end groups and the presence of residual monomer and catalyst (Li, 1999; Signori, 2009).
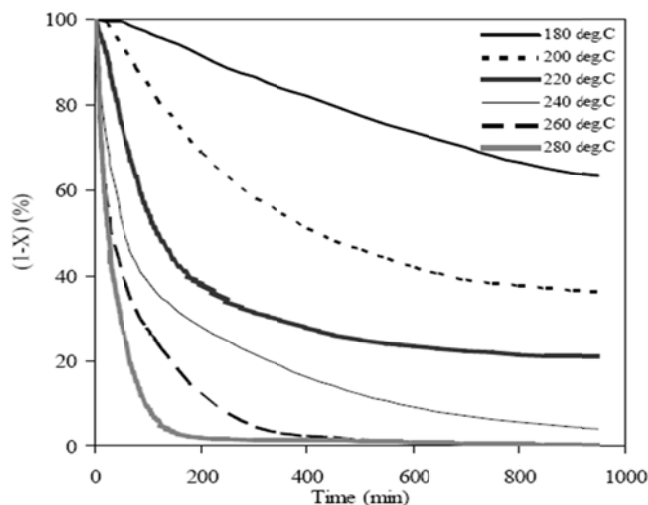
Figure 2-9: Isothermal weight loss of polylactic acid at different temperature, this test is conducted in TGA (Nicolae, 2008).

As a result of these side reactions, the molecular weight and melt viscosity of PLA can be significantly reduced, resulting in deteriorated mechanical properties and even barrier properties. For instance, the thermal-induced weight loss of PLA (X is weight loss) at different temperatures is shown as a function of time in Fig. 2-9 (Nicolae, 2008).

### 2.3.1.1 Hydrolysis

Hydrolysis is a water-based degradation mechanism of PLA in which a chain is split into two sub-chains. The molecular weight reduction of polyesters is primarily caused by the hydrolysis of the ester linkage, randomly taking place in the polymer (Amar, 2005). The general mechanism of the hydrolysis reaction is shown in Fig. 2-10. The rate of this side reaction is found to be dependent upon water concentration, acid or base catalyst, morphology of the polymer, and temperature (Amar, 2005; Jong, 2001).
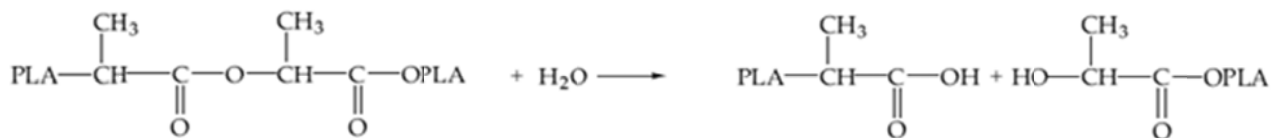


Figure 2-10: The hydrolysis reaction of PLA (Amar, 2005).

There are two major challenges in suppressing the PLA hydrolysis reaction which are: the high permeability of PLA and the autocatalytic nature of the hydrolysis reaction, leading to an easy penetration of water in the polymer and homogeneous and further progress of the degradation, respectively (Amar, 2005; Harris, 2010). To make matters worse, as Li and McCarthy pointed out (Li, 1999), the water uptake rate is markedly increased as the hydrolysis proceeded, due to the generation of more hydrophilic acid and alcohol end groups. The mechanism of this autocatalytic reaction is presented in Fig. 2-11.
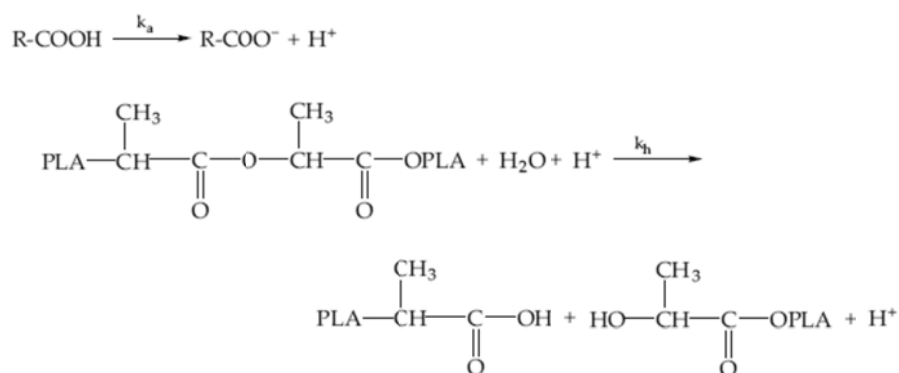


Figure 2-11: The autocatalytic hydrolysis mechanism of PLA (Amar, 2005).

The increase of the environment humidity, hydrophilic impurities such as lactide and carboxylic acid end groups in PLA strongly affects the equilibrium moisture content (EMC) and the subsequent hydrolysis rate (Amar, 2005; Sharp, 2001; Siparsky, 1998). Therefore, to hinder the progress of this reaction, in addition to reduce the EMC and rate of autocatalysis, the level of the residual monomer in PLA should be reduced as much as possible (Amar, 2005; Siparsky, 1998).

Another efficient route to impede the hydrolysis is to functionalize the end groups' chemistry of PLA. According to the literature (Amar, 2005; Cameron, 2011; Lee, 2001), a PLA terminated with Cl or $NH_2$ by the use of additives has more resistance to thermal and hydrolysis degradation in comparison to a PLA terminated with an hydroxyl group, since those former groups suppress the lactide formation.

Furthermore, temperature is another critical parameter in controlling the hydrolysis reaction considering that the rate of hydrolysis remarkably increases above the glass transition temperature. Based on the study performed by Witzke (Witzke, 1997), at a temperature between

150-215 °C, the hydrolysis is the dominant degradation mechanism. The $M_w$ loss of PLA stored at different temperatures and humidity conditions is shown in Fig. 2-12 (Amar, 2005).
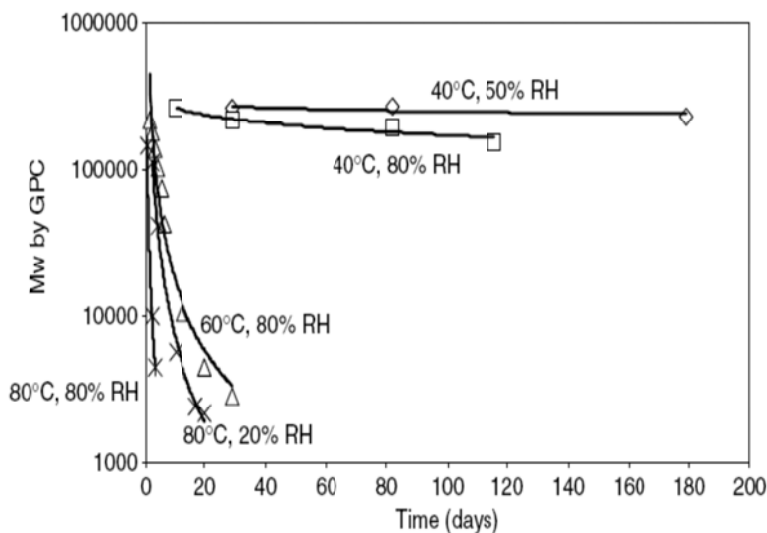


Figure 2-12: Variation of molecular weight for amorphous PLA stored at different temperatures and humidity concentration (Amar, 2005).

## 2.3.1.2 **Chain-Scission reaction**

The chain-scission reaction is another common degradation pathway leading to a gradual reduction of the number average molecular weight and subsequently decreased physical properties. Sodergard *et al* (Sodergard, 1994) studied the melt degradation of the PLA at temperatures above 180 °C. The thermal degradation was also found to proceed by random main-chain scission in such temperatures. There have been numerous reports on PLA (Li, 1990; Nostrum, 2004; Shih, 1995) indicating that the random chain-scission cannot alone describe the degradation kinetics, but that the end groups may also make an important contribution to the degradation through chain end scission. The chain ends contribution becomes more pronounced as the degradation proceeds since the number of polymer chain tails per mass is increased (Nostrum, 2004) and in the temperature range of 270-360 °C considering that it is the dominant degradation pathway of PLA at such temperature range (Kopinke, 1997).

The possible chain scission reactions of the PLA chain are presented in Fig. 2-13. Based on the chemical structure of a polyester, at least two susceptible linkages can undergo scission, which are carbonyl carbon-oxygen linkages, and carbonyl carbon-carbon linkages. However, it was argued that the carbonyl carbon-oxygen bond would be cleaved in the early stage of PLA thermal degradation (Gupta, 1982).
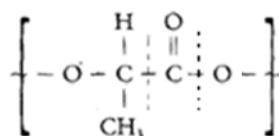


Figure 2-13: Possible chain-scission reaction in polylactic acid (Gupta, 1982).

The mechanism of degradation occurring at chain ends is shown in Fig. 2-14 (Lucas, 2008). Gupta *et al.* (Gupta, 1982) revealed that the cleavage of polymer chains was initiated by such a mechanism from unstable chain ends, having weak links.
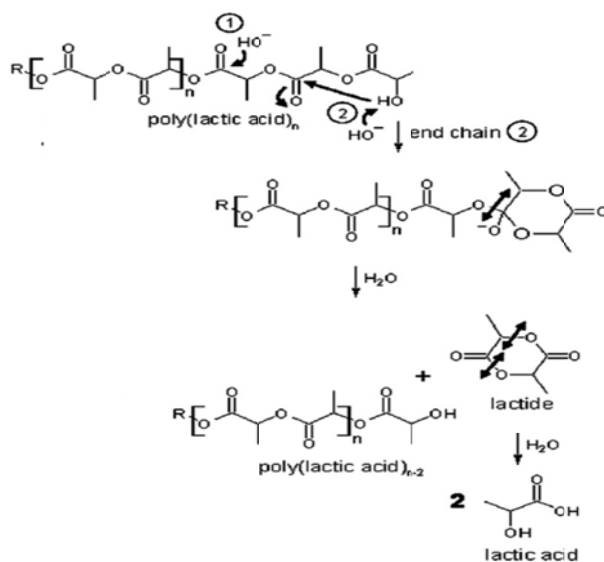


Figure 2-14: Degradation of PLA through chain end scission (Lucas, 2008).

## 2.3.1.3 Transesterification Reactions

Transesterification is generally considered as an undesirable phenomenon since it reduces the polymer $M_w$ and increases the polydispersity (Lipik, 2010). This mechanism was found as a dominant degradation mechanism of PLA at high temperatures (above 200 ℃), leading to the formation of cyclic oligomers (Kopinke, 1997; Li, 2009; Wachsen, 1997). In addition to temperature, the presence of monomers, oligomers, and hydroxyl groups are other factors accelerating transesterification. There are two different types of transesterification: intramolecular and intermolecular. Intramolecular transesterification or "back-biting" leads to polymer degradation and the formation of cyclic polylactide oligomers (Fig. 2-15a and b), while intermolecular transesterification affect the sequence of different polymeric segments (Fig. 2-15c) (Kricheldorf, 1988).

Besides these common mechanisms of transesterification, a cyclic transition state, called *cis*-elimination, and thermo-oxidative take place at high temperature range (300-500 ℃), leading to formation of an olefinic double bond (Kopinke, 1997; Li, 2009; Wachsen, 1997) and free radical (Gupta, 1982), respectively. The mechanism of *cis*-elimination reaction is given in Fig. 2-16 (Kopinke, 1997)
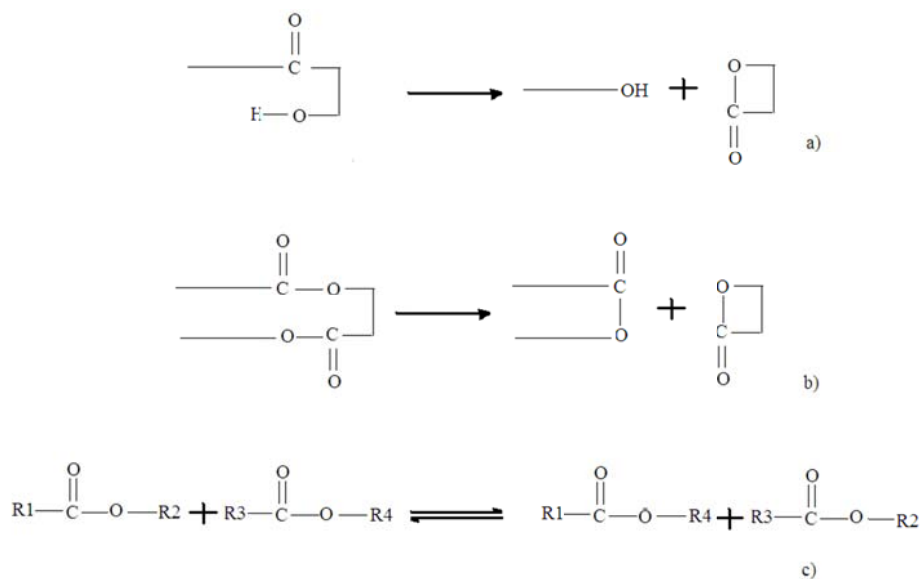


Figure 2-15: Transesterification reactions of polylactic acid degradation (Kricheldorf, 1988).
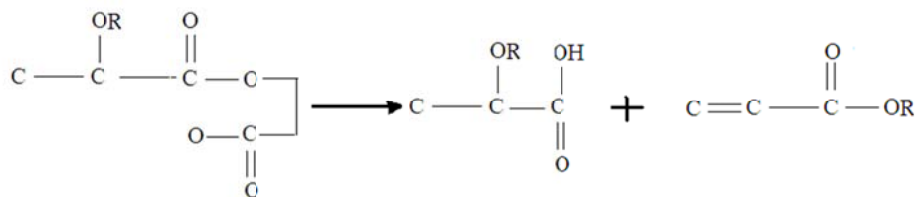
Figure 2-16: *Cis-* elimination reaction of PLA (Kopinke, 1997).

## 2.3.2 Thermal Stabilization of PLA

On reviewing the literature, it was found that hydrolytic and non-hydrolytic mechanisms control PLA thermal degradation, being accelerated by an increased moisture content and catalyst concentration. Hence, their concentration should be kept as low as possible. Furthermore, the addition of a chain-extender is another warranted approach that can control the molecular weight reduction. Tris (nonylphenyl) phosphite (TNPP) and polycarbodiimide (PCDI) are two chain extenders which have been used to thermally stabilize PLA during processing.

### 2.3.2.1 Stabilization of PLA by TNPP

TNPP is a chain extender through which cleaved polymer chains during thermal processing reconnect together (Lehermeier, 2001). The chemical structure of TNPP is shown in Fig. 2-17. TNPP can rapidly react with hydroxyl and carboxylic end groups present in PLA and those created by any hydrolysis mechanism. Then, the resulting phosphited end groups react with a carboxylic acid terminated PLA, leading to chain extension through transesterification (Cicero, 2002).
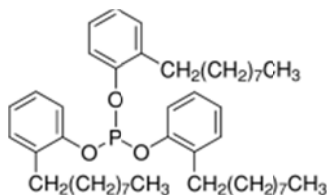


Figure 2-17: Structure of TNPP (Cicero, 2002).

The mechanism of these reactions is depicted in Figs. 2-18 and 19 (Cicero, 2002). It should be mentioned that phosphorous may or may not be incorporated into the backbone of the polymer chain during chain extension.
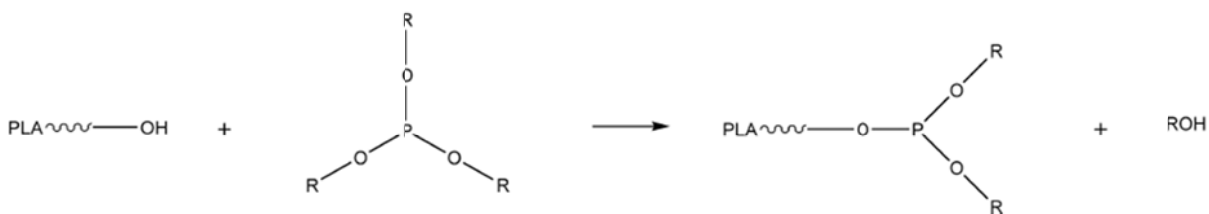


Figure 2-18: Reaction of TNPP with hydroxyl group of PLA (Cicero, 2002).
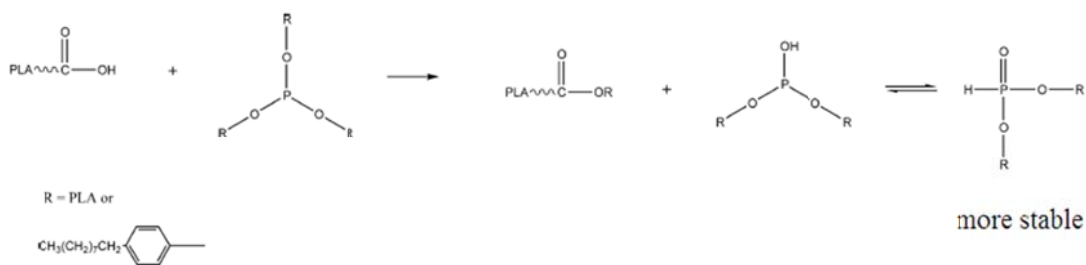


Figure 2-19: Reaction of TNPP with carboxylic acid group of PLA (Cicero, 2002).

TNPP can also react with the existing oxygen in the system. The product of this reaction is an organic phosphate. The hydroxyl end group of PLA can then react with the organic phosphate through the reaction shown in Fig. 2-20 (Cicero, 2002). This product (structure D) will react with the carboxylic acid end group of PLA to create other structures (Cicero, 2002), finally yielding phosphoric acid.
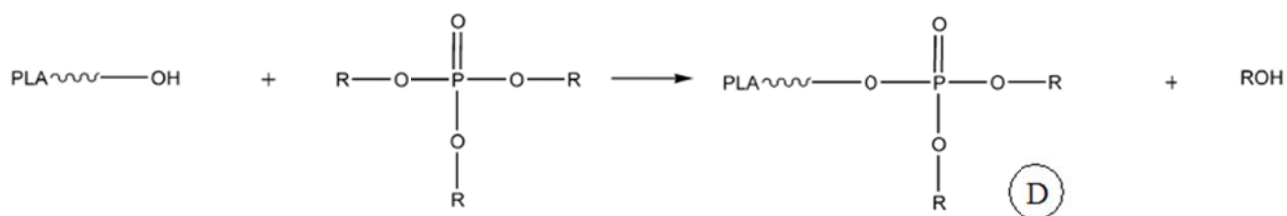


Figure 2-20: Reaction of organic phosphate with hydroxyl group of PLA (Cicero, 2002).

The addition of TNPP in less or more amounts than the required value may considerably affect the molecular weight of the polymer chains; hence the amount of required TNPP should be determined accurately. Dorgan and *et al*. considered (Lehermeier, 2001) the influence of different concentration of TNPP on PLA thermal stability. Their result is shown in Fig. 2-21 (Lehermeier, 2001). As illustrated, in order to stabilize the PLA thermally, 0.35 % wt of TNPP should be added (Burlet, 2005; Cicero, 2002; Lehermeier, 2001).
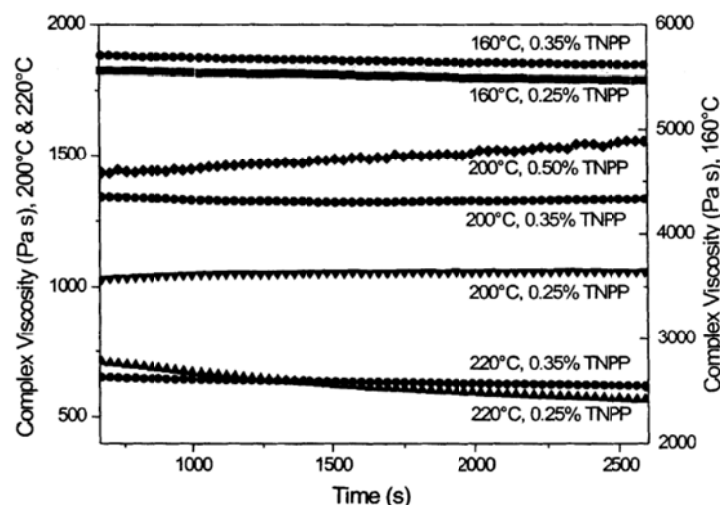


Figure 2-21: Time sweep test of PLA-TNPP at different temperatures (Lehermeier, 2001).

### 2.3.2.2 **Stabilization of PLA by PCDI**

Polycarbodiimide (PCDI), carboxyl reactive chain extender, has been employed to stabilize the PLA during thermal processing (Mantia, 2002). The carbodiimide (-N=C=N-) groups of this polymer chain are greatly reactive. They will react with –COOH band of PLA to decrease active site for degradation. Since the concentration of the end groups in PLA is too low to investigate reaction between PLA and PCDI well, they react with small molecules, which are mostly produced by degradation, presence of moisture, lactic acid monomer and acetic acid to suppress any further self-catalyzed degradation. PCDI can also directly react with water and lactic acid monomer, leading to eliminating residual moisture and monomer from the matrix (Yang, 2008). Yang *et al.* (Yang, 2008) results demonstrate that the addition of PCDI is even more effective than the drying process in removing the residual moisture in the matrix (Yang, 2008). Moreover, based on the reaction of PCDI with polylactic acid, the COOH and OH group of PLA may diminish according to the reactions depicted in Fig. 2-22 (Yang, 2008).

Therefore, as a consequence of reduced active COOH and OH group concentration, PLA becomes more stable in comparison with PLA with no PCDI chain extender (Yang, 2008).
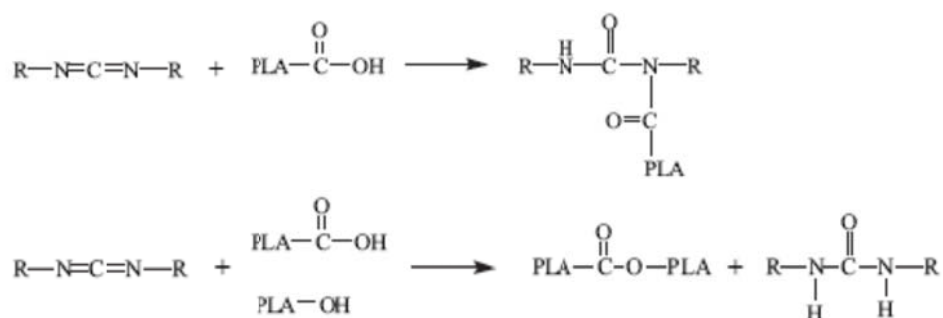


Figure 2-22: Reaction of PCDI with hydroxyl and carboxylic groups of PLA (Yang, 2008).

The effect of PCDI on thermal stabilization of the neat PLA, investigated by Yang *et al.* (Yang, 2008),is shown in Fig. 2-23. Based on these results,  0.7 % wt of PCDI should be added to the neat PLA to achieve reasonable thermal stability during processing (Yang, 2008).
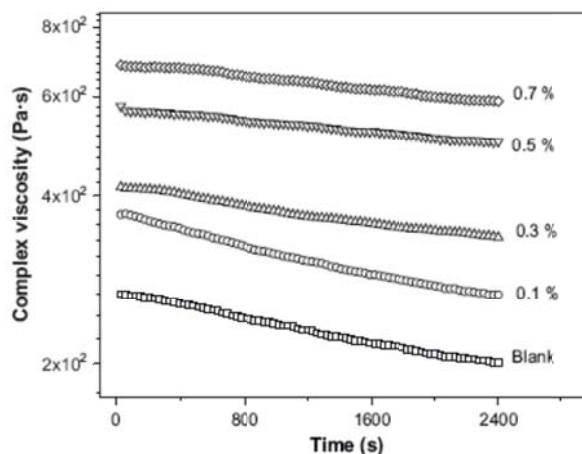


Figure 2-23:  Variation of the neat PLA viscosity containing different percentages of at a temperature of 210 ºC, frequency of 5 Hz, and strain of 5% PLA (Yang, 2008).

## 2.4  Nanocomposites

A nanocomposite is a composite filled with a reinforcing material having dimensions at the nanometric scale and a high surface area. Despite the existence of different nano-reinforcements, layered silicate clay minerals have attracted great attention due to their wide availability, low cost, and also low environmental impact. Clay is a type of commonly used fillers in composite

manufacturing with nanoscale dimensions thereby providing an increased surface area (Fukushima, 2009b; Sperling, 2006).

## 2.4.1 Clay

The most commonly used layered silicates in nanocomposites belong to the phyllosillicates structural family. Its structure is shown in Fig.2-24. Their crystal lattice is made of two dimensional layers in which a central octahedral sheet of either alumina or magnesia is inserted between two external tetrahedron silicon atoms so that the oxygen ions of the octahedral sheet also belong to the tetrahedral sheets. The thickness of the layers is around 1 nm and the other dimensions of these layers vary from 30 nm to several microns or even larger depending on the particulate layered silicate. They are organized in layers with a regular van der Waals gap between layers termed gallery or interlayer spacing. There are alkali or alkaline earth cations inside these galleries, which can be counterbalanced by generated negative charge through isomorphous substitution within the layers (for instance, $Al^{3+}$ replaced by $Mg^{2+}$ or $Fe^{2+}$) (Alexandre, 2000; Ray, 2005).

To enhance the affinity between the clay minerals and the polymer matrix, modification of their surface chemistry through ion-exchange reactions with organic and inorganic cations have been considered (Alexandre, 2000).

The natural clay is hydrophilic, thus, makes the intercalation of hydrophobic polymer chains into the gallery difficult and prevents clay delamination (Paul, 2003). Therefore, clay modification with a surfactant is required to make it organophilic and compatible with common hydrophobic polymers. To achieve such hydrophobic surface characteristic, a cationic surfactant like alkylammonium or alkylphosphonium should be substituted for the hydrated cations of the interlayer (Alexandre, 2000; Ray, 2005).

The most commonly used layer silicates are montmorillonite, hectorite, and saponite, having two types of structure including tetrahedral-substituted and octahedral-substituted. Contrary to the octahedral-substituted structure, the negative charges are located on the silicate layer surface in the tetrahedral-substituted structure, leading to enhanced polymer-clay interaction in comparison with the octahedral-substituted one. Clays are usually characterized by a moderate negative

surface charge called cation exchange capacity, CEC. Since, this charge is not locally constant and varies from layer to layer, an average value over the whole crystal must rather be considered.
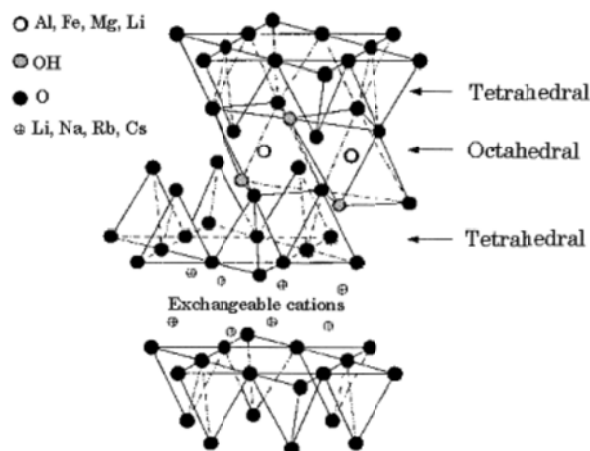


Figure 2-24: Structure of phyllosillicates (Ray, 2005).

The hydrophilic nature of montmorillonite makes it poorly suited for mixing and interacting with most polymer matrices, and thus, the stacks of clay platelets are held tightly together by electrostatic forces. Nowadays, several organically modified clays have been commercially produced at a rather low cost, yielding a larger interlayer spacing (d-spacing), besides enhancing the affinity of clays toward the polymer phase (Alexandre, 2000; Ray, 2005). Some of them are presented in Table 2-1. The incorporation of a polar functional group in the polymer matrix as a compatibilizer is another proposed approach to improve clay-polymer interaction (Alexandre, 2000; Ray, 2005) but is out of the scope of this project.

## 2.4.2 **Nanocomposite Structures**

Depending on the degree of compatibility between the clay and the polymeric matrix, thermodynamic properties and mixing conditions, three broad classes of nanocomposites can be distinguished (Chen, 2005b; Krikorian, 2003).

1- Intercalated nanocomposites, where the polymer chains penetrate inside the gallery and enhance the interlayer spacing, while still maintaining the overall ordered structure of clay. This structure is schematically illustrated in Fig. 2-25a.

Table 2.1: Structural formula and characteristics of some nano-clays (produced by *Southern Clay product Co.*) (Matana, 2007).

$$CH_3 - \overset{\overset{\displaystyle CH_3}{|}}{\underset{\underset{\displaystyle HT}{|}}{N^+}} - CH_2 - \bigcirc$$

Cloisite 10 A

$$CH_3 - \overset{\overset{\displaystyle CH_3}{|}}{\underset{\underset{\displaystyle HT}{|}}{N^+}} - HT$$
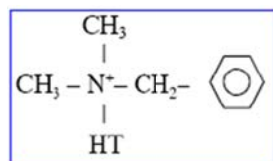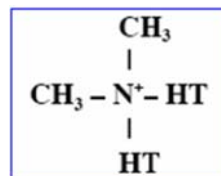
Cloisite 15A, 20 A

| | | 15A | 20A |
|---|---|---|---|
| CEC *(meq/100mg) | 125 | | |
| d-spacing (nm) | 1.92 | | |
| CEC (meq/100mg) | | 125 | 95 |
| d-spacing (nm) | | 3.15 | 2.42 |

$$CH_3 - \overset{\overset{\displaystyle CH_3}{|}}{\underset{\underset{\displaystyle HT \quad CH_3}{|}}{N^+}} - CH_2CHCH_2CH_2CH_2CH_3$$
$$CH_2$$

Cloisite 25 A

$$CH_3 - \overset{\overset{\displaystyle CH_2CH_2OH}{|}}{\underset{\underset{\displaystyle CH_2CH_2OH}{|}}{N^+}} - T$$
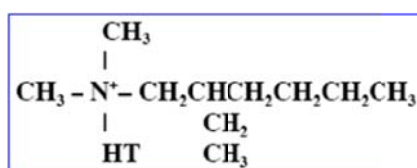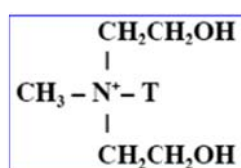
Cloisite 30 B

| | | | |
|---|---|---|---|
| CEC (meq/100mg) | 95 | CEC (meq/100mg) | 90 |
| d-spacing (nm) | 1.86 | d-spacing (nm) | 1.85 |

$$H3 -\overset{+}{N}- CH2(CH2)10\, COO^-$$
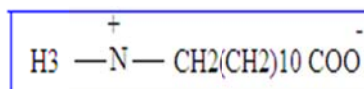
Nanomer I.24TL

Nanomer I.34 TCN

| | | | |
|---|---|---|---|
| CEC | - | CEC | - |
| d-spacing (nm) | 1.99 | d-spacing (nm) | 1.73 |

*cation exchange capacity

2- Flocculated nanocomposites (Fig. 2-25b), which conceptually are similar to the intercalated nanocomposites, nevertheless, due to hydroxylated edge-edge interactions of the silicate layers, the stacked and intercalated silicate layers occasionally flocculate.

3- Exfoliated nanocomposites (Fig. 2-25c), where the individual silicate layers are totally and homogeneously dispersed and distributed in a continuous polymer matrix, while the average distance generally depends on the silicate layer loading (Ray, 2003c).
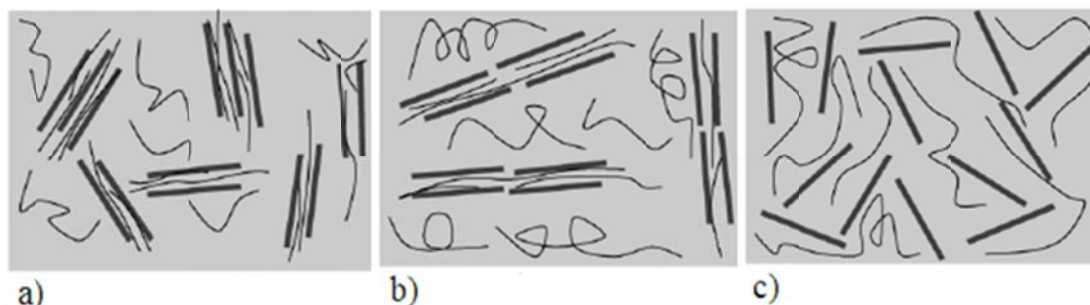
Figure 2-25: Schematic illustrations of three broad classes of thermodynamically achievable polymer-clay nanocomposites; a) Intercalated, b) Intercalated and flocculated, c) Exfoliated structures (Ray, 2003b).

Furthermore, the enthalpic interaction of the clay organic modifier with the matrix is another important factor significantly affecting the degree of clay dispersion. A high miscibility between the matrix and the modified clay yields a larger driving force for the exfoliation of layered silicates. Among different clays presented in Table 2-1, Cloisite® 30B and I.34 TCN are further miscible with PLA since a chemical interaction occurs between the carboxyl groups of PLA and the hydroxyl groups of the organomodifier. Despite higher d-spacing in other clays such as; Cloisite 15A and 25A (see Table 2-1), they are less exfoliated than Cloisite® 30B and Nanocor I.34TCN in PLA (Krikorian, 2003), indicating the importance of compatibility in achieving an exfoliated clay structure (Krikorian, 2003).

## 2.4.3 Nanocomposites Preparation

Based on results reported in the literature, the incorporation of nanoclay into a polymer matrix significantly improves the mechanical and functional properties in comparison with the neat polymer or even with those of micro or macrocomposites (Chen, 2005a, 2005b; Ozkoc, 2009; Paul, 2003; Ray, 2002, 2003b, 2003c).

The intercalation of polymers in layered silicates has proven to be a successful approach to develop a polymer nanocomposite. According to the initial materials used and processing techniques, three main methods are distinguished for the preparation of nanocomposites; these techniques are *in-situ* intercalative polymerization, intercalation of polymer and prepolymer from solution, and melt intercalation (Alexandre, 2000; Ray, 2005).

2.4.3.1    **In-situ Intercalative Polymerization**

In this approach, the layered silicates are swollen by a liquid monomer or a monomer solution so that the polymerization can take place mainly in the gallery space. To initiate the polymerization process, the mixture is exposed to either heat or radiation. Diffusion of a suitable initiator or attachment of an organic initiator or catalyst to the clay surface through cation exchange before the swelling step leads to a polymerization reaction inside the galleries, and consequently to clay delamination (Paul, 2003; Urbanczyk, 2009). Despite the fact that this method is the most efficient technique to achieve an exfoliated structure, this is not the most practical approach for the industry (Alexandre, 2000; Paul, 2003; Ray, 2005).

2.4.3.2   **Intercalation of Polymer and Pre-polymer from Solution**

This approach is based on a solvent system where the polymer or pre-polymer is soluble, while the layered silicates are swellable. First, the layered silicates are swollen in a solvent suitable for the polymeric matrix. Then, a mixing step is carried out after the addition of the polymer.  During mixing, the dissolved polymer chains diffuse within the interlayer of the swelled silicate sheets. Finally, a polymer-clay nanocomposite is obtained upon solvent removal through evaporation or precipitation of the mixture (Krikorian, 2003; Ogata, 1997). This approach usually results in the production of an intercalated-type nanocomposite for favored polymer-solvent pairs. It should be noted that this technique is usually performed to intercalate slightly polar or apolar polymers into the layered silicate, but the frequent use of harmful solvents restricts its range of applications to water-soluble polymers (Alexandre, 2000; Ray, 2005).

2.4.3.3   **Melt-Intercalation Techniques**

The melt intercalation technique is a method where the molten polymer is blended with the layered silicate at a temperature above the polymer melting point. During the blending, the polymer chains may diffuse from the bulk polymer melt into the interlayer gallery of the clay, depending on the amount of interaction between the polymer matrix and the clay (Chen, 2005a, 2005b). Nowadays, the technique has been used as the most practical method for polymer-layered silicate nanocomposites development since it has some advantages as compared to other approaches. For instance, the high shear applied during mixing can promote the diffusion of the polymer chains from the bulk to the gallery spacing, leading to further clay delamination.

Moreover, the absence of solvent and compatibility with current industrial mixing and processing techniques make this technique environmentally friendly and economical.

The thermodynamics involved in polymer melt intercalation differ from those in solution intercalation. For the overall process where oligomers or polymer molecules are exchanged with the previously intercalated solvent in the gallery, a negative variation in the Gibbs free energy is required. For the solution state, the driving force for the polymer chain confinement into the gallery spacing is the increased entropy resulting from desorption of the solvent molecules. However in melt-intercalation, the outcome of polymer intercalation is determined by an interplay of enthalpic and entropic factors (Shen, 2002). Indeed, the energy required to confine the polymer chains to the layered silicates is supplied by an increased conformational freedom of tethered alkyl surfactants as the inorganic layers separate. Since the increase in gallery spacing is too small to strongly affect entropy change, the change in the total enthalpy determines whether intercalation occurs or not. The mixing enthalpy can be broadly classified into two contributions: the first contribution is apolar, resulting from the interaction between polymer and surfactant aliphatic chains, which is generally unfavorable. The second contribution, which is favorable, is the polar interaction, originating from an interaction of polymer chains with polar layered silicates (Giannelis, 1999). A favorable enthalpy change is accentuated by maximizing the number of desirable polymer-clay interactions, while minimizing the number and magnitude of unfavorable apolar polymer-aliphatic chains interactions (Alexandre, 2000; Giannelis, 1999).

Successful melt intercalation process involves blending of the polymer and the layered silicate above the polymer melting point, leading to penetration of the polymer chains from the bulk into the gallery spacing. Depending on the degree of polymer diffusion in the clay gallery, an intercalated or exfoliated structure may be obtained. The degree of polymer diffusion is significantly dependent on the silicate functionalization and constituent interactions. Moreover, it was found that in addition to processing conditions such as temperature, level of shear field, and the processing residence time, there are two other parameters which have a strong impact on the structure of resulting nanocomposites. These parameters are: an optimal interlayer structure on the organically modified clay (number of surfactant chains per unit area and their size), and the existence of polar interactions between the layered silicates and the polymeric matrix (Ray, 2005; Vaia, 1997).

Accordingly, to achieve an exfoliated structure the undesirable interactions between the aliphatic chains and the polymer should be minimized by increasing the polarity or hydrophilicity of the polymer, and making shorter the chain length of the functional groups present in the modified layered silicates (Alexandre, 2000; Ray, 2005; Shen, 2002).

Although the mechanical and barrier properties of PLA could be potentially improved by adding the organically modified clays into the polymeric matrix, however, the thermal degradation of PLA may be intensified after clay incorporation, resulting in a molecular weight $M_w$ decrease (Fukushima, 2009a; Hwang, 2009), as explained in the previous chapter.

## 2.5  Summary of Literature Review

Based on the literature review, the principal drawbacks of polylactide in terms of industrial application like packaging are its poor thermal and mechanical resistance, and limited gas barrier properties. These drawbacks could be overcome by improving the thermomechanical properties through filling techniques. There are different techniques for nanocomposites preparation, however, melt intercalation has advantages as compared to others. For example, it is solvent free and compatible with common polymer processing methods.

Depending on the specific interactions between the polymeric matrix and clay, different structures such as intercalated or exfoliated can be formed in the nanocomposite. The addition of nano-sized fillers (clays) can improve the mechanical and barrier properties provided that they are well dispersed in the matrix. It is however hard to achieve such a structure since the thermodynamic interactions between the nano-fillers and the polymeric matrix is relatively weak. Hence high thermo-mechanical stress is required and may contribute to matrix degradation, especially in the case of PLA.

In addition, clay loading in PLA promotes the matrix degradation and consequently leads to a reduction of the mechanical and barrier properties of PLA-based nanocomposites. Consequently, the main problems in producing PLA-clay nanocomposites which are the thermal instability of the matrix and the difficult dispersion of the clay particles in the PLA matrix, are addressed in this study.

# CHAPITRE 3

# OBJECTIVE

# Objective

The literature reviewed in Chapter 2 indicates that the thermal stability of PLA-based nanocomposites and dispersion of clay present major challenges.

The main objective of this work is **to control the thermal degradation of PLA nanocomposites and improve their thermo-mechanical and barrier properties**. To meet this goal, the following specific objectives are considered:

**Step 1:** To control the thermal degradation of PLA nanocomposites during processing by using chain extenders;

**Step 2:** To achieve a well dispersed and exfoliated structure of nanoclay into PLA nanocomposites to gain increased mechanical properties, through control of the degradation and processing conditions.

In the scope of these specific objectives, different chain extenders are used and their ability to control the degradation, improve the thermal and rheological behavior are examined. Then, the most efficient chain extender is used further to study the strategy of chain extender incorporation into nanocomposites on clay dispersion, mechanical and barrier properties.

# CHAPITRE 4

# ORGANIZATION OF ARTICLES

## Organization of Articles

Chapters 5 and 6 present the main scientific findings of this work and represent the core of this Master's thesis. Each of these chapters consists of an article that has been submitted to a peer reviewed journal. The following is a brief description of each chapter:

The results of the first part of this study are presented in an article presented in Chapter 5. The effect of the organically modified clay and different chain extenders on the thermal degradation, rheological properties and molecular structure of the resulting nanocomposites are investigated using rheometry, thermogravimetric analysis (TGA), gel permeation chromatography (GPC) and Fourier transform infrared spectroscopy (FT-IR). Based on the results obtained in this first part, it can be stated that that the incorporation of a chain extender into the nanocomposite has a profound effect on controlling the degradation and even increasing the molecular weight in some cases. Thermogravimetric analysis shows an increase in the onset temperature of thermal degradation of the nanocomposite after chain extender loading. The reported rheology data and FT-IR spectroscopy reveals that the mechanism of stabilization is most likely chain extension. The chain extension results presumably in the formation of longer linear chains in the PCDI and TNPP-modified nanocomposites, and long chain branching (LCB) structure in Joncryl-based nanocomposites.  The change of molecular structure caused by LCB strongly influences the linear viscoelastic response such as the zero shear viscosity and loss angle behavior. It is found that Joncryl is the most efficient chain extender among the ones used in this study, properly controlling the thermal degradation over a wide range of processing temperatures.

In the second part of the work, the effect of processing conditions on the degree of clay dispersion in the presence of a chain extender (Joncryl® ADR) are investigated. The results are presented in the form of a second article in Chapter 6. Different strategies are used to promote the degree of clay dispersion. The morphology, thermal, barrier and mechanical properties of the resulting nanocomposites are discussed in details. Morphological observations as well as quantification of clay dispersion show that the incorporation of the chain extender can enhance the degree of clay dispersion provided that it is judiciously added to the nanocomposites.  An investigation of the oxygen permeability of PLA and PLA nanocomposites with and without chain extender is also conducted. The corresponding results reveal that the Joncryl-based nanocomposites, where nanoclay platelets were well-dispersed, provide a significantly reduced

permeability as compared to others. The mechanical properties of the neat PLA, the PLA and Joncryl-based nanocomposites were also examined. The increased molecular weight in Joncryl-based nanocomposites causes a significant increase in the mechanical properties of the samples.

# CHAPITRE 5

# CONTROL OF THERMAL DEGRADATION OF POLYLACTIC ACID (PLA)-CLAY NANOCOMPOSITES USING CHAIN EXTENDERS

# Article 1: Control of thermal degradation of polylactic acid (PLA)-clay nanocomposites using chain extenders[1*]

**N. Najafi C.[a], M.C. Heuzey[a], P. J. Carreau[a], Paula M. Wood-Adams[b]**

*Center for Applied Research on Polymers and Composites, CREPEC*
*a-Ecole Polytechnique, Department of Chemical Engineering, Montreal, QC, Canada*

*b- Concordia University, Department of Mechanical and Industrial Engineering, Montreal, QC, Canada*

**Abstract**:

The control of thermal degradation of polylactide (PLA) during processing is still a challenge for the industry.  In addition, the presence of an organically modified clay intensifies the rate of PLA degradation and molecular weight ($M_W$) reduction. In this work, three different chain extenders: polycarbodiimide (PCDI), tris (nonyl phenyl) phosphite (TNPP) and Joncryl® ADR 4368, were incorporated into PLA and PLA-based nanocomposites containing 2 wt% clay (Cloisite ®30B) in an effort to control thermal degradation. The thermal and rheological properties of the PLA and PLA nanocomposites with and without chain extender were investigated. Thermogravimetric analysis showed an increase in the onset temperature for thermal degradation after the incorporation of PCDI (2 wt. %), TNPP (1 wt. %), or Joncryl (1 wt. %) into the nanocomposite. The rheological results revealed that the addition of such a concentration of chain extender had a profound effect on the degradation and even increased the molecular weight in some cases. The mechanism of stabilization is most likely chain extension that results in the formation of longer linear chains in the PCDI and TNPP-modified nanocomposites, and a long chain branched (LCB) structure in Joncryl-based nanocomposites.  It was found that Joncryl was the most efficient chain extender among the ones used in this study.

---

1 - *Submitted to* Polymer Degradation and Stability *in August 2011.*
[*] The title is changed from Polylactic acid to Polylactide in new version of submitted article

**Keywords:** polylactide, thermal degradation, chain extender, nanocomposite

## 5.1   Introduction

The use of non-degradable petrochemical-based polymers for disposable items has considerably disturbed the ecosystem. A large portion is discarded into the environment after use and there are limitations on what can be put in landfills. Incineration of these materials leads to increased carbon dioxide emission and, subsequently, global warming. Hence, many attempts have been made to substitute petrochemical-based plastics by environmentally benign products. Recently, increasing attention has been paid to biodegradable and biocompatible polymers originating from renewable sources. Among the renewable source-based biodegradable plastics, polylactide (PLA) has attracted the most attention since it is a thermoplastic, biocompatible, bioresorbable and biodegradable material, while it has good processability and transparency after processing [1].

Polylactide is a linear, aliphatic thermoplastic polyester that can either be semi-crystalline or amorphous depending on the stereopurity of the polymer backbone. PLA can be synthesized from 100 % renewable resources such as fermentation products of corn and sugar beets [2]. It can be produced by direct polycondensation of lactic acid [3], but higher molecular weights are achieved by ring-opening polymerization of a cyclic lactide dimer [4]. Initially, the high production cost of PLA had confined its applications to biomedical areas; however, a new technology has decreased the production cost and enlarged its range of applications, especially in packaging [1, 2]. Despite all the advantages of PLA, there are, however, some difficult issues that make PLA unsuitable for some end uses. PLA suffers from poor thermal stability, low mechanical resistance, limited gas barrier properties and low melt strength [5]. To overcome these drawbacks, copolymerization, blending and filling techniques can be used. Indeed, the incorporation of organically modified nano-scale particles into PLA to produce nanocomposites is attractive due to its lower cost in comparison with other techniques [5-10].

Polymer nanocomposites based on thermoplastic matrices can be mainly prepared by three different methods: *in-situ* polymerization where the dispersed nanoclay is incorporated to the monomer followed by polymerization [8]; solution intercalation where nanoclay is mixed with the polymer in solution followed by solvent evaporation [11, 12]; and melt compounding in which the nanoclay is blended with the polymer in the molten state [13, 14]. Melt compounding

is the simplest and most common method for industrial applications due to the absence of solvent and its compatibility with current industrial mixing and processing techniques. In this approach, the polymer and nanoparticles are generally blended using a twin-screw extruder at a temperature above the polymer melting point. Under the right conditions, the stress applied during mixing may result in the diffusion of the polymer chains from the bulk into the gallery spacing of the clay, and formation of an intercalated or exfoliated structure, depending on the degree of polymer penetration [15].

Although the mechanical and barrier properties of PLA can potentially be improved by adding the organically modified clays into the polymeric matrix, thermal degradation of PLA appears to be intensified with clay incorporation, resulting in a loss of molecular weight [6, 7]. It is well known that PLA degrades upon thermal processing due to several undesirable reactions that occur during processing. These reactions include hydrolysis, inter-chain transesterification and depolymerization by back-biting (intramolecular transesterification) [16]. Hydrolysis is a water-based degradation mechanism of PLA in which a chain is split into two sub-chains. The molecular weight reduction of polyesters is primarily caused by the hydrolysis of the ester linkage, randomly taking place in the polymer. As for transesterification, there are of two types: intramolecular and intermolecular. Intramolecular transesterification, or "back-biting", leads to polymer degradation and the formation of cyclic polylactide oligomers. On the other hand, intermolecular transesterification affect the sequence of different polymeric segments [17]. As a result of such reactions, the molecular weight, and hence the mechanical properties decrease. Considering that the rate of thermal degradation increases after clay loading, controlling the thermal degradation of PLA nanocomposites is a major challenge that we address in this work.

The control of the degradation of neat PLA using chain extenders such as tris (nonyl-phenyl) phosphite (TNPP), polycarbodiimide (PCDI) and Joncryl has been previously considered [18-20]. Based on reported results, the addition of 0.35 wt. % of TNPP, 0.7 wt. % PCDI or < 1.5% of Joncryl as a stabilizer has a profound influence on the melt stability of neat PLA. The mechanisms proposed to explain the increased thermal stability was chain extension and the consumption of small molecules such as lactic acid and moisture, which are known to accelerate thermal degradation. However, to our knowledge no report has been published on controlling the degradation of PLA nanocomposites using chain extenders. In this work, we analyze the rheological and thermophysical properties of PLA nanocomposites containing different chain

extenders with special attention being paid to their effect on the molecular structure of the polymeric matrix.

## 5.2    Experimental

### 5.2.1 Materials

The poly (lactic acid) investigated was supplied by NatureWorks, PLA 4032D, and is a semi-crystalline material comprising 2% of D-LA. It has a reported glass transition temperature, $T_g$, and melting temperature, $T_m$, of 60 and 167 ºC, respectively [21]. The organically modified nanoclay, Cloisite ® 30B, was supplied by Southern Clay Products Inc. Three different chain extenders were used in this study:  polycarbodiimide (PCDI), a carboxyl-reactive chain extender, and tris (nonylphenyl) phosphite (TNPP), both purchased from Sigma Aldrich; and finally Joncryl® ADR 4368, supplied by BASF, a modified acrylic copolymer with epoxy functions. The molecular formula of these chain extenders are presented in Fig. 5-1. The organoclay and the chain extenders were used as received.

.
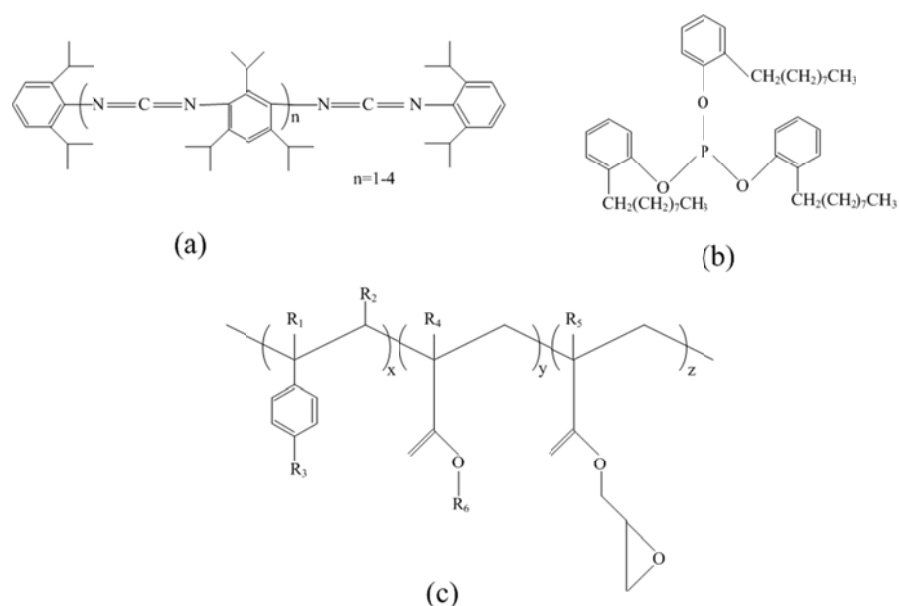


Figure 5-1:   Chemical structure of a) polycarbodiimide (PCDI) [20] b) tris (nonylphenyl) phosphate (TNPP) [24], and c) Joncryl® ADR, where x, y, and z are all between 1 and 20 [19].

## 5.2.2  **Nanocomposite Preparation**

Before mixing, PLA and clay were dried at 70 ºC in a vacuum oven for 48 h. Mixing of PLA with clay and chain extender was, in most cases, carried out in a counter-rotating Brabender Plasti-Corder® internal mixer. In addition, to investigate further the role of the Joncryl chain extender on controlling the degradation at different processing temperatures, a twin-screw extruder described below was used to prepare some of the nanocomposites.

**Internal Mixer**

The previously dried PLA was blended in the molten state with 2 wt. % dried clay and chain extender in the internal mixer. The mixing was conducted under a nitrogen atmosphere at a rotation speed of 100 rpm for 11 min, while the temperature was set to 190 ºC. After mixing, the nanocomposites were immediately immersed in liquid nitrogen to avoid thermo-oxidative degradation during cooling. The processed materials were placed in a vacuum oven (70 ºC) for at least 24h. Disks of 25 mm diameter and 1.5 mm thickness were produced by compression molding under a nitrogen atmosphere at 190 ºC using a pressure of 20 MPa during 8 min.  The molded samples were dried again in the vacuum oven at 70 ºC before rheological characterization.

**Twin-screw extruder**

The dried PLA, 2 wt. % clay and 1 wt. % Joncryl were initially dry-mixed. The mixture was then melt-extruded in a closely intermeshing co-rotating 18 mm twin-screw extruder (CICO-TSE) from Leistritz with an L/D ratio of 40, at a rotation speed of 150 rpm. The extruder was operated using the temperature profiles presented in Table 5-1, respectively called low, medium and high temperature profiles. After exiting the die, the material was immediately cooled in an ice-water bath. The cooled extrudate was then pelletized and placed in a vacuum oven (70 ºC) for at least 24h. Disks of 25 mm diameter and 1.5 mm thickness were prepared and stored as stated above.

Table 5.1: Temperature profiles for different processing conditions.

| TSE zones | 1 | 2 | 3 | 4 | 5 | 6 | 7 | 8 |
|---|---|---|---|---|---|---|---|---|
| Low temperature  profile (LT) (in °C) | 172 | 175 | 178 | 180 | 185 | 185 | 185 | 185 |
| Medium temperature  profile (MT) (in °C) | 172 | 185 | 190 | 195 | 200 | 200 | 200 | 200 |
| High temperature  profile (HT) (in °C) | 172 | 205 | 210 | 215 | 220 | 220 | 220 | 220 |

### 5.2.3 **Characterization**

The weight average molecular weight ($M_W$), polydispersity index, and the intrinsic viscosity ($IV$) of PLA before and after processing, as well as PLA containing 1 wt. % Joncryl were measured using gel permeation chromatography (GPC, Varian, analysis done by Polymer Source, Montreal, QC). The samples were initially dissolved in chloroform and then eluted. Polystyrene standards were used to generate calibration curve. These tests were conducted using tetrahydrofurane (THF) as a carrier solvent at 35 ºC with a flow rate of 0.5 mL/min.

Fourier transform infrared absorption spectra were collected in the IR range from 4000 to 500 cm$^{-1}$ using a Perkin Elmer FT-IR spectrometer in attenuated total reflectance (ATR) mode. The beam was polarized by means of a Spectra-Tech zinc selenide wire grid polarizer from Thermo Electron Corp. Samples (4 g) were dissolved in chloroform (10 mL), and tests were conducted in the solution state at a spectral resolution of 4 cm$^{-1}$ and a scanning speed of 32 kHz. The spectra were acquired after subtraction of the chloroform absorption obtained under the same conditions.

Thermal gravimetric analysis ($TGA$) was performed using a TGA-Q500 thermogravimetric analyzer from TA Instruments. Samples of 10-15 mg were heated from 100 to 700 ºC with a heating ramp of 10 ºC /min in an inert ($N_2$) atmosphere. Only data in the temperature range from 280-440 ºC were collected.

Dynamic rheological measurements of the PLA, PLA containing chain extender and PLA-based nanocomposites, excluding Joncryl-enriched PLA, were carried out using a strain-controlled ARES rheometer (Rheometric Scientific Inc.) with a 25 mm parallel plate flow geometry. Strain amplitude was fixed at 0.08, large enough to give a reliable signal while keeping the measurement in the linear viscoelastic region. To consider the thermal stability of the nanocomposites, the storage modulus and complex viscosity were monitored as a function of time. The time sweep measurements were conducted under a nitrogen atmosphere, at 190 ºC, a frequency of 6.28 rad/s and a gap size of 1-1.3 mm. Frequency sweep tests over a frequency range of 0.1-100 rad/s were also performed from low to high frequencies under the same conditions as stated above, during which the contribution of thermal degradation was less than 10% and considered to be negligible. Dynamic rheological measurements of Joncryl-enriched PLA were performed using a controlled stress rheometer, AR-2000 (TA Instruments) from low to high frequencies, over a frequency range of 0.06-100 rad/s. These measurements were performed

at an applied stress of 800 Pa, at 190 ºC and under a nitrogen atmosphere to minimize thermal degradation. In addition, for these specific samples the zero-shear viscosity was obtained from creep tests using the controlled stress rheometer, AR 2000, at an applied stress of 50 Pa and at 190 ºC.

## 5.3 Results and discussion

### 5.3.1 Gel permeation chromatography (GPC)

According to Yang *et al.* [20], the molecular weight of PLA generally decreases during melt processing, and also with increasing processing temperature. The GPC data obtained from the sample processed in the internal mixer (Table 5-2) show that the molecular weight and intrinsic viscosity of PLA are decreased and the MWD also becomes narrower after melt processing. These changes can be related to the cleavage of the long chains to shorter ones via the degradation mechanisms that favor the longer chains (hydrolysis and intermolecular transesterification). The incorporation of Joncryl into PLA during processing however significantly increases the $M_W$ and the breadth of the molecular weight distribution as expected for chain extension [22]. In the case of chain extenders of functionality greater than 2, such as Joncryl, the formation of branched structures is expected which will lead to an increase in average molecular weight and polydispersity index [23], consistent with the GPC results.

.

Table 5.2: GPC analysis of neat PLA, processed PLA and PLA treated by Joncryl.

|  | $\bar{M}_w$ (g/mol) | PD | $IV$ (dL/g) |
| --- | --- | --- | --- |
| Neat PLA | 100900 | 1.86 | 1.78 |
| Processed PLA | 95400 | 1.53 | 1.77 |
| Processed PLA with 1 wt% Joncryl | 668000 | 2.85 | 2.68 |

### 5.3.2 Fourier-transform infrared spectroscopy (FT-IR)

In order to detect any reaction that may have occurred between the matrix and chain extender, we have used FT-IR to compare the processed PLA-chain extender systems with their physical

mixtures having the same composition and their two pure components. The physical mixtures were produced by mixing PLA and the chain extender in chloroform at room temperature, conditions under which a reaction is unlikely.

The results for the PCDI systems are shown in Fig. 5-2. The reactive functional group of PCDI, carbodiimide (-N=C=N-) exhibits a characteristic infrared bond at 2130 cm$^{-1}$ in the FT-IR spectra of PCDI. This peak also exists in the FT-IR spectrum of the physical mixture of PLA and PCDI.
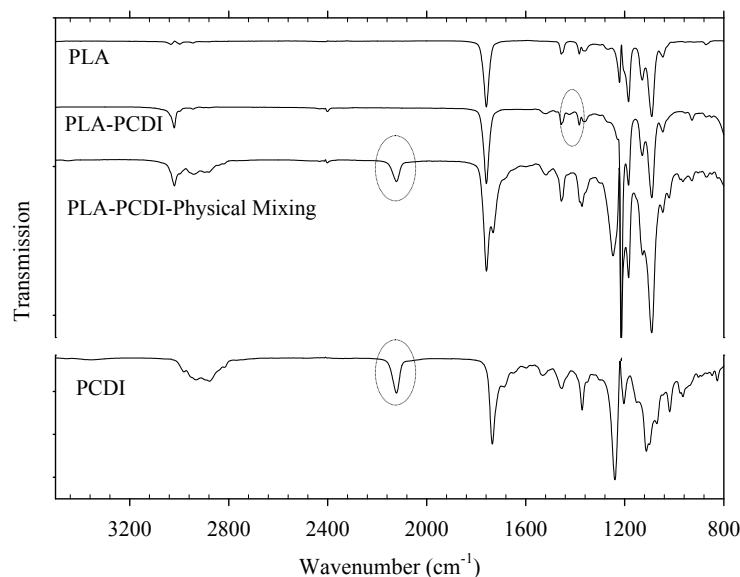


Figure 5-2:   FT-IR spectra of PCDI, PLA, physically mixed PLA-PCDI, and PLA treated by PCDI.

The absence of this peak in the FT-IR spectrum of PLA treated by PCDI indicates that the carbodiimide groups have been consumed by reaction. Yang *et al* [20] have identified two possible reactions between the terminal groups of PLA and carbodiimide (Fig. 5-3).  The first reaction implies incorporation of the PCDI into the backbone of the chain.  Since the PCDI contains more than one carbodiimide group, Reaction I is expected to produce a nonlinear polymer chain.   In Reaction II, the carbodiimide acts as an intermediary to facilitate transesterification and the joining of two PLA chains. This reaction is expected to produce longer, linear chains. Both of the reactions produce similar amide groups (N-C), with a peak between 1000-1250 cm$^{-1}$. Because of this, it is not possible to determine from the PLA-PCDI spectrum which of these reactions occur.  We will show later that our rheological results are not

consistent with the formation of a branched structure in this case. For this reason, we propose that reaction II is the most likely mechanism for chain extension with PCDI.
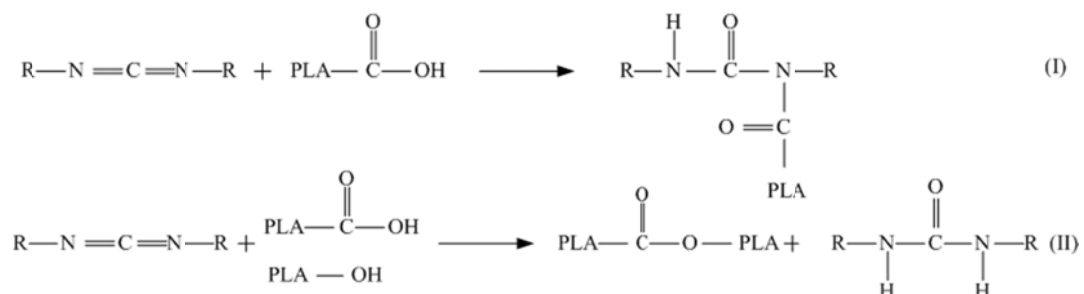


Figure 5-3: Potential Reactions involving PLA and PCDI [20].

Fig. 5-4 shows the corresponding FT-IR spectra for the PLA/TNPP systems. The peaks located at 914 cm$^{-1}$ and 1201 cm$^{-1}$, observed in the spectra of TNPP and physical mixture of PLA-TNPP, are assigned to aromatic phosphates (P-O-C), while that located at 1016 cm$^{-1}$ is related to aliphatic phosphates. There are two other peaks at approximately 1500 cm$^{-1}$ and 1600 cm$^{-1}$ attributed to aromatic compounds. In the spectrum for the treated PLA-TNPP system, there are no peaks at 914, 1016, 1201, 1500 or 1600 cm$^{-1}$, indicating the absence of phosphate and aromatic groups.
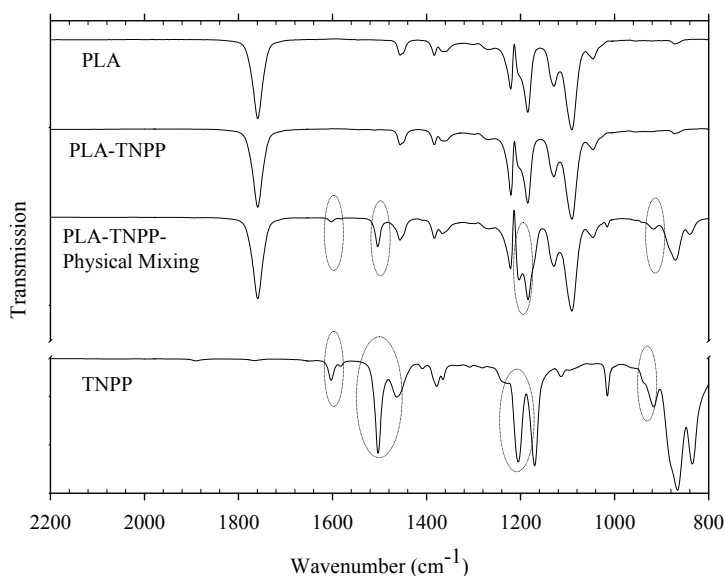


Figure 5-4: FT-IR spectra of TNPP, PLA, physically mixed PLA-TNPP, and PLA treated by TNPP.

According to the reaction mechanisms presented by Cicero *et al.* [24], the phosphate groups of TNPP react with the hydroxyl end groups of the PLA chains to produce a chain with a phosphited end group and nonylphenol (Reaction I in Fig. 5-5). Since the boiling point of nonylphenyl (180-181 °C [25]) is lower than the processing temperature (190 °C), it is expected to evaporate as it is produced. The phosphited PLA chain then under goes transesterification with a carboxyl terminated chain (Reaction II), resulting in the production of the longer PLA chain and bis(nonylphenyl) phosphite. The two remaining active groups on this substance can then proceed to react with another terminal hydroxyl group. If all of the active groups in TNPP are reacted in this manner then the final product is expected to be free of aromatic and phosphate groups, as in our treated PLA-TNPP system.
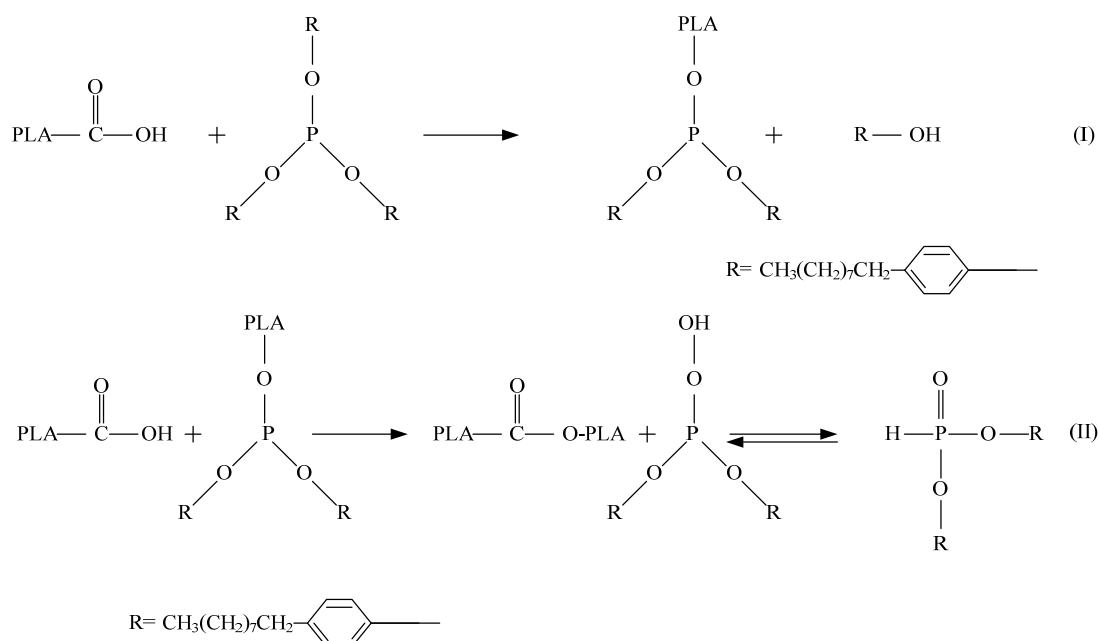


Figure 5-5: Potential reactions in the PLA -TNPP system [24]. (I) Reaction between terminal hydroxyl groups of PLA with TNPP, and (II) Transesterification between a phosphited PLA end group and a carboxylic acid PLA end group.

The FT-IR spectra of the PLA containing Joncryl are presented in Fig. 5-6. The peaks at 842 cm$^{-1}$, 908 cm$^{-1}$, and 1255 cm$^{-1}$, found in the spectra of Joncryl and the physical mixture of PLA and Joncryl, are attributed to the C-O stretching modes of the epoxy groups. These peaks do not occur

in the spectrum of the treated PLA-Joncryl, indicating that all of the epoxide groups have been consumed.
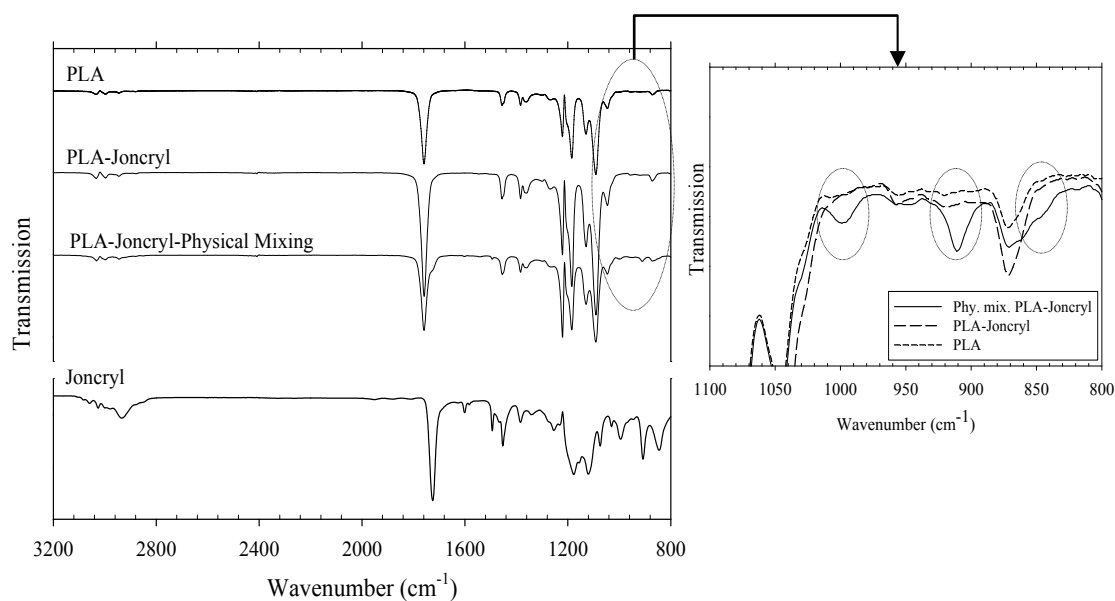


Figure 5-6: FT-IR spectra of Joncryl, PLA, physically mixed PLA-Joncryl, and PLA treated by Joncryl.
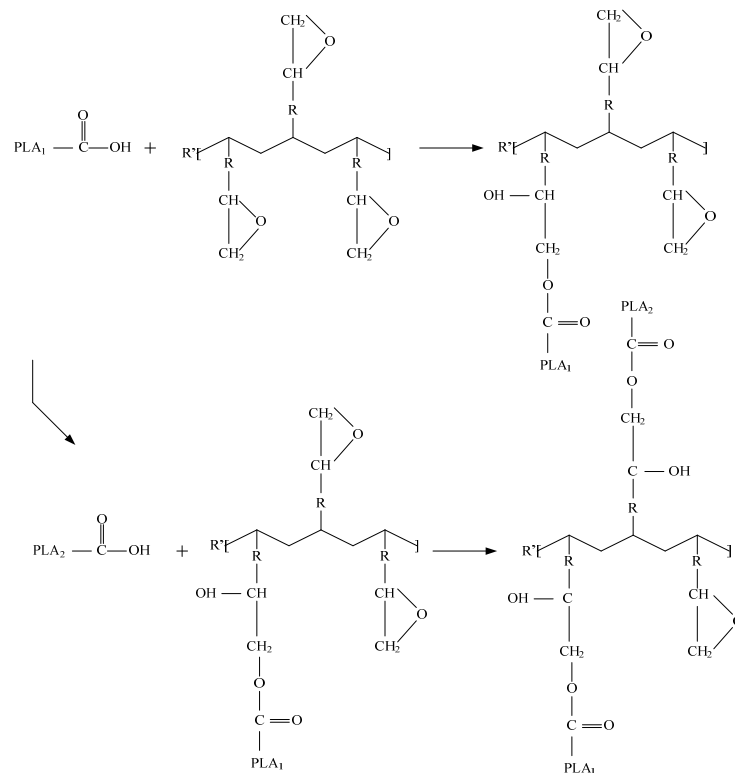


Figure 5-7: Reaction scheme of Joncryl-PLA end groups and possible long chain branching structures.

The epoxy groups of Joncryl can theoretically react with both hydroxyl and carboxyl groups of the polyester although the reaction with electrophilic groups such as epoxide is more favorable in the case of carboxyl groups [26]. Bikiaris and Karayanndis [27] have demonstrated that epoxide groups on chain extenders react with the carboxyl end groups on polyesters. They also concluded that excess epoxide groups likely react with terminal hydroxyl groups and with the new hydroxyl groups formed from the joining of the epoxide and carboxyl groups. The reaction between the epoxy-based chain extender and carboxylic acid end group of polyester is shown schematically in Fig. 5-7. We note that gelation is possible in the case of more than 2 epoxide groups per chain extender molecule if both the hydroxyl and carboxyl groups react with the epoxide.

### 5.3.3  **Thermal gravimetric analysis (TGA)**

TGA was carried out to investigate the effect of clay and chain extenders on the thermal degradation behavior of PLA under nitrogen, and the results are displayed in Fig. 5-8. The onset temperature for thermal degradation decreases with the addition of clay, consistent with the data of Wu *et al.* [10]. To explain this behavior, we propose that the clay promotes chain-scission (hydrolysis) of the PLA during processing, leading to the presence of shorter polymer chains and an increase in the number of chain ends per mass. Chain ends then promote the depolymerization by back-biting (chain end scission or intramolecular transesterification) during the TGA test considering that it is the dominant degradation pathway of PLA at the temperature range of 270-360 °C [28].
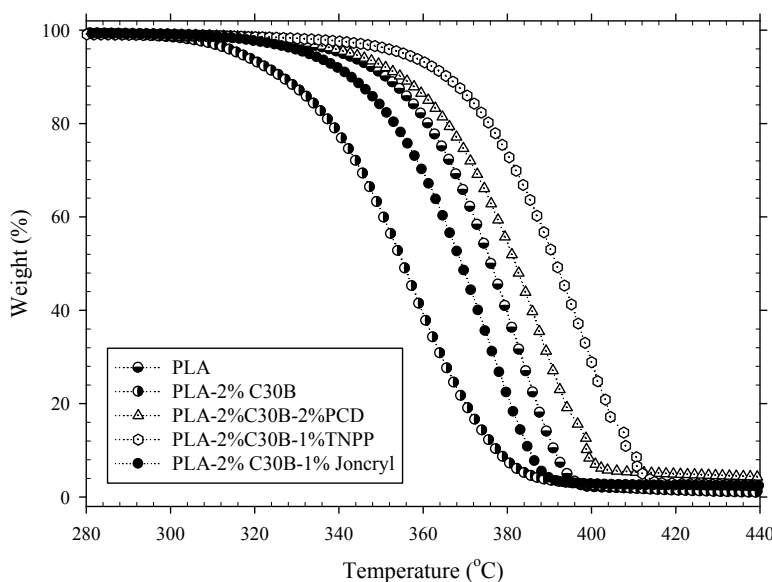


Figure 5-8: Effect of clay and different chain extenders on thermal degradation of PLA nanocomposites.

Since this degradation reaction occurs due to the presence of active sites on the chain ends, an increased number of chain ends per mass is expected to lead to an enhanced rate of degradation.

An increase in the temperature for the onset of degradation is observed after the incorporation of two of the chain extenders, TNPP and PCDI (Fig. 5-8). This improvement in the thermal stability can be attributed to the longer polymer chains in the nanocomposites containing these chain extenders and hence the reduced number of chain ends per mass. A comparison between the nanocomposites treated by TNPP and PCDI shows that TNPP increases the onset of degradation temperature more than PCDI. This suggests that TNPP is more efficient at extending the molecular weight of PLA than PCDI under the conditions considered here. Later in this work, we will show that our rheological data support this conclusion. Interestingly, Joncryl is not as efficient at increasing the temperature for the onset of degradation of the nanocomposites as compared to the other two chain extenders. This could indicate a significantly branched structure, having an increased number of ends per chain (and overall) than the linear systems produced by the use of TNPP and PCDI. Our rheological results will also support this conclusion.

### 5.3.4 Rheological characterization of PLA and PLA nanocomposites

The complex viscosity as well as the storage modulus at a frequency of 6.28 rad/s, normalized by their initial values at $t = 0$, are presented as a function of time for PLA and PLA nanocomposites with and without chain extender in Fig. 5-9. The initial complex viscosity and storage modulus values are presented in Table 5-3.  It is evident that the neat PLA and PLA nanocomposite without chain extender exhibit significant reductions in viscosity and storage modulus over time, with the PLA nanocomposite having by far the fastest rate of decrease (complex viscosity and storage modulus drops by 17 and 30 %, respectively, over 30 min). According to the literature [9, 29, 30], the decrease in viscosity corresponds to a loss in molecular weight. Shear mixing at high temperature and presence of the clay intensify the hydrolysis of the PLA matrix, leading to a faster loss of molecular weight in the nanocomposites without chain extenders in comparison with the neat PLA.  In fact, the interaction between the hydroxyl groups of Cloisite® 30B and the carboxylic groups of PLA may result in  scission of the polymer backbone into shorter chains [31].
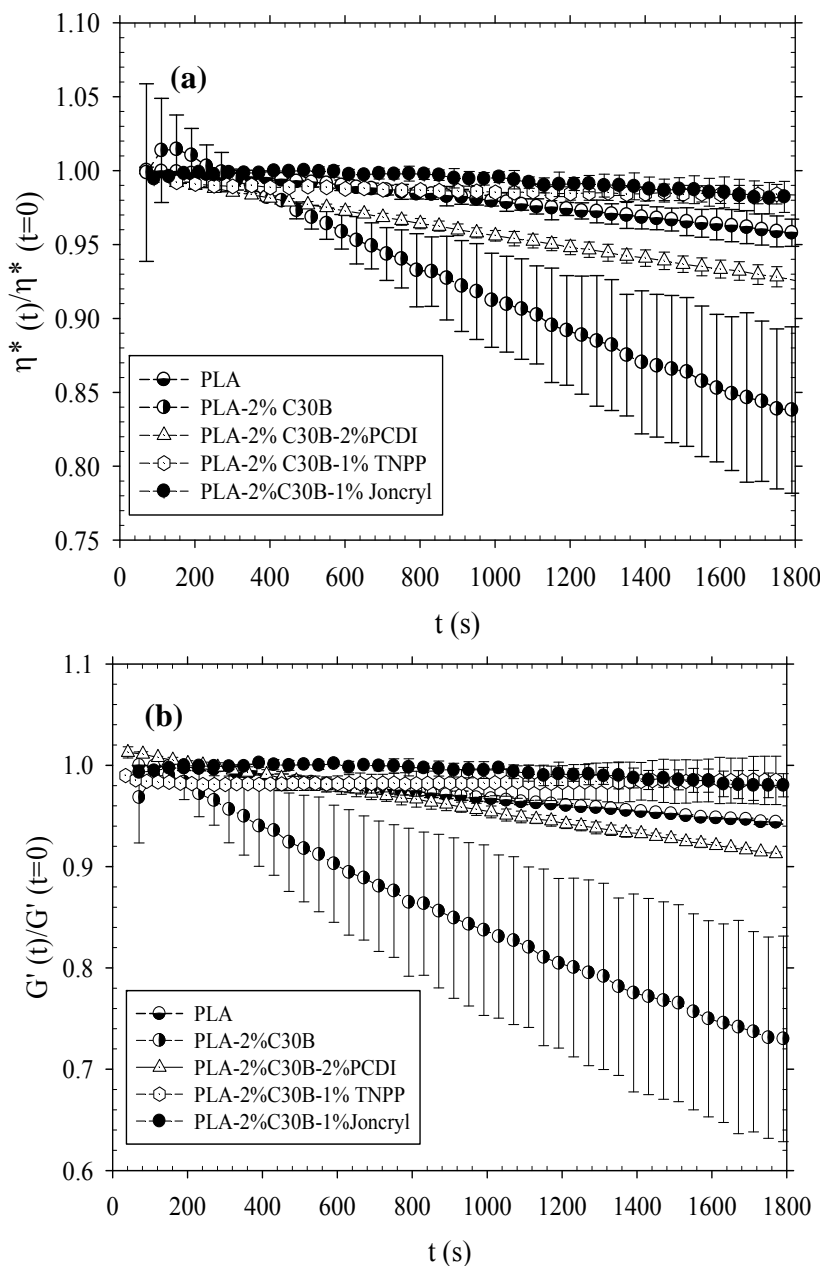
Figure 5-9: Normalized complex viscosity (a) and storage modulus (b) of neat PLA and PLA nanocomposites with and without chain extender as a function of time at $\omega = 6.28$ rad/s and T=190 °C. The initial values used for normalization are reported in Table 5-3.

To compensate for such chain scission reactions, a chain extender is incorporated as suggested by Yang *et al*. [20]. They showed that 0.7 wt. % of PCDI should be added to neat PLA to achieve a reasonable thermal stability during processing at 190 to 210 °C. However, our preliminary studies showed that this concentration is not sufficient to compensate for chain scission reactions in PLA nanocomposites (data not shown). Further studies demonstrated that 2 wt. % of PCDI

was required to control to an acceptable level the degradation in PLA nanocomposites containing 2 wt. % clay, as shown in Fig. 5-9.

Table 5.3: Initial values of the complex viscosity and storage modulus, at $t$=0, $\omega$=6.28 rad/s and the crossover frequency of the neat PLA and PLA nanocomposites containing various chain extenders used for normalization. All tests conducted at $T$=190 ºC.

| | $\eta$* (Pa.s) | G' (Pa) | (G'/ G'') | Crossover frequency, $\omega_c$, (rad/s) |
|---|---|---|---|---|
| PLA | 1320 | 1100 | 0.83 | - |
| PLA-2% C30B | 1050 | 750 | 0.71 | ~300 [*] |
| PLA-2% C30B-2% PCDI | 1400 | 1740 | 1.24 | ~300 [*] |
| PLA-2% C30B-1% TNPP | 2480 | 7600 | 3.1 | ~100 |
| PLA-2% C30B-1% Joncryl | 8570 | 35740 | 4.2 | ~12 |

[*] The crossover frequency of these samples is out of range of the frequency covered during the experiments and predicted by Akima cubic spline interpolation [38]

At this concentration of PCDI, the complex viscosity and storage modulus decreases by just 7 and 8%, respectively, over 30 min. The need for a larger concentration of chain extender in clay-containing systems is likely related to the accelerated hydrolysis rate of PLA in the presence of clay. In the nanocomposite with no chain extender, hydroxyl and carboxylic acid terminal groups may be left during the polymerization of PLA and/or produced by any hydrolysis reaction [32], leading to further depolymerization by back-biting (intramolecular transesterification) [20] and chain-scission mechanisms. In addition, carboxylic acid end groups may act as a catalyst in the hydrolysis reaction and bring about self-catalyzed degradation of PLA [20]. However, the addition of PCDI to the nanocomposites reduces the rate of degradation, thereby reducing the production of small molecules such as water, lactic acid monomer and acetic acid. These small molecules normally increase the rate of degradation leading to a self-catalyzed degradation scheme [20].

TNPP is known to stabilize polyesters by taking part in complex reaction sequences that strongly preclude hydrolytic degradation and ester exchange reactions [33]. Lehermrier *et al*. [18] showed that 0.35 wt. % of TNPP yielded an acceptable stability of the complex viscosity of PLA at 160 to 200 °C over 30 min. However, in our work this concentration was found to be inadequate for

PLA nanocomposites, and even in some cases to promote viscosity reduction. For example a complex viscosity reduction of 35 % over 30 min was observed for PLA-2 wt. % clay containing 0.35 wt. % TNPP, as opposed to 17 % for the same nanocomposite without chain extender (Fig. 5-9a). As shown in Fig. 5-9, at 190 °C the addition of 1 wt. % of TNPP considerably improves the melt stability of the PLA nanocomposite (the decrease in viscosity and storage modulus over 30 min is limited to 1.5 and 2%, respectively). According to Cicero *et al.* [24], the incorporation of TNPP into neat PLA causes a rapid reaction between the hydroxyl groups of PLA and TNPP. Then, the resulting phosphited end groups can react with any carboxylic acid terminated PLA, leading to chain extension through transesterification [24].

Joncryl is another chain extender designed to reverse the degradation of condensation polymers. The results of rheological tests, shown in Fig. 5-9, demonstrate that a stable viscoelastic response could be obtained by adding 1 wt. % of Joncryl to the PLA nanocomposite containing 2 wt. % of clay (the decrease in complex viscosity and storage modulus over 30 min is identically 1.5%). The linear viscoelastic functions, $\eta*$ and $G'$, of nanocomposites containing various chain extenders are plotted as a function of frequency in Fig. 5-10. Since the frequency sweep tests were completed in 10 min, the thermal degradation was considered to be negligible, except for the PLA nanocomposite without chain extender for which a 10% decrease of the storage modulus (Fig. 5-9b) should be taken into account. The complex viscosity gradually decreases with increasing frequency, which is a typical shear-thinning behavior. As shown in Fig. 5-10a, the complex viscosity of the nanocomposite with no chain extender is lower than that of the neat PLA. This behavior is even observed in the high frequency range, where the response of the nanocomposite should be dominated by the matrix properties. This reduction can be explained by a decrease of the matrix molecular weight due to thermal degradation, which is slightly more pronounced in the presence of the organomodifed clay (Fig. 5-9a, at 600s). The storage modulus ($G'$) of these composites is also presented in Fig. 5-10b. As expected for a polymer melt, the storage modulus of PLA monotonically increases with increasing frequency. However, the incorporation of clay into PLA leads to a pronounced change in $G'$. In the low frequency range the PLA nanocomposites display higher $G'$ than the neat PLA due to a spatially-linked structure and geometric constraints as a result of clay loading, while a contrary trend is observed in the high frequency range where the neat PLA has a higher $G'$ value than the PLA nanocomposite without chain extender. This is evidently caused by the degradation occurring over the frequency

test for the PLA nanocomposite without chain extender (Fig. 5-9b, at 600 s), as discussed above. Strong differences in the rheological response of the nanocomposites containing a chain extender (especially TNPP and Joncryl) in comparison with that of the neat PLA and the nanocomposite containing no chain extender are observed in Fig. 5-10a and 5-10b.
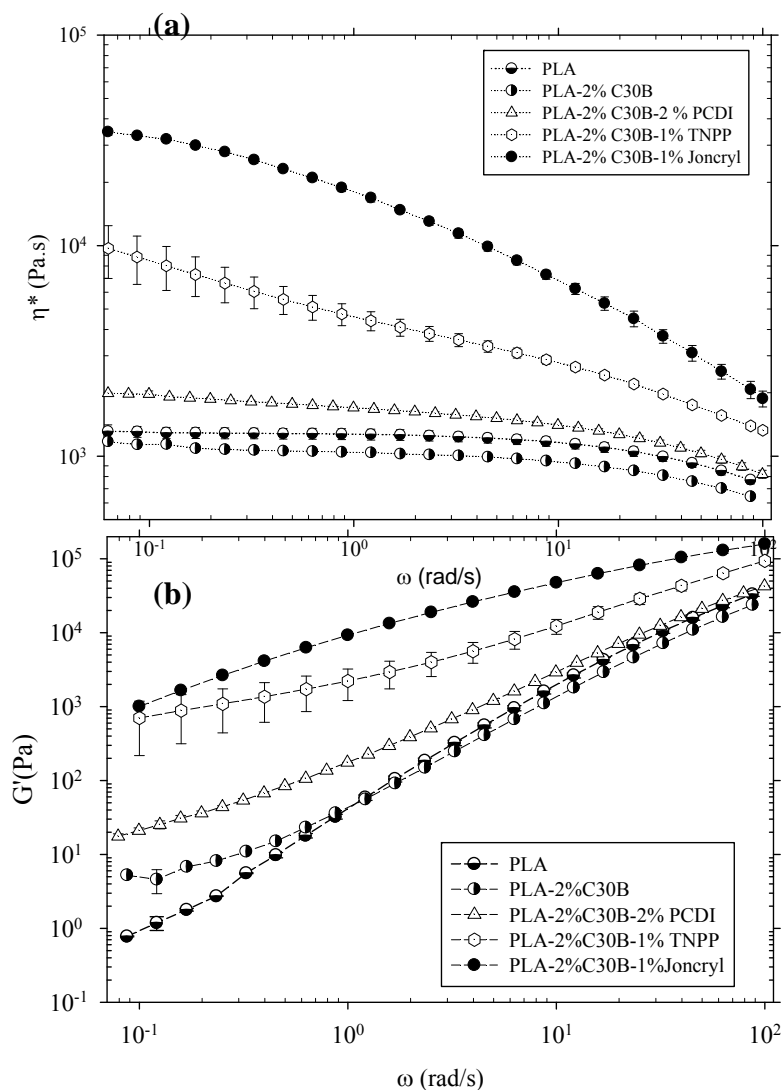


Figure 5-10: Complex viscosity (a) and storage modulus (b) of neat PLA and PLA nanocomposites containing different chain extenders, as functions of frequency(T=190 °C).

Using a chain extender not only stabilizes the viscosity and modulus with time (Fig. 5-9) but also increases their magnitudes (see also Table 5-3), facilitating further processing since high melt viscosity and elasticity are required in processes such as blow molding, thermoforming and

foaming. The viscosity and modulus enhancement of the nanocomposites containing a chain extender can be attributed to an increased molecular weight, resulting from a reattachment of cleaved polymer chains or branching as discussed later.

The crossover frequency ($\omega_c$) of the storage and loss moduli, where the transition from liquid-like to solid-like behavior takes place, is also reported in Table 5-3. As shown, the magnitude of the crossover frequency shifts toward lower frequencies in TNPP and Joncryl-based nanocomposites, consistent with an increase in matrix molecular weight or the addition of long chain branching.

Since chain extenders allow for the possible formation of nonlinear chains, it is important to consider the likelihood of gelation or the formation of local microgels. It is obvious from the ratio of the storage modulus to the loss modulus at low frequency (Table 5-3) that the elasticity of the nanocomposites increases with the addition of chain extenders, especially Joncryl. A gel content test was therefore performed using chloroform as a solvent on all of the nanocomposites containing chain extenders. All samples were completely dissolved in the solvent after 1.5 h suggesting that we are far from the gelation threshold in all cases. We may also estimate the critical mole fraction of chain extender, $\alpha_C$, for gelation from Eq. 1.

$$\alpha_c = \frac{1}{f-1} \qquad \qquad (1)$$

where $f$ is the functionality of the chain extender [34]. Joncryl [19] has a functionality of $f \sim 4$ and $\alpha_C \sim 0.33$. Since Joncryl has $M_N = 3\ 000$ g/mol and the virgin PLA has $M_N = 54\ 000$ g/mol, this corresponds to a critical weight fraction of 2.7%, which is higher than the contents used here. This confirms that we are below the gelation threshold with all of our Joncryl-based systems. The formation of branched structures leading to gelation is not expected with TNPP and PCDI since these chain extenders have an effective functionality of two, which leads to longer, but still linear chains. In the case of TNPP, the active phosphite groups simply act to form intermediate compounds facilitating the joining of two PLA chains by transesterification and do not remain in the backbone of the resulting chain [24]. The carbodiimide groups in PCDI [20] act similarly to the phosphate groups in TNPP.

To observe the effect of a chain extender on controlling the degradation over a large range of processing temperatures, the PLA nanocomposite, Joncryl-PLA based nanocomposite and PLA

containing Joncryl were processed in a twin-screw extruder using three different temperature profiles, and subsequently rheological measurements were conducted at 190 °C. The temperature profiles used are listed in Table 5-1 and abbreviated by LT, MT, and HT, for low, medium and high temperature profiles, respectively. The resulting complex viscosity and storage modulus are plotted as a function of frequency in Fig. 5-11. For nanocomposites without chain extender, the viscosity decreases with processing temperature at all frequencies (Fig. 5-11a). This indicates that the processing-induced degradation increases with processing temperature, as expected. In comparison, for the Joncryl-based nanocomposites the properties of the nanocomposites produced at LT and MT overlap over the entire frequency range, while they differ slightly from the properties of that processed at HT in the low frequency range (Fig. 5-11b). This may indicate a slightly enhanced PLA degradation in this nanocomposite at HT or a poorer clay dispersion relating to the degradation of the organic clay modifier [12, 35].

For comparison, the viscosity and storage modulus of PLA containing 1 wt. % Joncryl is also considered under the same three processing conditions. As shown in Fig. 5-11c, the rheological functions are independent of the processing temperature over the entire frequency range, indicating that no degradation occurred during processing at any temperature. Based on the results in Fig. 5-11, we can conclude that the rate of thermal degradation of PLA-nanocomposites is increased with increasing temperature and that Joncryl effectively maintains the molecular weight in PLA nanocomposites.

To gain further understanding of the polymer molecular structure after the incorporation of the chain extender, the examination of the linear viscoelastic behavior (LVE) is refined. To create a weight average molecular weight, $M_W$, independent plot, the complex viscosity is shifted on both axes using the zero-shear viscosity as illustrated in Fig. 5-12. The zero-shear viscosities of the PLA systems containing PCDI and TNPP were observed in the range of frequency covered during the dynamic experiments; however, the zero-shear viscosity of PLA containing Joncryl was not observed in these tests and therefore was determined by a creep test. The values of the zero- shear viscosities are reported in Table 5-4. It is interesting to note that the addition of a chain extender beyond a certain value results in a viscosity reduction. The reason for this decrease is discussed later.
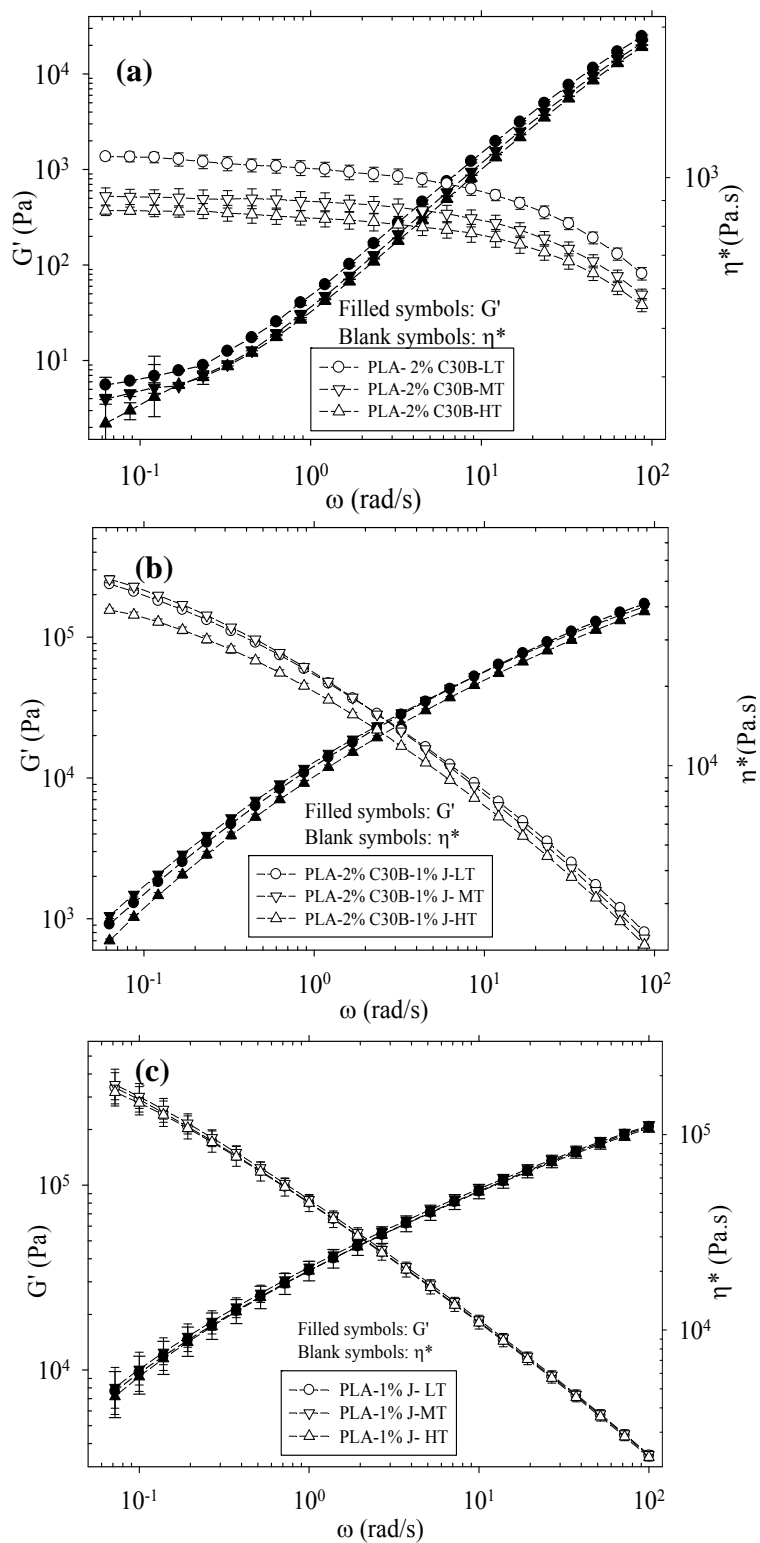
Figure 5-11: Complex viscosity and storage modulus of samples processed at LT, MT, and HT (Table 1): a) PLA nanocomposite, b) Joncryl-enriched nanocomposite, c) PLA containing 1 wt. % Joncryl. The rheological measurements are conducted from low to high frequencies at 190 ºC.

Plots such as Fig. 5-12 show the effect of molecular weight distribution (MWD) and long chain branching (LCB) on the rheological properties, independent of $M_W$. Narrow molecular weight distributed polymers tend to exhibit a broad Newtonian plateau, followed by a narrow transition to the power-law region. A narrower Newtonian plateau and a broad transition region can be caused by broadening of the MWD or branching. The results in Fig. 5-12 therefore indicate that there is a significant difference between the molecular structure (MWD and LCB) of the Joncryl-enriched PLA and those of the other samples. Since the curves for the neat PLA, PLA containing PCDI, and PLA containing TNPP superpose even though the materials have different zero shear viscosities, we can assume that these three materials have the same shaped molecular weight distribution and no LCB. Their different zero shear viscosities indicate however that they have different $M_W$. The curves for the Joncryl-enriched PLA are consistent with either a very broad MWD and/or long chain branching.
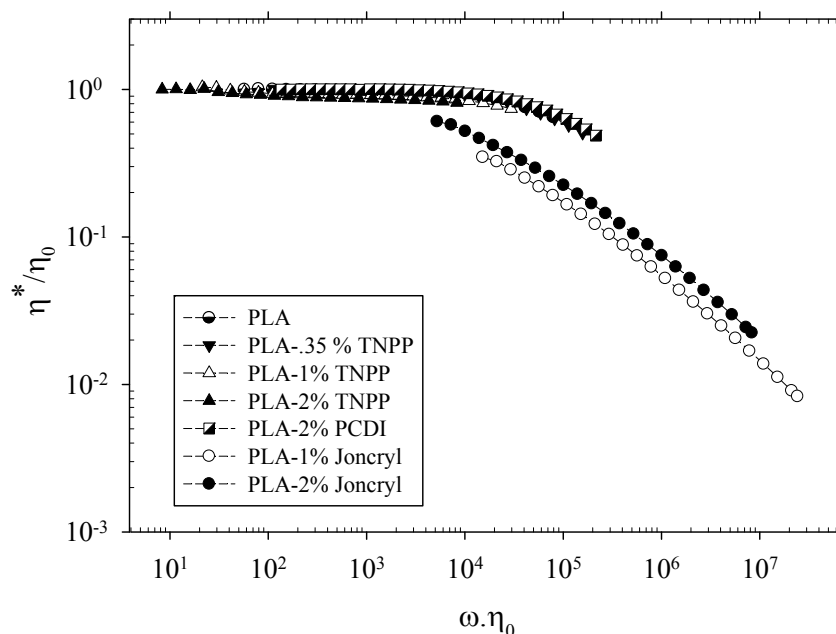


Figure 5-12: Shifted complex viscosity curves of neat PLA and PLA containing different chain extenders (T=190 ºC).

Another useful plot to consider is the loss angle as a function of frequency (Fig. 5-13) which clearly illustrates the differences between our materials. As in Fig. 5-12, the materials are clearly segregated into two classes: those with δ=90° at low frequency and those with lower δ at all frequencies. The first class consists of our linear systems (the neat PLA and the systems with

TNPP and PCD), and the second consists of the Joncryl systems which we believe to be branched. The nature of these data is consistent with previous studies of the effect of molecular structure on LVE properties [36].

Table 5.4: Zero-shear viscosity of neat PLA and PLA containing different chain extenders.

|  | Zero-shear Viscosity (Pa.s) |
|---|---|
| PLA | 1300 |
| PLA-0.35% TNPP | 2300 |
| PLA-1% TNPP | 400 |
| PLA-2% TNPP | 100 |
| PLA-2% PCDI | 1700 |
| PLA-1% Joncryl | 242000 |
| PLA-2% Joncryl | 83100 |

For linear chains, the frequency at which elasticity starts to play an important role decreases as the molecular weight increases, leading to a more pronounced decrease in the loss angle with increasing frequency. Based on this and the zero shear viscosities in Table 5-4, it can be concluded that the incorporation of 0.35 wt. % of TNPP and 2 wt. % of PCDI into the neat PLA leads to an increase of the PLA molecular weight. However, further addition of TNPP to the neat PLA decreases the molecular weight (see Table 5-4 and the curves related to PLA containing 1 and 2 wt. % TNPP). This behavior is in good agreement with the observations of Jacques *et al*. for TPP-enriched PET/PBT blends [37]. These authors propose that the reduction in the molecular weight and subsequent viscosity in the polyester containing a chain extender could be explained by condensation-hydrolysis mechanisms, taking place in polycondensates. The molecular weight of polyesters is usually determined by an equilibrium between ester groups and chain ends [37].
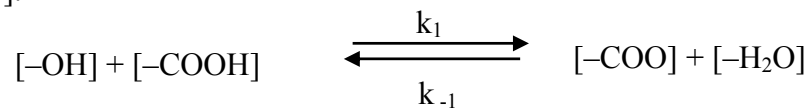
$$[-\text{OH}] + [-\text{COOH}] \underset{k_{-1}}{\overset{k_1}{\rightleftharpoons}} [-\text{COO}] + [-\text{H}_2\text{O}]$$

The equilibrium constant can be written as Eq. 2

$$K = \frac{k_1}{k_{-1}} = \frac{[-COO-][H_2O]}{[-OH][-COOH]} \tag{2}$$

Once the chain extender, TNPP, is added, a reaction takes place between the phosphite groups of the chain extender and the hydroxyl groups of the PLA chain ends, leading to a reduction of the active chain end concentration in the polyester. Accordingly, incorporation of more TNPP than required to react with all of the hydroxyl groups results in a large displacement away from the condensation equilibrium [37]. To compensate and put the system back into equilibrium, new hydroxyl groups are released by the cleavage of ester bonds in the polymer backbone, decreasing the polymer molecular weight.
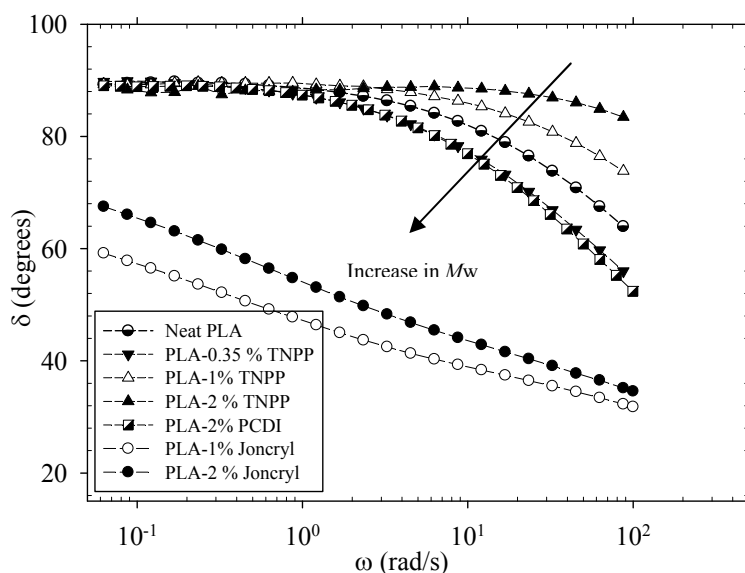


Figure 5-13: Effect of molecular structure on loss angle of neat PLA and PLA containing different chain extenders (T=190 ºC).

A similar mechanism may also be responsible for the reduction in zero shear viscosity when increasing from 1% to 2% Joncryl (Table 5-4). We note that since LCB is present, it is not possible to unequivocally ascribe the reduction in zero shear viscosity to a reduction in molecular weight because of the presence of LCB, which can have a non-monotonic effect on zero shear viscosity. We can replot the data in Fig. 5-13 as in Fig. 5-14 to emphasize the impact of long chain branching (LCB). Due to the presence of relaxation modes at long times related to the branched chains, the shape of the loss angle curve changes completely in long chain branched systems [36].
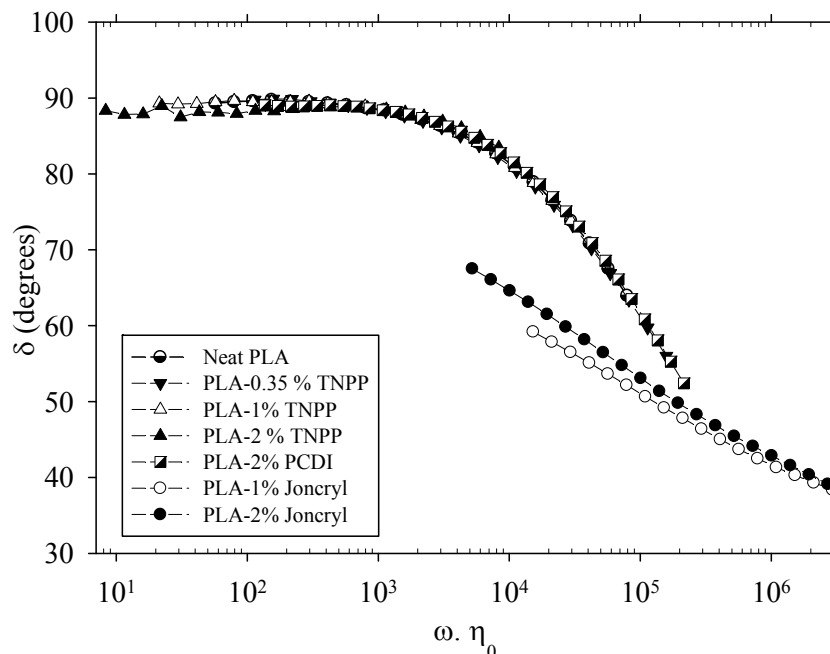
Figure 5-14:  Shifted loss angle curves of neat PLA and PLA containing different chain extenders (T=190 ºC).

The shape of the curves for both Joncryl containing systems is consistent with LCB.  Fig. 5-14 confirms that TNPP and PCDI systems are linear with the same shape of MWD since these curves also superimpose. We recall that these observations are consistent with the functionality of 2 for TNPP and PCDI (producing longer, linear chains) and the functionality of 4 for Joncryl (producing longer linear and branched chains).

## 5.4   Conclusion

In the present study, the thermal stability of PLA-clay nanocomposites was investigated through rheometry and thermal gravimetric analysis. Rheological data revealed a rapid thermal degradation of PLA in the presence of an organo-modified clay (Cloisite® 30B). It has been found that the incorporation of a chain extender into the nanocomposites, at an appropriate concentration for a given temperature, had a profound effect not only on controlling the degradation but also on increasing the $M_W$, resulting in an increase of the polymer viscosity. Based on the rheological data and an FT-IR spectroscopic study of the reaction products, the mechanism of stabilization is most likely chain extension.   The chain extension led to the

formation of longer linear chains in the PCDI and TNPP based nanocomposites, and long chain branched (LCB) structure in Joncryl-based nanocomposites. The LCB strongly influenced the linear viscoelastic response such as the zero-shear viscosity and loss angle. Thermal gravimetric analysis revealed that the addition of clay into the PLA decreases its thermal stability, whereas the incorporation of a chain extender increased the onset temperature for thermal degradation for a PLA containing 2 wt. % of the organoclay. Joncryl was found to be the most efficient chain extender under the studied processing conditions, which strongly influenced the rheological properties of PLA and properly controlled the degradation over a wide range of processing temperatures.

## Acknowledgments

## References

[1] Garlotta D. A literature review of poly(lactic acid). J Polym Environ. 2001;9:63-84.

[2] Lunt J. Large-scale production, properties and commercial applications of polylactic acid polymers. Polym Degrad Stab 1998;59:145-52.

[3] Achmad F., Yamane K., Quan S., Kokugan T. Synthesis of polylactic acid by direct polycondensation under vacuum without catalysts, solvents and initiators. Chem Eng J. 2009;151:342–50.

[4] Mehta R., Kumar V. , Bhunia H., Upadhyay S. N. Synthesis of poly(lactic acid): a review. J Macromol Sci,: Polym Rev. 2005;45:325–49.

[5] Alexandre M., Dubois P. Polymer-layered silicate nanocomposites: preparation, properties and uses of a new class of materials Mater Sci Eng. 2000;28:1-63.

[6] Fukushima K. , Abbate C., Tabuani D., Gennari  M., Camino G. Biodegradation of poly(lactic acid) and its nanocomposites. Polym Degrad Stab 2009;94:1646–55.

[7] Hwang S.-S., Hsu P. P., Yeh J.-M., Chang K. -C. , Lai Y. -Z. The mechanical/thermal properties of microcellular injection-molded poly-lactic-acid nanocomposites Polym Comp. 2009:1625-30.

[8] Paul M-A, Alexandre M., Degée P., Calberg C., Jérôme R., Dubois P. Exfoliated polylactide/clay nanocomposites by in-situ coordination-insertion polymerization. Macromol Rapid Commun. 2003;24:561-6.

[9] Ray S. S., Yamada K., Okamoto M., Ogami A., Ueda K. New polylactide/layered silicate nanocomposites. 3. high-performance biodegradable materials. Chem Mater. 2003;15:1456-65.

[10] Wu D., Wu L., Zhang M. Rheology and thermal stability of polylactide/clay nanocomposites. Polym Degrad Stab 2006;91:3149-55.

[11] Chiang M.-F., Wu T.-M. Synthesis and characterization of biodegradable poly(L-lactide)/layered double hydroxide nanocomposites. Comp Sci Tech. 2010; 70:110–5.

[12] McLauchlin A. R., Thomas N. L. Preparation and thermal characterisation of poly(lactic acid) nanocomposites prepared from organoclays based on an amphoteric surfactant. Polym Degrad Stab. 2009;94:868–72.

[13] Fukushima K. , Tabuani D., Camino G. Nanocomposites of PLA and PCL based on montmorillonite and sepiolite. Mater Sci Eng C 2009;29:1433–41.

[14] Ray S.S., Maiti P., Okamoto M., Yamada K., Ueda k. New polylactide/layered silicate nanocomposites. 1. Preparation, characterization, and properties. Macromolecules. 2002;35:3104-10.

[15] Vaia R. A., Giannelis E. P. Polymer melt intercalation in organically-modified layered silicates: model predictions and experiment. Macromolecules. 1997;30:8000-9.

[16] Kopinke F. D., Mackenzie K. Mechanistic aspects of the thermal degradation of poly(lactic acid) and poly(b-hydroxybutyric acid). J Anal Appl Pyrolysis. 1997;40:43–53.

[17] Mohanty A. K., Misra M., Drzal L. T. Natural fibers, biopolymers, and biocomposites: CRC Press; 2005.

[18] Lehermrier H. J., Dorgan J. R. Melt rheology of poly( lactic acid): consequences of blending chain architectures. Polym Eng Sci. 2001;41:2172-84.

[19] Villalobos M., Awojulu A., Greeley T. , Turco G., Deeter G. Oligomeric chain extenders for economic reprocessing and recycling of condensation plastics. Energy. 2006;31.

[20] Yang L. X., Chen X. S., Jing X. B. Stabilization of poly(lactic acid) by polycarbodiimide. Polym Degrad Stab. 2008;93:1923–9.

[21] Li B., Dong f.-X., Wang X.-L. Organically modified rectorite toughened poly(lactic acid): nanostructures, crystallization and mechanical properties. Europ Polym J. 2009;45:2996–3003.

[22] Yan L.-T., Xu J., Qian Z.-Y., Guo B.-H. Carboxyl terminated polymer chain extension using a bisoxazoline coupling agent: monte carlo simulation. Macromol Theory Simul. 2005;14:586–95.

[23] Hea C., Costeuxa S., Wood-Adams P., Dealy J.- M. Molecular structure of high melt strength polypropylene and its application to polymer design. Polymer. 2003;44:7181–8.

[24] Cicero J. A., Dorgan J. R., Dec S. F., Knauss D. M. Phosphite stabilization effects on two-step melt-spun fibers of polylactide Polym Degrad Stab 2002;78 95–105.

[25] Vincent M. D., Sneddon J. Nonylphenol: an overview and its determination in oysters and wastewaters and preliminary degradation results from laboratory experiments. Microchem J 2009 92 112–8.

[26] Inata H., Matsumura S. Chain extenders for polyesters. I. Addition-type chain extenders reactive with carboxyl end groups of polyesters. appl Polym Sci. 1985;30:3325-37.

[27] Bikiaris D. N., Karayanndis G. P. Chain extension of polyesters PET and PBT with two new Diimidodiepoxides. II. Appl Polym Sci: Polym Chem. 1996;34:1337-42

[28] Kopinke F.-D., Remmler M., Mackenzie K., Milder " M., Wachsen O. Thermal decomposition of biodegradable polyesters -ll. Poly(lactic acid). Polym Degrad Stab. 1996;43:329-42.

[29] Zaidi L., Kaci M., Bruzaud S. Effect of natural weather on the structure and properties of polylactide/Cloisite 30B nanocomposites. Polym Degrad Stab 2010;95 1751-8.

[30] Yuryev Y., Wood-Adams P. Rheological properties of crystallizing polylactide: detection of Induction time and modeling the evolving structure and properties. Polym Sci Part B: Polym Phys. 2010;48:812-22.

[31] Krikorian V., Pochan D. J. Poly (L-lactic acid)/layered silicate nanocomposite: fabrication, characterization, and properties. Chem Mater 2003;15:4317-24.

[32] Fan Y., Nishida H., Hoshihara S., Shirai Y., Tokiwa Y., Endo T. Pyrolysis kinetics of poly(L-lactide) with carboxyl and calcium salt end structures. Polym Degrad Stab. 2003;79:547–62.

[33] Palade L. I., Dorgan J. R. Melt rheology of high L-content poly(lactic acid). Macromolecules. 2001;34:1384-90.

[34] Flory P. J. Principles of polymer chemistry: Cornell Unversity Press; 1953.

[35] Pavlidou S. , Papaspyrides C.D. A review on polymer–layered silicate nanocomposites. Prog Polym Sci. 2008;33:1119–98.

[36] Wood-Adams P. M., Dealy J. M. Effect of molecular structure on the linear viscoelastic behavior of polyethylene. Macromolecules. 2000;33:7489-99.

[37] Jacques B., Devaux J., Legras R. Reactions induced by triphenyl phosphite addition during melt mixing of PET/PBT blends: chromatographic evidence of a molecular weight increase due to the creation of bonds of two different natures. Polymer 1997; 38 5367- 77.

[38] Akima H. A new method of interpolation and smooth curve fitting based on local procedures. J Associat Comput Machin. 1970; 17:589-602.

# CHAPITRE 6

# POLYLACTIC ACID (PLA)-CLAY NANOCOMPOSITES PREPARED BY MELT COMPOUNDING IN THE PRESENCE OF A CHAIN EXTENDER

# Article 2: Polylactic acid (PLA)-clay nanocomposites prepared by melt compounding in the presence of a chain extender[1]*

N. Najafi C., M. C. Heuzey, P. J. Carreau

*Center for Applied Research on Polymers and Composites, CREPEC*
*Ecole Polytechnique, Department of Chemical Engineering, Montreal, QC, Canada*

**Abstract:**

Polylactide -layered silicate nanocomposites with and without a chain extender were prepared by melt mixing using a twin-screw extruder. An organo-modified clay, Cloisite® 30B, and a chain extender Joncryl®-ADR 4368F were employed in this study. The effect of the chain extender and processing conditions on the properties of the PLA-clay nanocomposites were investigated for different strategies of mixing. The resulting nanocomposites were characterized by X-ray diffraction (XRD), while their morphology was observed by SEM and TEM. The incorporation of the chain extender could enhance the degree of clay dispersion provided that it is judiciously added to the nanocomposite. The corresponding results revealed that the Joncryl-based nanocomposites, where nanoclay platelets were well-dispersed, exhibited a significantly reduced permeability as compared to others. The mechanical properties of the neat PLA, the PLA and Joncryl-based nanocomposites were also examined. The increased molecular weight in Joncryl-based nanocomposites caused a significant increase in the modulus, drawability and toughness of the samples.

---

# 6.1 Introduction

A significant attention has been devoted to biodegradable and biocompatible polymers in recent years, both from ecological and biomedical perspectives. The predominant biopolymers are polycaprolactone (PCL), polylactic acid (PLA), polyglycolic acid (PGA) and polyhydroxyalkanoate (PHA), among which PLA is the most promising candidate since it is made from renewable agricultural sources and can keep its transparency after processing [1-3]. Although biocompatibility, biodegradability, and bioresorbability of PLA make it an appropriate candidate for packaging end-use applications, there are, however, some issues such as a low drawability [1, 4, 5], insufficient toughness [6, 7] and limited gas barrier properties [8, 9] that should be properly overcome. Copolymerization, blending and filling techniques are generally used to prevail over these drawbacks [10]. However, the incorporation of a filler into the PLA matrix has attracted the most attention since it pairs low cost with good results. Recently, there have been several attempts to broaden the end-use properties of PLA by developing PLA/clay nanocomposites [1, 5-7, 9, 11]. Three main techniques can be distinguished for nanocomposites preparation based on thermoplastic matrices: *in-situ* polymerization, solution intercalation and melt intercalation. The melt intercalation method is the most useful approach for industrial applications due to the absence of solvent, and compatibility with current industrial compounding and processing techniques [12].

The delamination of natural hydrophilic clay in the hydrophobic polymer matrix is a crucial issue [13]; hence, the modification of the clay surface with a surfactant is required to make it organophilic and compatible with common hydrophobic polymers. Cloisite® 30B is an organo-modified montmorillonite having two hydroxyl groups. The reaction occurring between its hydroxyl groups and the carboxyl groups of PLA makes this clay favorable for producing PLA-clay nanocomposites [1]. On the other hand, many attempts have been made to enhance PLA physical and mechanical properties through modification of the polymer and increased molecular weight [14, 15]. It has been shown that using a chain extender could make the molecular weight increase and improve properties [14, 16]. The effect of different chain extenders such as polycarbodiimide (PCDI), tris (nonylphenyl) phosphite (TNPP) and Joncryl ®ADR 4368F on the thermal degradation of PLA and PLA-clay nanocomposites was investigated in our previous

work [17]. Joncryl was found to be the most efficient chain extender, strongly influencing the molecular weight of PLA and rheological properties of PLA and PLA/clay nanocomposites.

The aim of the present work is to investigate the effect of processing conditions on clay dispersion in the presence of the chain extender Joncryl. The impact on the resulting morphology, rheological, mechanical, and barrier properties of PLA/clay nanocomposites is examined. Different strategies for the incorporation of the chain extender into the PLA nanocomposites are investigated.

## 6.2 Experimental

### 6.2.1 Materials

The polylactide (PLA) used in this study was purchased from NatureWorks Co. (USA). The selected grade, PLA 4032 D, is a semi-crystalline material in pellet form with an L-lactide: D-lactide ratio of 98:2. The glass transition temperature $T_g$ and the melting point $T_m$ are 60 and 170 ºC, respectively, as reported by the manufacturer. The organo-modified nanoclay used was Cloisite® 30B (Southern Clay Products Inc.). Finally, Joncryl® ADR-4368F, an epoxy-based chain extender supplied by BASF, was used as a chain extender. It is a modified acrylic copolymer with epoxy functions.

### 6.2.2 Nanocomposite Preparation

Before compounding, the polylactide (PLA) and clay were dried at 70 ºC in a vacuum oven for 48 h. To prepare a benchmark nanocomposite (without chain extender), dried PLA and 2 wt. % clay were initially mixed. The mixture was then extruded using a corotating twin-screw extruder (CICO-TSE) of Leistritz Corp. with an $L/D$ ratio of 40 ($L$ = 720 mm), at a rotation speed of 150 rpm. The extruder was operated using the temperature profile set at 175, 180, 185, 190, 195, 195 °C (for the different zones from hopper to die).  To examine the effect of chain extender and processing conditions on clay dispersion, the Joncryl-based nanocomposites were prepared using five different strategies. In the first strategy (S1), the nanocomposite was prepared by direct mixing of PLA, 2 wt. % clay and 1 wt. % Joncryl and subsequently extruded using the conditions stated above. In the second strategy (S2), the nanocomposite was prepared using a master batch approach: pre dry-mixed PLA and 4 wt. % clay were fed into the extruder operated under the

same conditions.  The obtained master batch was dried in a vacuum oven (70 ºC) for 24 h. The master batch, PLA and Joncryl were then used to prepare the nanocomposite for a nominal content of 2 wt. % clay and 1 wt. % Joncryl. In the third strategy (S3), PLA and Joncryl were blended in the extruder, and then dried in a vacuum oven (70 ºC) for 24 h. Afterwards, the nanocomposite was prepared by extruding a mixture of this blend, along with PLA and 2 wt. % clay. To further investigate the effect of residence time on clay dispersion, two other strategies were also used. In the fourth and fifth strategies (S4 and S5, respectively), first the benchmark nanocomposite (PLA and 2 wt. % clay) was passed through the extruder two or four times, respectively, and put in the vacuum oven. Then, these nanocomposites and 1 wt. % Joncryl were compounded in twin-screw extrusion to prepare the final nanocomposites.  After each processing, the materials were cooled in an ice-water bath right after emerging from the extrusion die, pelletized and then dried in a vacuum oven (70 ºC) for at least 24h. The characteristics of the strategies considered in this study are summarized in Table 6-1

Table 0.1: Characteristics of the compounding strategies considered in this study

| Strategy | Composition | Ext. proc. times | Procedure |
|---|---|---|---|
| Benchmark nanocomposite (S0) | PLA-2 wt% C30B | 1 | PLA and clay were extruded simultaneously |
| S1 | PLA-2 wt% C30B-1wt% Joncryl | 1 | PLA, clay and Joncryl were extruded simultaneously |
| S2 | PLA-2 wt% C30B-1wt% Joncryl | 2 | PLA and 4 wt% clay were blended in the first extrusion pass, while Joncryl was added to the nanocomposite in the second pass |
| S3 | PLA-2 wt% C30B-1wt% Joncryl | 2 | PLA and Joncryl were blended in the first extrusion pass, while clay was added to the nanocomposite in the second pass |
| S4 | PLA-2 wt% C30B-1wt% Joncryl | 3 | PLA and clay were  extruded  two times, Joncryl was added in the third extrusion pass |
| S5 | PLA-2 wt% C30B-1wt% Joncryl | 5 | PLA and clay were  extruded four times, Joncryl was added in the fifth extrusion pass |

## 6.2.3  Characterization

The nanoclay interlayer spacing ($d_{001}$) was determined by X-ray diffraction (XRD) measurements performed on a Philips X'Pert X-ray diffractometer using Cu-K$\alpha$ radiation ($\lambda$ = 0.1542 nm), while the generator was set up at 50 kV and 40 mA. The data was collected over a range of scattering angles (2$\theta$) of 1 to 10°. The morphology of the disk-shaped nanocomposites was investigated by scanning and transmission electron microscopy (SEM and TEM, respectively) at

room temperature. A high resolution Hitachi S-4700 microscope operated at 2 kV accelerating voltage was employed for SEM to observe nanofiller agglomeration and distribution. The specimens were prepared using an ultramicrotome equipped with a diamond knife and then coated with platinum vapor. Finally, TEM images were obtained using a JEOL JEM-2100F microscope at a 200 kV accelerating voltage. TEM was done on ultramicrotomed samples using a diamond knife at temperature -100 °C.

In order to characterize the rheological properties, disks of 25 mm diameter and 1.5 mm thickness were produced by compression molding at 190 ºC and a pressure of 20 MPa under a nitrogen atmosphere. Dynamic rheological measurements of PLA nanocomposites were performed using a strain-controlled ARES rheometer (Rheometric Scientific) equipped with a 25 mm parallel plate flow geometry. The strain amplitude was set at 8 %, strain large enough to provide a reliable signal while keeping the measurements in the linear viscoelastic region. All the time sweep tests, at a frequency of 6.28 rad/s, and frequency sweep tests, over a frequency range of 0.1-100 rad/s (from high to low frequency), were carried out under a nitrogen atmosphere, at 190 ºC and using a gap size of 1-1.3 mm. The contribution of thermal degradation during the frequency sweep tests was less than 10% and considered to be within experimental error.

Differential scanning calorimetry (DSC) tests were carried out using a TA Instruments calorimeter (DSC-Q 1000) under a nitrogen atmosphere. Samples were heated at a scanning rate of 10 ºC /min from 30 to 250 ºC. To investigate the effect of processing conditions on the degree of crystallinity of the resulting nanocomposites, crystallization enthalpy ($\Delta H_c$), melting enthalpy ($\Delta H_m$), and degree of crystallinity were determined from the first heating cycle.

The oxygen permeability of PLA and PLA nanocomposites was measured using the methodology described in standard ASTM 1434-82S, using an Ox-Tran Model 2/21 apparatus (Mocon Inc.) at 25 °C. The samples were compression molded, at 190 °C and a pressure of 20 MPa under a nitrogen atmosphere, into films with a thickness of approximately 400 µm for this purpose. The permeability values reported in this work have been normalized by the film thickness. All the presented values are averages of at least three films for each specimen.

Dog-bone-shaped specimens of 150 mm in total length, with a gage section of 12 mm wide by 4 mm thick and 80 mm long, type I based on standard ASTM D638, were prepared by compression molding at 190 ºC and a pressure of 25 MPa and subsequent cooling down to 5 ºC to avoid

sample shrinkage. An Instron tensile machine (model 4400R) was used to measure the tensile strength, tensile modulus, elongation at break and toughness according to standard ASTM D638. All tests were carried out under ambient conditions using a cross-head speed of 5 mm/min. In order to accurately measure the strain, an Instron extensometer was employed. All the reported values were obtained by averaging over four specimens for each processing condition.

## 6.3    Results and Discussion

### 6.3.1 Morphology

The structure of the nanocomposites obtained using the various compounding strategies (Table 6-1) was first characterized on the compression molded samples using X-ray diffraction. The XRD patterns of Cloisite 30B, PLA and Joncryl-based nanocomposites are presented in Fig. 6-1.
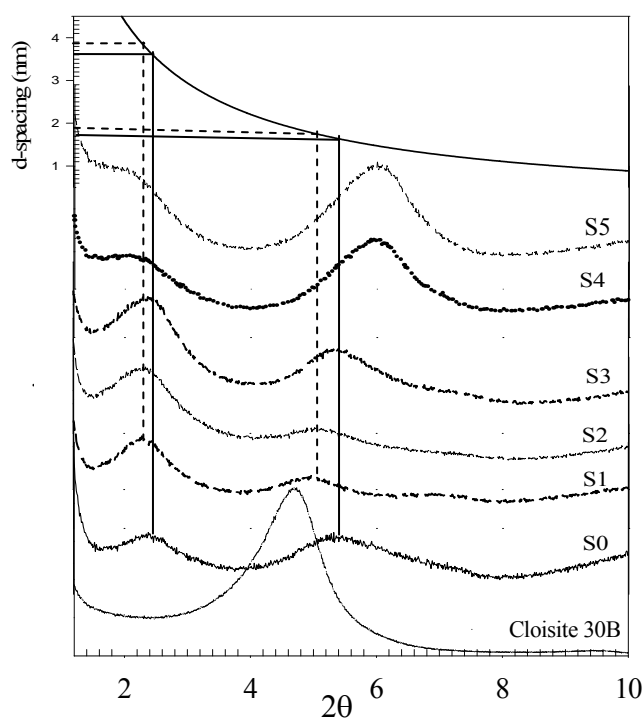


Figure 0-1:  XRD pattern of PLA and Joncryl-based nanocomposites prepared by different compounding strategies. The intensity axis has been shifted for clarity.

The diffraction pattern of the organo-clay (Cloisite 30B) reveals a sharp reflection peak at $2\theta = 4.73°$ that corresponds to a mean interlayer space of 1.86 nm. The insertion of polymer chains inside the clay gallery in the nanocomposites leads to an increase in the $d_{001}$ basal spacing and

hence shifting of the peak towards a lower diffraction angle (around $2.2^\circ$). Moreover, a second diffraction peak also appears at a higher angle (around 5-5.5 $^\circ$). The second observed peak may result from clay gallery collapsing and/or the $d_{002}$ reflection. Most of these results represent a combination of both mechanisms, except in the nanocomposite prepared by S1 and S2 strategies, where the second peak position and intensity correspond to the $d_{002}$ reflection. The first direct comparison between the PLA benchmark nanocomposite and Joncryl-based nanocomposites prepared by the S1 and S2 strategies shows that both the first peak shifts towards a lower diffraction angle (from 2.4 to 2.2°) when the chain extender is incorporated into the nanocomposites, which corresponds to a slight increase of the gallery spacing. Note that although the basal $d$-spacing and peak position of the Joncryl-based nanocomposites prepared by the third strategy (S3) are similar to those of the PLA benchmark nanocomposite, its second peak is more intense and sharper in comparison with the benchmark nanocomposite, indicating a more ordered silicate layer structure. For the Joncryl-based nanocomposites prepared by the fourth (S4) and fifth (S5) strategies significant increases in intensity of the second peak suggest an important collapse of the gallery due to thermal degradation of the organo component of the clay. As expected the formation of clay aggregates due to silicate layer collapse is more pronounced upon increasing the residence time due to multiple extrusion passes encountered in S4 and S5 strategies. However, the Joncryl-based nanocomposites prepared by the third strategy, where the chain extender was first added to the matrix, also exhibits a poor clay dispersion even though it was prepared in a single extrusion pass. The reason for the poor result of the S3 strategy is explained below. To study the morphological details of the nanocomposites prepared by the best strategies, i.e. S1 and S2, SEM and TEM are employed.

The SEM micrographs for samples prepared using the first and second strategies are presented in Fig. 6-2. The bright spots represent clay particles. The micrographs of the nanocomposite without the chain extender (Fig. 6-2a) reveal a fairly uniform distribution of clay particles, whereas there are some aggregates in the Joncryl-based nanocomposite processed by the first strategy (S1) (Fig. 6-2b). However, the incorporation of the chain extender in the second strategy (S2) results in a good level of clay dispersion since clay aggregates have almost disappeared (Fig. 6-2c).
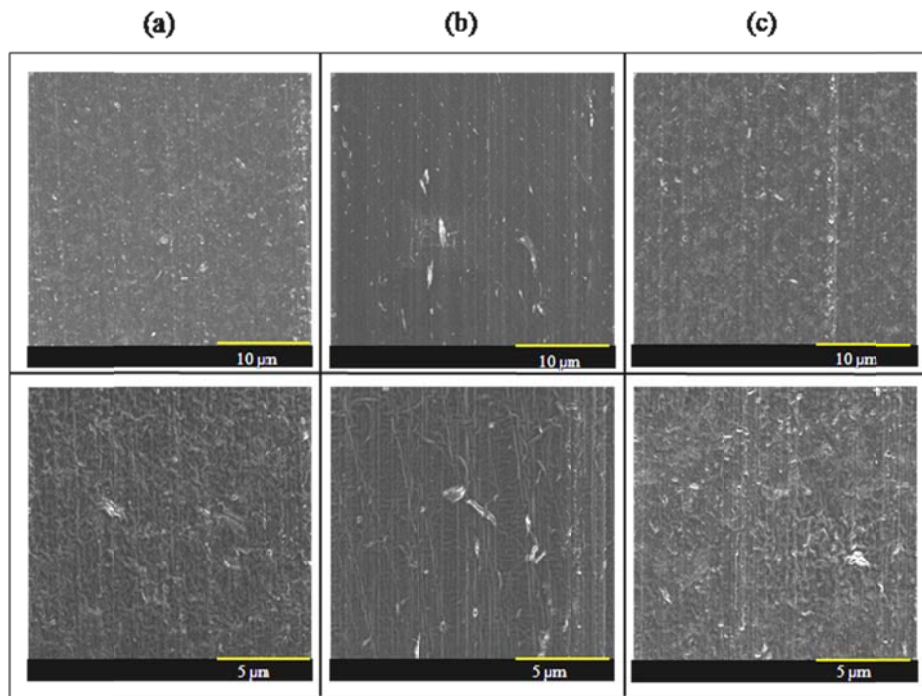
Figure 0-2: SEM micrographs of (a) PLA nanocomposites; and Joncryl-based nanocomposites prepared by the (b) first and (c) second strategies, the top and the bottom micrographs are related to low and high magnifications, respectively.

Fig. 6-3 shows the TEM micrographs of PLA and Joncryl-based nanocomposites prepared by the first (S1) and second (S2) strategies at different magnifications. Dark lines or spots correspond to clay sheets. The micrographs are arranged from low to high magnification, indicating the quality of the distributive mixing and revealing the coexistence of intercalated, disordered and delaminated clay platelets. Fig. 6-3a presents the TEM micrographs of benchmark nanocomposite (S0) at different magnifications, indicating the coexistence of intercalated, disordered and delaminated clay platelets. In the case of Joncryl-based nanocomposites prepared by the first strategy (S1), mainly intercalation is observed in Fig. 6-3b, although there is partial delamination. These observations are consistent with the SEM and XRD results. The micrographs reveal that the simultaneous incorporation of clay and chain extender deteriorates the degree of clay dispersion as compared to the benchmark nanocomposite containing no Joncryl. In order to understand the reason behind this finding, the effect of the chain extender on the molecular structure of PLA was investigated. According to GPC results reported in our previous study [17], the incorporation of 1 wt. % Joncryl into PLA results in a significant increase in the molecular

weight, from 95 000 to 668 000 g/mol, and to the probable formation of a long chain branched structure. The epoxy groups of the epoxy-based chain extender may preferentially react with carboxylic acid groups of the polyester [18].
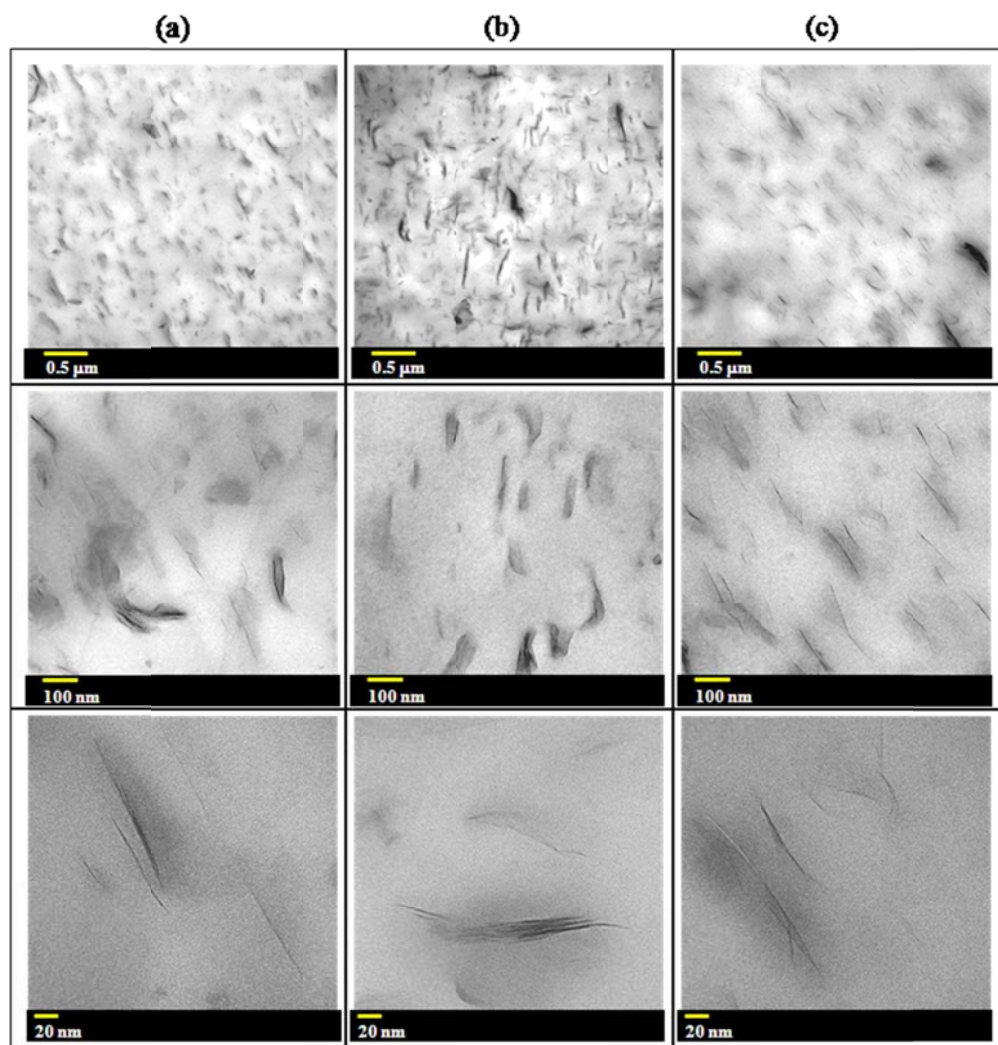


Figure 0-3: TEM micrographs of (a) PLA nanocomposites and Joncryl-based nanocomposites prepared by (b) the first and (c) second strategies, the top, middle and the bottom micrographs are related to different magnifications.

Moreover, the reaction occurring between the hydroxyl groups of the clay and the carboxyl groups of the PLA promotes the dispersion of the clay. As both clay and chain extender tend to react with the carboxyl groups of PLA [1, 18], the deterioration of the clay dispersion in the Joncryl-based nanocomposites prepared by the first strategy can be explained by the competing effects between clay and Joncryl to react with the carboxyl groups of PLA.

Such a competing effect is also responsible for the poor clay dispersion in Joncryl-based nanocomposites developed by the third strategy (S3) where clay is incorporated into the blend of PLA and Joncryl. The addition of the chain extender to PLA prior to clay loading consumes most of the carboxyl end groups present in the polymer. Consequently, no more compatibility reaction can be carried out between the PLA chains and the modified clay surface. Moreover, increasing the polymer molecular weight in the early stage of compounding makes it difficult for the penetration of polymer chains into the clay gallery spacing. In contrast, in the case of Joncryl-based nanocomposite prepared by the second strategy (S2) a more homogeneous clay dispersion is obtained (see Fig. 6-3c) as a result of the reaction occurring between clay and PLA during melt blending and the increased shear force provided by the higher molecular weight matrix in the following extrusion step.

The clay dispersion can be quantified using the method proposed by Luo *et al.* [19], called free-path spacing measurement (FPSM). It is based on the free-path spacing, $x_i$, which is defined as the distance between clay platelets, and the dispersion parameter, $D_{0.1}$, given by Eq.3:

$$D_{0.1} = 1.1539 \times 10^{-2} + 6.6838 \times 10^{-4} \left( \frac{\mu}{\sigma} \right)^2 - 1.9169 \times 10^{-4} \left( \frac{\mu}{\sigma} \right)^3 + 3.9201 \times 10^{-6} \left( \frac{\mu}{\sigma} \right)^4 \qquad (3)$$

where, $\mu$ and $\sigma$ are the mean free-path and standard deviation, respectively. Based on this approach, an exfoliated structure is achieved when the dispersion factor $D_{0.1}$ is over 8%, while an intercalated structure has a dispersion factor between 4 and 8% [19]. This factor has been calculated for the benchmark PLA (S0) and Joncryl-based nanocomposites prepared by the first and second strategies using approximately 100 measurements. The obtained values for $D_{0.1}$ are 6.84, 5.72 and 7.86 % for nanocomposite prepared by S0, S1 and S2 strategies, respectively, suggesting that the degree of clay dispersion is slightly decreased in Joncryl-based nanocomposite prepared by the first strategy (S1) as compared to the one containing no Joncryl. On the contrary, in the Joncryl-based nanocomposite prepared by the second strategy, the dispersion factor is very close to that corresponding to an exfoliated structure (~ 8%). Therefore, this statistical study confirms what was observed by XRD, SEM and TEM.

## 6.3.2 **Rheological properties**

The embedding of nano-size clay particles into polymeric matrices changes their rheological properties [20-22]. The filler-polymer and filler-filler interactions lead to an increase in the complex viscosity, particularly at low frequencies, and to a more pronounced shear-thinning behavior. The molecular weight of the matrix and the degree of clay dispersion strongly affect the rheological properties of the nanocomposites. Based on time sweep measurements performed to evaluate the thermal stability of various PLA nanocomposite melts [17], the incorporation of 1 wt. % Joncryl seems to hinder the chain scission reaction, leading to thermal stability during processing. The complex viscosity and storage modulus of the PLA and Joncryl-based nanocomposites prepared by various strategies in this work are plotted as functions of frequency in Fig. 6-4.
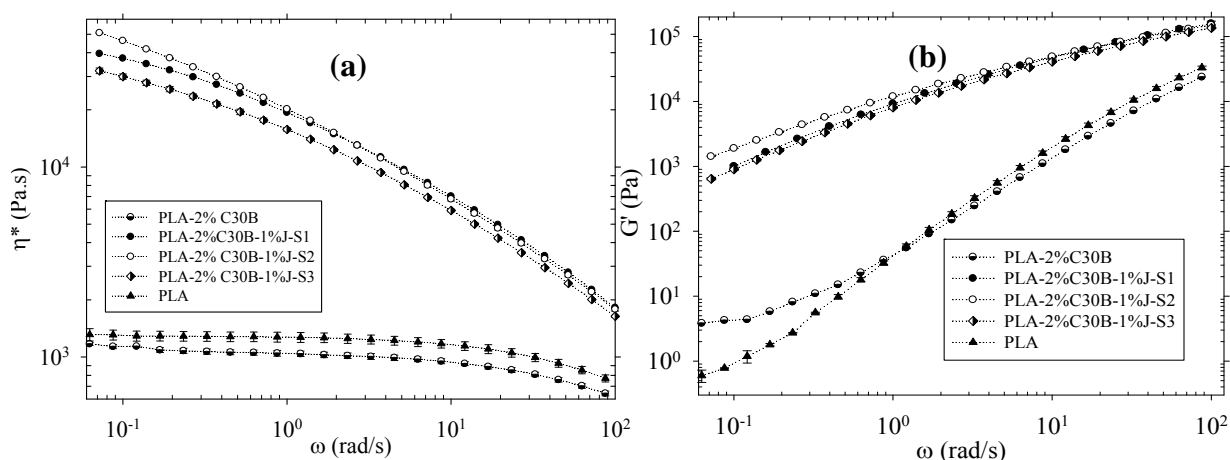


Figure 0-4:  Complex viscosity (a) and storage modulus (b) as a function of angular frequency of PLA and Joncryl-based nanocomposites prepared using different compounding strategies. The rheological measurements have been conducted from high to low frequencies at 190 °C.

As observed the nanoclay can have a significant effect on the rheological behavior of PLA nanocomposites provided that the PLA degradation is controlled. The Joncryl-based nanocomposite prepared by the second strategy exhibits the highest values of the complex viscosity and storage modulus in the low frequency region, indicating the finest clay dispersion, which was confirmed by the direct morphology observation. In fact, well-dispersed clay platelets have a much larger surface area that results in stronger interactions between the polymer and clay

in exfoliated structures. Such interactions in nanocomposites impede the motion of macromolecular chains and are reflected by an increase in viscosity and elasticity. The Joncryl-based nanocomposite prepared by the first strategy provides the second highest complex viscosity and storage modulus, even though less clay delamination occurred as compared to the benchmark PLA nanocomposite. This can be attributed to the degradation of the PLA matrix in the nanocomposite without chain extender, leading to a significant decrease of the matrix molecular weight that negatively impacts the rheological properties [17]. As expected the rheological properties of the nanocomposites prepared by the third strategy are lower than those for the S1 and S2 strategies.

### 6.3.3 Oxygen permeability

The permeation of gases through a polymeric film is a complex phenomenon that is governed by four processes: the sorption of gas molecules on the film surface; the dissolution of the gas in the polymer, the diffusion of the gas through it and, at last, desorption of the gas from the other surface of the film [20]. The gas permeation proceeds mainly in the amorphous phase of polymers. By this account, a semi-crystalline polymer is composed of a nearly impermeable crystalline phase dispersed in a permeable amorphous phase. Therefore, any increase in crystallinity leads to a decrease of the gas permeability due to a diminished contribution of the permeable amorphous phase and to an enhanced tortuosity of the diffusion path. The gas permeation mechanism in a nanoclay reinforced polymer is similar to that in a semi-crystalline polymer. The nanoclay platelets are considered as an impermeable phase dispersed in a semi-permeable polymeric phase. In addition to crystallinity, there are some other factors affecting the permeability, such as the fractional free volume (FFV), volume fraction of the nanoclay, its aspect ratio and orientation. Therefore, a reduction of gas permeability is expected in nanocomposites due to the decreased polymer phase volume fraction and mainly to the increased tortuous path. Since the reduction of the matrix volume fraction as a result of clay addition is small, tortuosity is the major factor influencing the barrier properties besides crystallinity.

Consequently, clay delamination and orientation could have a profound impact on the barrier properties considering that the tortuosity is generally controlled by the shape, dispersion level and orientation of the nano-platelets. The oxygen gas permeability ($P$) for the neat PLA, PLA

containing 1 wt. % Joncryl, and PLA- and PLA-Joncryl-based nanocomposites is presented in Fig 6-5.

As shown, the incorporation of the chain extender into the neat PLA increases the oxygen permeability of the corresponding blend ($P/P_{PLA}$=1.4). To explain this higher gas permeability, the crystallinity of the films used in these studies is considered. The first heating DSC thermogram data of PLA, PLA-Joncryl blend, and related nanocomposites are reported in Table 6-2. The degree of crystallinity ($X_c$) was determined from DSC analysis according to Eq. 4, where $\Delta H_m$, $\Delta H_c$ and $\phi$ are the measured melting enthalpy, crystallization enthalpy and weight fraction of PLA, respectively.

$$X_c\% = \left( \frac{\Delta H_m - \Delta H_c}{\Delta H_m^0 (\phi_{PLA}/100)} \right) \times 100 \qquad (4)$$

An enthalpy of fusion ($\Delta H_m^o$) of 93.6 J/g [11] was used for the perfectly crystalline PLA phase.



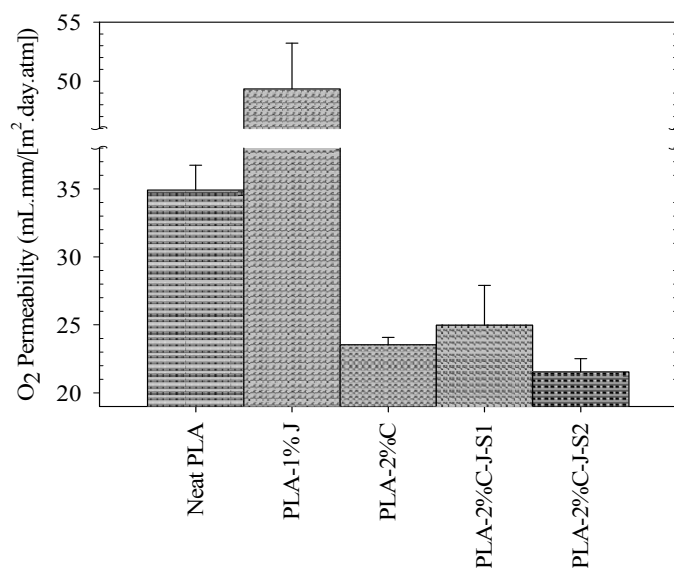Figure 0-5: Oxygen permeability of the neat PLA, PLA- and PLA-Joncryl-based nanocomposites prepared using different compounding strategies.

As shown in Table 6-2, the addition of the chain extender to the neat matrix leads to a decrease in crystallinity of the PLA from 7.7 to 1.4 %, due to the formation of a long chain branching structure in the Joncryl-PLA blend [17] that is not easily incorporated into the crystal lattice.

Table 0.2: Degree of crystallinity of the neat PLA, PLA-Joncryl blend and nanocomposites prepared by different strategies. These data are obtained from the first heating cycle in DSC thermograms.

| Composition | $\Delta H_c$ | $\Delta H_m$ | $X_c$ (%) |
|---|---|---|---|
| PLA | 27.1 | 34.3 | 7.7 |
| PLA-1% Joncryl | 25.5 | 26.8 | 1.4 |
| PLA-2% C | 29.3 | 36.6 | 8.0 |
| PLA-2% C-1% Joncryl (S1) | 27.2 | 29.3 | 2.3 |
| PLA-2% C-1% Joncryl (S2) | 26.5 | 28.6 | 2.3 |

Furthermore, a long chain branched structure hinders the packing of the main chains, leading to a considerable increase in the fractional free volume of the PLA chains that reacted with the chain extender [21]. The free volume plays an important role in the gas solubility and diffusion through polymers. Based on the free volume theory, the diffusion coefficient exponentially increases with the fractional free volume (FFV) [22]. Therefore, as a result of increased FFV as well as decreased crystallinity, the oxygen permeability is enhanced in the PLA-Joncryl blend. On the other hand, the formation of a tortuous path and also slightly increased crystallinity resulting from nanoclay loading diminishes the permeability of the PLA nanocomposites containing no Joncryl ($P/P_{PLA}$= 0.68). The decreased crystallinity and poorer clay dispersion in the nanocomposites prepared by the first strategy (S1) in the presence of the chain extender is responsible for the slightly lower barrier properties ($P/P_{PLA}$= 0.72) in comparison with the PLA nanocomposite containing no Joncryl ($P/P_{PLA}$= 0.68). However, further delamination and a better distribution of clay in the Joncryl-based nanocomposites produced by the second strategy (S2) provide a higher tortuosity, hence yielding the lowest permeability in comparison with the other samples ($P/P_{PLA}$= 0.64).

## 6.3.4 **Mechanical properties**

Typical stress-strain curves of the PLA and Joncryl-based nanocomposites are plotted in Fig. 6-6, while their mechanical properties are summarized in Fig. 6-7. PLA is found to be very brittle (failing without necking) while having a high modulus and a high tensile strength. A general increase in the tensile modulus and strength is observed in the Joncryl-PLA system due to the increased molecular weight and formation of a long chain branching structure [17]. The long chain branching increases the entanglement density of the polymer structure [23, 24] and thus

further hinders the slippage and orientation of the chains upon elongation. A similar behavior was also observed by Yim *et al.* [25] for ultra high molecular weight polyethylenes. Accordingly, the strain at break of the PLA containing the chain extender decreases, as shown in Fig.6- 6, leading to a reduced toughness despite increased tensile strength.
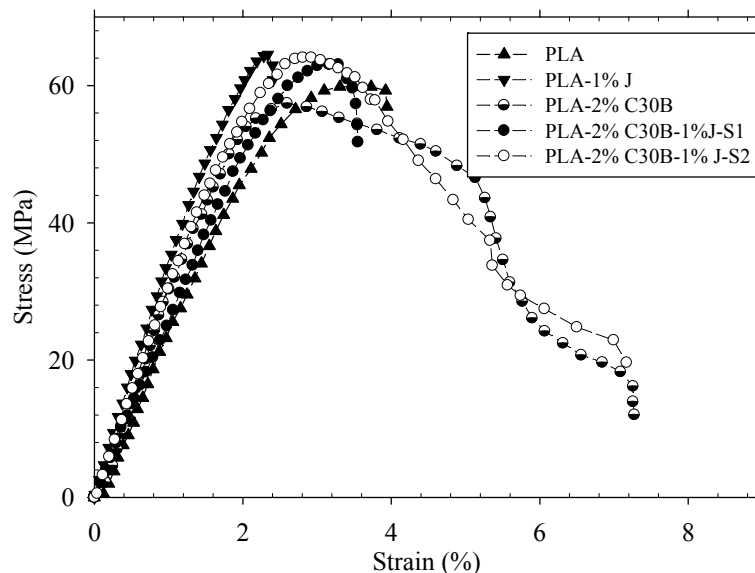


Figure 0-6:  Typical stress-strain behavior of dog-bone shaped samples for the neat PLA, PLA- and PLA-Joncryl-based nanocomposites prepared using different compounding strategies.

The Young modulus of the PLA nanocomposites increases after clay addition (see Fig. 6-7), while the tensile strength decreases as compared to the neat PLA. A reduction of the tensile strength in PLA nanocomposites was also reported by other authors [7, 9]. The reduction of molecular weight resulting from thermal degradation during processing may be responsible for such a strength reduction. The increase of ductility of PLA nanocomposites is clearly evident on the stress-strain curve shown in Fig. 6-6. The incorporation of Cloisite® 30B improves the deformation behavior of nanocomposites and causes the samples to experience significant necking, leading to an increased strain at break.

Generally, polymeric materials yield when shear yielding or crazing takes place during deformation [26]. Jiang and coworkers' study [6] indicates that micro-voiding and subsequent massive crazing are responsible for yielding in neat PLA exposed to uniaxial tension. The

incorporation of nanoclay platelets into PLA may play a dual role: the first role is providing micro-void nucleating sites due to interfacial debonding. The formation of micro-voids release strain constraint and induce local shear deformation, and hence brings about early material fracture. The second role is preventing the micro-voids from coalescing and forming cracks [6]. Since a favorable interaction occurs between the organo-modified clay and PLA, the clay platelets form a strong barrier between the micro-voids, leading to the inhibition of the micro-void coalescence and the craze propagation. As a consequence, a higher drawability is observed in PLA nanocomposites, resulting in an increase of the toughness despite a reduction of the tensile strength.
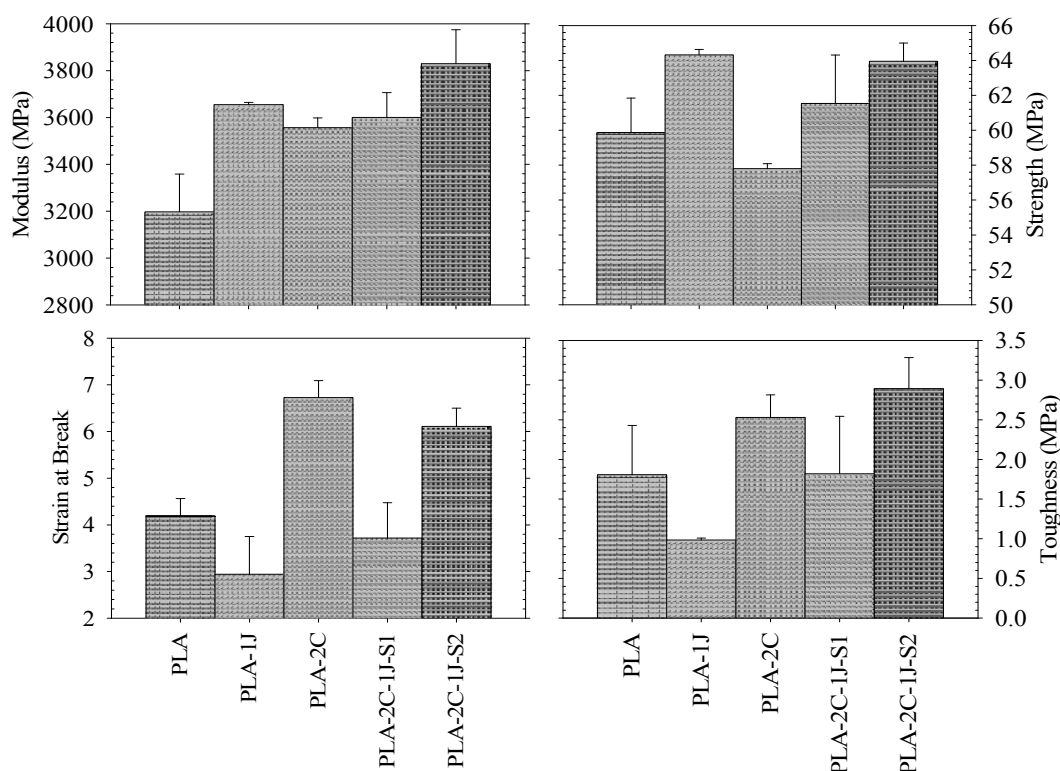


Figure 0-7: Effects of Joncryl and compounding strategy on a) Young's modulus, b) tensile strength, c) strain at break and d) toughness of the neat PLA, PLA- and PLA-Joncryl-based nanocomposites prepared using different compounding strategies.

The results presented in Figs.6- 6 and 6-7 reveal that the tensile modulus and tensile strength increase in the Joncryl-based nanocomposites prepared by the first strategy (S1), in comparison with the PLA nanocomposite containing no chain extender (S0). This can be related to the

increased molecular weight due to chain extension and the formation of a long chain branching structure [14, 27]. Nevertheless the nanocomposite toughness is decreased as a result of a reduction of the strain at break. Note that the strain at break is very sensitive to the dispersion of inclusions. As explained earlier, the simultaneous incorporation of clay and chain extender into the PLA decreased the clay dispersion and clay aggregates appeared (Fig. 6-2). These aggregates act as material flaws [6] around which a high stress is concentrated promoting PLA-clay debonding and material fracture. However, besides the enhanced $M_w$ of the matrix in the case of Joncryl-based nanocomposites prepared by the second strategy (S2), the increased degree of clay dispersion promotes the formation of a larger interfacial area and subsequent interfacial interaction between clay and PLA. Therefore, the stress transfer from the polymeric matrix to the inorganic phase increases, leading to a high tensile strength and modulus for the Joncryl-based nanocomposites. Furthermore, the lack of aggregates in these nanocomposites decreases craze density due to less interfacial debonding, and hence increases the polymer drawability and subsequent toughness (Fig. 6-7d). Based on the above findings, it can be concluded that the incorporation of the chain extender can significantly improve the mechanical properties provided that it is judiciously added to the nanocomposites.

## 6.4   Conclusion

In this work, the effects of a chain extender (Joncryl) and processing conditions on the clay dispersion and the final properties of PLA-clay nanocomposites were examined. PLA-nanoclay without Joncryl and Joncryl-based nanocomposites were prepared by melt compounding using different strategies. The morphological observations and quantification of clay dispersion revealed that an increased and homogeneous dispersion of clay was achieved in Joncryl-based nanocomposites prepared by the second strategy, based on a master batch of PLA/clay. In addition, the clay dispersion strongly affected the rheological properties of nanocomposites particularly in the low frequency region. The nanocomposites prepared by the second strategy also provided the highest complex viscosity and storage modulus at low frequencies despite the fact that it was processed twice. The measured oxygen permeability also indicated that the incorporation of the clay and chain extender into the nanocomposites using the second strategy provided the lowest permeability. The mechanical properties of the neat PLA, the PLA and Joncryl-based nanocomposites were also considered.  The semi-crystalline PLA exhibited a high

tensile modulus and strength while it had a very low elongation at break and toughness. However, a good dispersion and distribution of clay platelets and an increased molecular weight in Joncryl-based nanocomposites led to significant increases in the modulus, drawability and toughness compared to the neat PLA.

## Acknowledgments

## References

[1] Krikorian V, Pochan DJ. Poly (L-Lactic Acid)/Layered Silicate Nanocomposite: Fabrication, Characterization, and Properties. Chem Mater 2003;15(22):4317-4324.

[2] Ray SS, Okamoto M. New Polylactide/Layered Silicate Nanocomposites, 6 Melt Rheology and Foam Processing. Macromol Mater Eng. 2003;288(12):936–944.

[3] Urayama H, Kanamori T, Kimura Y. Properties and biodegradability of polymer blends of Poly(l-lactide)s with different optical purity of the lactate Unit. Macromol Mater Eng 2002;287:116-121.

[4] Baiardo M, Frisoni G, Scandola M, Rimelen M, Lips D, Ruffieux K, et al. Thermal and Mechanical Properties of Plasticized Poly(L-lactic acid). J Appl Polym Sci. 2003;90:1731–1738

[5] Chang JH, An YU, Cho DH, Giannelis EP. Poly(lactic acid) nanocomposites: comparison of their properties with montmorillonite and synthetic mica(II). Polymer. 2003;44(13):3715-3720.

[6] Jiang L, Zhang J, Wolcott MP. Comparison of polylactide/nano-sized calcium carbonate and polylactide/montmorillonite composites: reinforcing effects and toughening mechanisms. Polymer 2007; 48:7632-7644.

[7] Lewitus D, McCarthy S, Ophir A, Kenig S. The effect of nanoclays on the properties of PLLA-modified polymers part 1: mechanical and thermal Properties. J Polym Environ. 2006;14:171–177.

[8] Drieskens M, Peeters R, Mullens J, Franco D, Lemstar PJ, Hristova-Bogaerds DG. Structure Versus Properties Relationship of Poly(lactic acid). I. Effect of Crystallinity on Barrier Properties. J Polym Sci ;Part B, Polym Phys. 2009;47:2247–2258.

[9] Koh HC, Park JS, Jeong MA, Hwang HY, Hong YT, Ha SY, et al. Preparation and gas permeation properties of biodegradable polymer/layered silicate nanocomposite membranes. Desalination. 2008;233:201–209.

[10] Fukushima K, Tabuani D, Camino G. Nanocomposites of PLA and PCL based on montmorillonite and sepiolite. Mater Sci Eng C  2009;29:1433–1441.

[11] Huang J-W, Hung YC, Wen Y-L, Kang C-C. Polylactide/nano- and micro-scale silica composite films. II. melting behavior and cold crystallization. J Appl Polym Sci. 2009;112:3149–3156.

[12] Chen GX, Yoon JS. Clay functionalization and organization for delamination of the silicate tactoids in poly(L-lactide) matrix. Macromol Rapid Commun. 2005;26(11):899-904.

[13] Paul MA, Alexandre M, Degée P, Calberg C, Jérôme R, Dubois P. Exfoliated polylactide/clay nanocomposites by in-situ coordination-insertion polymerization. Macromol Rapid Commun. 2003;24(9):561-566.

[14] Liu J, Lou L, Yua W, Liao R, Li R. Long chain branching polylactide: Structures and properties. Polymer. 2010;51:5186-5197.

[15] Nallicheri RA, Rubner MF. Thermal and mechanical properties of Polyurethane-diacetylene segmented copolymers. 1. molecular weight and annealing effects. Macromolecules. 1990;23:1005-1016.

[16] Li H, Huneault MA. Effect of chain extension on the properties of PLA/TPS blends. J Appl Polym Sci. 2011(DOI 10.1002/app.33981).

[17] Najafi C. N, Heuzey MC, Carreau PJ, Wood-Adams PM. Control of thermal degradation of polylactic acid (PLA)-clay nanocomposites using chain extenders. Polym Degrad Stab (submitted). 2011.

[18] Bikiaris DN, Karayanndis GP. Chain extension of polyesters PET and PBT with two new Diimidodiepoxides. II. Appl Polym Sci: Part A, Polym Chem. 1996;34:1337-1342

[19] Luo ZP, Ko JH. Quantification of the layer dispersion degree in polymer layered silicate nanocomposites by transmission electron microscopy. Polymer. 2008;49 1841-1852.

[20] Choudalakis G, Gotsis AD. Permeability of polymer/clay nanocomposites: A review. Eur Polym J 2009; 45:967–984.

[21] Zhai W, Yu J, Ma W, He J. Influence of long-chain branching on the crystallization and melting behavior of polycarbonates in supercritical $CO_2$. Macromolecules. 2007;40:73-80.

[22] Hedenqvist M, Gedde UW. Diffusion of small-molecule penetrants in semicrystalline polymers. Prog Polym Sci 1996;21:299–333.

[23] Kennedy MA, Peacock AJ, Mandelkern L. Tensile properties of crystalline polymers: linear polyethylene. Macromolecules. 1994;27:5297-5310.

[24] Lin G-G, Shih H-H, Chai P-C, Hsu S. Influence of side-chain structures on the viscoelasticity and elongation viscosity of Polyethylene meIts. Polym Eng Sci. 2002;42( 11):2213-2221.

[25] Yim CI, Lee KJ, Jho JY, Choi K. Wear resistance of some modified ultra-high molecular weight polyethylenes and its correlation with tensile properties. Polym Bull 1999;42:433–440.

[26] Anderson TL. Fracture Mechanics: Fundamentals and Applications. Second ed: CRC; 1993.

[27] Grosvenor MP, Staniforth JN. The effect of molecular weight on the rheological and tensile properties of poly(e-caprolactone). Int J Pharm. 1996;135:103-109.

# CHAPITRE 7

# GENERAL DISCUSSION

# General Discussion

Different types of petrochemical-based thermoplastic polymers such as polyolefins, polystyrene, and polyamide have been widely used as packaging materials. In many cases, the recycling of these materials is not economically reasonable, while the disposal of such non-degradable plastic materials has seriously disturbed the ecosystem. As such, the development of biodegradable "green polymeric materials", has gained a great interest. Nowadays several biodegradable polymers such as poly (butylene succinate) (PBS), poly (ε-caprolactone) (PCL), poly (lactic acid) (PLA) and poly (vinyl alcohol) (PVOH) are commercially produced.

Among them, PLA can be made from renewable sources such as starch from corn or sugar beets, and decompose into non-toxic components in the environment. Moreover, the remarkable properties such as biodegradability, biocompatibility, high processability, transparency after processing and organoleptic characteristic of PLA makes it as a good candidate for food packaging (Amar, 2005; Schwach, 1997). Although these features make PLA an appropriate candidate for massive production, there are however some important issues which should be considered for industrial applications. PLA suffers from poor thermal stability, low mechanical resistance, and limited gas barrier properties. These problems were addressed in this project and methods for producing PLA-clay nanocomposites with improved properties were developed.

Our findings in the first step of this project indicated that the incorporation of a chain extender into the nanocomposites, at an appropriate concentration for a given temperature, had a profound effect on controlling the thermal degradation and increasing the molecular weight, leading to an increase of the polymer viscosity.

Chain extension leads to the formation of longer linear chains in the PCDI- and TNPP-based nanocomposites, and to a long chain branching (LCB) structure in Joncryl-based nanocomposites. The LCB strongly influences the linear viscoelastic response such as the zero-shear viscosity and loss angle. Thermogravimetric analysis showed that the clay loading in PLA decreases its thermal stability, whereas the incorporation of the chain extender increased the onset temperature of thermal degradation. Based on the obtained results, Joncryl was found the most efficient chain extender under the present processing conditions over a wide range of temperatures.

In the second step of this study, the most efficient chain extender under processing conditions, Joncryl, is used further to study the strategy of chain extender incorporation into PLA nanocomposites on promoting the degree of clay dispersion, rheological, mechanical and barrier properties. PLA/nanoclay without Joncryl and Joncryl-based nanocomposites were prepared by melt compounding using different strategies. The morphological observations, using XRD, SEM and TEM, and quantification of clay dispersion revealed that an increased and homogeneous dispersion of clay was achieved in Joncryl-based nanocomposites prepared by the second strategy, based on a master batch of PLA-clay. The chemical reaction occurring between carboxylic acid groups of the PLA chains and hydroxyl groups of the organically modified clay, as well as increased $Mw$, were responsible for the further delamination of clay platelets in the nanocomposites prepared by the second strategy. These samples provided the highest complex viscosity and storage modulus at low frequencies, despite the fact that they were processed twice.

The measured oxygen permeability also indicated that the incorporation of the clay and chain extender into the nanocomposites using the second strategy provided the lowest permeability. This finding could be well explained by an increase in the tortuosity path. The mechanical properties of the neat PLA, the PLA and Joncryl-based nanocomposites were also considered. Semi-crystalline PLA exhibited a high tensile modulus and strength while it had a very low elongation at break and toughness. However, a good dispersion and distribution of clay platelets and an increased molecular weight in Joncryl-based nanocomposites led to a significant increase in the mechanical properties of the PLA nanocomposites in comparison with the neat PLA.

Although the incorporation of the chain extender into the nanocomposites slightly increase the final cost of the resulting filled product (less than $1 per kg), it is still found to be more cost efficient than other alternatives.

Considering the fact that its level of crystallinity is usually low, PLA is a transparent polymer, and this is undoubtedly advantageous for food packaging applications and other consumer products. However, there is a risk that PLA-based nanocomposites loose this essential characteristic. Photographs of neat PLA and a PLA-based nanocomposite prepared in this work are presented in Figure 7-1.  It is evident that the nanocomposite sheet retains a good transparency, and that the sample color is only slightly affected by the presence of the additives.
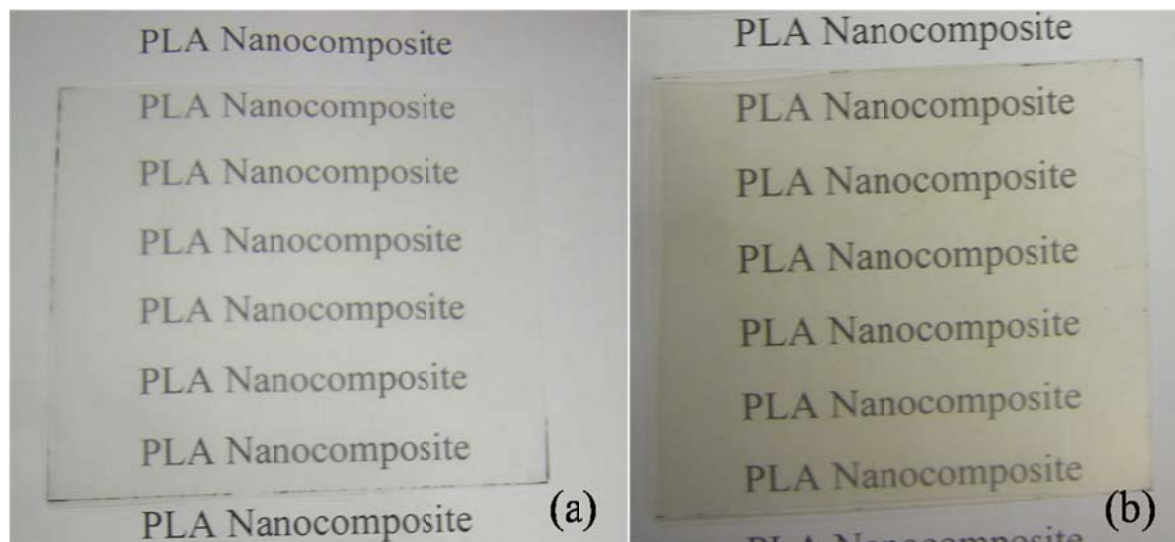
Figure 7-1: Photographs of (a) neat PLA and (b) Joncryl-based nanocomposite prepared by the second strategy.

Another aspect of food grade plastics is matching the appropriate type of plastic to the food considered. Since plastic additives can be leached from the packaging or container into the food, the Food and Drug Administration's (FDA) must approve materials to be used in food-contact applications. Among the materials used in this project, Joncryl (up to 1 wt. %) and TNPP have been approved as food additives by the FDA, while polycarbodiimide and Cloisite® 30B are still not FDA approved, which may be a drawback for the future development of these materials.

# CHAPITRE 8

## CONCLUSION AND RECOMMENDATIONS

# Conclusion

Based on the literature review, the thermal stability of PLA-based nanocomposites and clay dispersion are the major challenges in the development of PLA-clay nanocomposites with improved mechanical and barrier properties. Hence, in the first step of this work, control of the thermal degradation of PLA nanocomposites was aimed for. In the scope of this objective, different chain extenders were used and their ability to control the degradation was examined. The rheological and thermal properties of PLA nanocomposites containing different chain extenders were comprehensively investigated. Rheological data revealed a rapid thermal degradation of PLA in the presence of an organo-modified clay (Cloisite® 30B). It has been found that the incorporation of a chain extender into the nanocomposites, at an appropriate concentration, had a profound effect on controlling the degradation by increasing the $M_w$. The mechanism of stabilization was most likely chain-extension. The chain extension led to formation of longer linear chains in the PCDI and TNPP based nanocomposites, and long chain branching (LCB) structure in Joncryl-based nanocomposites. Thermogravimetric analysis revealed that the addition of clay into the PLA decreases its thermal stability, whereas the incorporation of the chain extender increased the onset temperature of thermal degradation due to a decreased number of chain tails per mass.

In the second step, the most efficient chain extender, Joncryl, was used to increase the degree of clay dispersion, leading to enhanced mechanical and barrier properties. To achieve this target, PLA-nanoclay without Joncryl and Joncryl-based nanocomposites were prepared using different strategies. The effect of chain extender, Joncryl, and polymer processing conditions on the clay dispersion and the final properties of nanocomposites were examined. The morphological observation and quantification of clay dispersion revealed that an increased and homogeneous dispersion of clay was achieved in Joncryl-based nanocomposites prepared by the master batch of PLA-clay (S2 strategy), while those prepared by the direct mixing (S1strategy) showed the worst morphology. This nanocomposite also provided the highest complex viscosity at low frequencies despite the fact that its matrix was processed twice. The measured oxygen permeability and mechanical properties also indicated that the incorporation of the clay and chain extender into the nanocomposites using the S2 strategy provided the lowest permeability and the highest mechanical properties.

Consequently, in addition to control the thermal degradation of the nanocomposite and enhance *M*w, the opportune addition of the chain extender resulted in further clay dispersion, and subsequently improved mechanical and barrier properties.

## 8.1  Originality of the work

As mentioned in Chapter 2, control of the degradation of neat PLA using chain extenders such as tris (nonyl-phenyl) phosphite (TNPP) and polycarbodiimide (PCDI) have been previously considered. Based on the reviewed literature and our own results, the incorporation of an organically modified clay intensifies the degradation of PLA during processing, resulting in decreased mechanical and even barrier properties.

To our knowledge no report has been published on controlling the degradation of PLA nanocomposites using chain extenders. This dissertation was aimed at the study of the rheological and thermophysical properties of PLA nanocomposites containing different chain extenders with a special attention being paid to their effect on the molecular structure of the polymeric matrix. In addition, different strategies for the incorporation of the chain extender into the nanocomposites were considered.

## 8.2  Recommendations for future work

The following unexplored topics are recommended for future research:

- Considering that melt compounding was selected as a preferred technique to prepare polymer-clay nanocomposites, the twin-screw configuration used during extrusion and the geometry of the mixing elements such as their staggering angle, the use of forward/backward transport elements and the width of kneading blocks should be optimized for the sake of increasing the degree of clay dispersion.

- Considering that the crystallinity and orientation of the clay platelets reduce the volume fraction of the gas permeable amorphous phase and increase the tortuosity path, respectively, post-processing conditions such as draw ratio and cooling rate could be investigated in the preparation of PLA nanocomposite films.

# REFERENCES:

Achmad, F., Yamane, K., Quan, S., Kokugan, T. (2009). Synthesis of polylactic acid by direct polycondensation under vacuum without catalysts, solvents and initiators. *Chem. Eng. J., 151*, 342–350

Alexandre, M., Dubois, P. (2000). Polymer-layered silicate nanocomposites: preparation, properties and uses of a new class of materials. *Mater. Sci. Eng., 28*(1-2), 1-63.

Amano, M. (2004). *PET bottle system in Sweden and Japan: an integrated analysis from a life-ccycle perspective* Master of Science, LUND

Amar, K., Mohanty, M. M., Lawrence T. D. (Ed.). ( 2005). *Natural fibers, biopolymers, and biocomposite* (Vol. 1-Chapter **16**). Michigan: Taylor & Francis

Bamford, C. H., Tipper  C. F.H. (Ed.). (1976). *Chemical kinetics* (Vol. 15- Non-Radical Polymerisation): Elsevier Scientific Publishing Company

Burlet, J., Heuzey,  M.-C., Dubois, C.,  Wood-Adams, P. (2005). *Thrmal stabilization of high-molecular weight l-polylactide*. Paper presented at the ANTEC

Cameron, D. J. A., Shaver, M. P. (2011). Aliphatic polyester polymer stars: synthesis, properties and applications in biomedicine and nanotechnology. *Chem.  Soc. Rev., 40*, 1761–1776

Chen, G. X., Kim, H. S., Shim, J. H., Yoon, J. S. (2005a). Role of epoxy groups on clay surface in the improvement of morphology of poly(L-lactide)/clay composites. *Macromolecules, 38*(9), 3738-3744. doi: Doi 10.1021/Ma0488515

Chen, G. X., Yoon, J. S. (2005b). Clay functionalization and organization for delamination of the silicate tactoids in poly(L-lactide) matrix. *Macromol. Rapid Comm., 26*(11), 899-904. doi: DOI 10.1002/marc.200500046

Cicero, J. A., Dorgan, J. R., Dec, S. F., Knauss, D. M. (2002). Phosphite stabilization effects on two-step melt-spun fibers of polylactide. *Polym. Degrad. Stab., 78*(1), 95-105. doi: Pii S0141-3910(02)00123-4

Drumright, R. E., Gruber, P. R., Henton, D. E. (2000). Polylactic acid technology. *Adv. Mater., 12*(23), 1841-1846

Fan, Y. J., Nishida, H., Shirai, Y., Tokiwa, Y., Endo, T. (2004). Thermal degradation behaviour of poly(lactic acid) stereocomplex. *Polym. Degrad. Stab., 86*(2), 197-208. doi: DOI 10.1016/j.polymdegradstab.2004.03.001

Fomin, V. A., Guzeev V. V. (2001). Biodegradable polymers, their present state and future prospects. *Prog  Rubber Plast Tech, 17*(3), 186-204

Fukushima, K., Abbate,  C., Tabuani, D.,  Gennari, M. . (2009a). Biodegradation of poly(lactic acid) and its nanocomposites. *Polym. Degrad. Stab. , 94*, 1646–1655

Fukushima, K., Tabuani, D., Camino, G. (2009b). Nanocomposites of PLA and PCL based on montmorillonite and sepiolite. *Mater. Sci. Eng., C-Biomimetic and Supramolecul. Sys. , 29*(4), 1433-1441. doi: DOI 10.1016/j.msec.2008.11.005

Garlotta, D. (2001). A literature review of poly(lactic acid). *J. Polym. Environ., 9*(2), 63-84. doi: Unsp 1566-2543/01/0400-0063/0

Giannelis, E. P., Krishnamoorti, R., Manias, E. (1999). Polymer-silicate nanocomposites: model systems for confined polymers and polymer brushes. *Adv. Polym. Sci., 138*, 107-147.

Gupta, M. C., Deshmukh, V.G. ( 1982). Thermal oxidative degradation of poly-lactic acid, part II. *Colloid  Polymer Sci,, 260*, 514-517

Harris, A. M., Lee E. C. ( 2010). Heat and humidity performance of injection molded PLA for durable applications. *Appl. Polym. Sci., 115*(3), 1380–1389

Hrkach, J. S., Lotan N. O., Langer R. (1995). Synthesis of Poly(L-lactic acid-co-L-lysine) Graft Copolymers. *Macromolecules, 28*, 4736-4739

Hwang, S. S., Hsu, P. P., Yeh, J.-M., Lai, Y. -Z. (2009). The mechanical/thermal properties of microcellular injection-molded poly-lactic-acid nanocomposites *Polym. Comp.*(DOI: 10.1002/pc.20736), 1625-1630

Hyon, S. H., Jamshidi, K., Ikada, Y. (1997). Synthesis of polylactides with different molecular weights. *Biomaterials, 18*(22), 1503-1508

Jong, S. J. D., Arias, E. R., Rijkers, D. T., Nostrum, C. F., Hennink, W. E. (2001). New insights into the hydrolytic degradation of poly(lactic acid): participation of the alcohol terminus. *Polymer, 42*(7), 2795-2802

Kim, S. H., Han, Y. -K., Kim Y. H., Hong S. I. (1992). Multifunctional initiation of lactide polymerization by stannous octoate/pentaerythritol. *Macromol. Chem.  Phys., 193*(7), 1623–1631

Kopinke, F. D., Mackenzie K. (1997). Mechanistic aspects of the thermal degradation of poly(lactic acid) and poly(b-hydroxybutyric acid). *J Anal Appl Pyrolysis, 40*, 43–53

Kricheldorf, H. R., Berl, M., Scharnagl, N. (1988). Poly(lactones) polymerization mechanism of metal alkoxide initiated polymerizations of lactide and various lactones. *Macromolecules, 21*(2), 286-293

Krikorian, V., Pochan, D. J. (2003). Poly (L-lactic acid)/layered silicate nanocomposite: fabrication, characterization, and properties. *Chem. Mater., 15*(22), 4317-4324. doi: Doi 10.1021/Cm034369

Lee, S. H., Kim, S. H., Han, Y. K., Kim, Y. H. (2001). Synthesis and degradation of end-group-functionalized polylactide. *J. Polym. Sci. Part A-Polym. Chem., 39*(7), 973-985

Lehermeier, H. J., Dorgan, J. R. (2001). Melt rheology of poly(lactic acid): consequences of blending chain architectures. *Polym. Eng. Sci., 41*(12), 2172-2184

Li, J., Zheng, W., Li, L., Zheng, Y. F., Lou, X. (2009). Thermal degradation kinetics of g-HA/PLA composite. *Thermochimica Acta, 493*(1-2), 90-95. doi: DOI 10.1016/j.tca.2009.04.009

Li, S. M., Garreau, H., Vert, M. (1990). Structure property relationships in the case of the degradation of massive aliphatic poly-(alpha-hydroxy acids) in aqueous-media .1. Poly(dl-lactic acid). *J. Mater. Sci.-Mater. in Med., 1*(3), 123-130

Li, S. M., McCarthy, S. (1999). Influence of crystallinity and stereochemistry on the enzymatic degradation of poly(lactide)s. *Macromolecules, 32*(13), 4454-4456

Ligadas, G., Ronda, J. C., Galia, M., Cadiz, V. (2007). Poly(ether urethane) networks from renewable resources as candidate biomaterials: synthesis and characterization. *Biomacromol., 8*(2), 686-692. doi: Doi 10.1021/Bm060977h

Lima, L.-T., Aurasb, R., Rubinob, M. (2008). Processing technologies for poly(lactic acid). *Prog Polym Sci, 33*, 820–852

Lipik, V. T., Widjaja, L. K., Liow,S. S., Venkatraman S. S. (2010). Effects of transesterification and degradation on properties and structure of polycaprolactoneepolylactide copolymers. *Polym. Degrad. Stab., 95*, 2596-2602

Lucas, N., Bienaime, C., Belloy, C., Queneudec, M., Silvestre, F., Nava-Saucedo, J. E. (2008). Polymer biodegradation: mechanisms and estimation techniques. *Chemosphere, 73*(4), 429-442. doi: DOI 10.1016/j.chemosphere.2008.06.064

Mantia, F. L. (2002). *Handbook of plastic recycling*: Rapra Technology Limited

Matana, L. M., Faruk, O. . (2007). *Hybrid HDPE/Wood-flour/ montmorillonite*. Paper presented at the 9 [th] wood and biofiber plastic composites, Madison, USA

Mehta, R., Kumar, V., Bhunia, H., Upadhyay, S. N. . (2005). Synthesis of poly(lactic acid): a review. *J. Macromol. Sci. Part C: Polym.Rev., 45*, 325–349

Nagahata, R., Sano, D., Suzuki, H., Takeuchi, K. ( 2007 ). Microwave-assisted single-step synthesis of poly(lactic acid) by direct polycondensation of lactic acid. *Macromol. Rapid Commun, 28*, 437–442

Ndreopoulos, G., Tzi, E. H., KIS M. D. S. (1999). Synthesis and properties of polylactic acid. *Kluwer Academic Publisher*, 5

Nicolae, C. A., Grigorescu, M. A., Gabor R. A. . (2008). An investigation of thermal degradation of poly(lactic acid). *Adv. online publication*

Nostrum, C. F., Veldhuis, T. F. J., Bos, G. W., Hennink, W. E. . (2004). Hydrolytic degradation of oligo(lactic acid): a kinetic and mechanistic study. *Polymer, 45*(20), 6779-6787. doi: DOI 10.1016/j.polymer.2004.08.001

Ogata, N., Jimenez, G., Kawai, H., Ogihara, T. (1997). Structure and thermal/mechanical properties of poly(l-lactide)-clay blend. *J. Polym. Sci. Part B-Polym. Phys., 35*(2), 389-396

Ozkoc, G., Kemaloglu, S. (2009). Morphology, biodegradability, mechanical, and thermal properties of nanocomposite films based on PLA and plasticized PLA. *Appl. Polym. Sci., 114*(4), 2481-2487. doi: Doi 10.1002/App.30772

Patel, R. M., Jain, P., Story, B**.,** Chum S. (2008). Polyethylene: an account of scientific discovery and industrial innovations *Innovations in industrial and engineering chemistry* (pp. 74-102): American chemical society

Paul, M. A., Alexandre, M., Degee, P., Calberg, C., Jerome, R., Dubois, P. (2003). Exfoliated polylactide/clay nanocomposites by in-situ coordination-insertion polymerization. *Macromolecu. Rapid Comm., 24*(9), 561-566

Ray, S. S., Bousmina, M. (2005). Biodegradable polymers and their layered silicate nano composites: in greening the 21st century materials world. *Prog. Mater. Sci., 50*(8), 962-1079. doi: DOI 10.1016/j.pmatsci.2005.05.002

Ray, S. S., Maiti, P., Okamoto, M., Yamada, K., Ueda, K. (2002). New polylactide/layered silicate nanocomposites. 1. preparation, characterization, and properties. *Macromolecules, 35*(8), 3104-3110. doi: Doi 10.1021/Ma011613e

Ray, S. S., Okamoto, M. (2003a). New polylactide/layered silicate nanocomposites, 6 melt rheology and foam processing. *Macromol Mater Eng., 288*, 936–944

Ray, S. S., Yamada, K., Okamoto, M., Fujimoto, Y., Ogami, A., Ueda, K. (2003b). New polylactide/layered silicate nanocomposites. 5. designing of materials with desired properties. *Polymer, 44*(21), 6633-6646. doi: DOI 10.1016/j.polymer.2003.08.021

Ray, S. S., Yamada, K., Okamoto, M., Ueda, K. (2003c). New polylactide-layered silicate nanocomposites. 2. concurrent improvements of material properties, biodegradability and melt rheology. *Polymer, 44*(3), 857-866. doi: Pii S0032-3861(02)00818-2

Schwach, G., Coudane, J., Engel, R., Vert, M. (1997). More about the polymerization of lactides in the presence of stannous octoate. *J. Polym. Sci. Part A-Polym. Chem., 35*(16), 3431-3440

Sharp, J. S., Forrest, J. A., Jones R. A. L. (2001). Swelling of poly(dl-lactide) and polylactide-co-glycolide in humid environments. *Macromolecules, 34*, 8752-8760

Shen, Z. Q., Simon, G. P., Cheng, Y. B. (2002). Comparison of solution intercalation and melt intercalation of polymer-clay nanocomposites. *Polymer, 43*(15), 4251-4260. doi: Pii S0032-3861(02)00230-6

Shih, C. (1995). Chain-end scission in acid-catalyzed hydrolysis of poly(dl-lactide) in Solution. *J. Control. Release, 34*(1), 9-15

Signori, F., Coltelli, M. B., Bronco, S. (2009). Thermal degradation of poly(lactic acid) (PLA) and poly(butylene adipate-co-terephthalate) (PBAT) and their blends upon melt processing. *Polym. Degrad,.Stab., 94*(1), 74-82. doi: DOI 10.1016/j.polymdegradstab.2008.10.004

Siparsky, G. L., Voorhees, K. J., Miao F. (1998). Hydrolysis of polylactic acid (PLA) and polycaprolactone (PCL) in aqueous acetonitrile solutions: autocatalysis. *J. Environ. Polym. Degrad., 6*(1), 31-41

Siracusa, V., Rocculi, P., Romani, S., Dalla R. (2008). Biodegradable polymers for food packaging: a review. *Trend Food Sci. Tech., 19*(12), 634-643. doi: DOI 10.1016/j.tifs.2008.07.003

Sodergard, A., Näsman J. H. (1994). Stabilization of poly(Image -lactide) in the melt *Polym. Degrad. Stab., 46*(1), 25-30

Soppimath, K. S., Aminabhavi, T. M., Kulkarni, A. R., Rudzinski W. E. (2001). Review, biodegradable polymeric nanoparticles as drug delivery devices. *J. Control. Release 70*, 1–20

Sperling, L. H. (2006). Introduction to physical polymer science (pp. 866)

Theinsathid, P., Chandrachai, A., Keeratipibul, S. (2009). Managing bioplastics business innovation in start up phase. *J. Tech. Manage.Innov., 4*(1), 81-93

Urbanczyk, L., Ngoundjo, F., Alexandre, M., Jerome, C., Detrembleur, C., Calberg, C. (2009). Synthesis of polylactide/clay nanocomposites by in situ intercalative polymerization in supercritical carbon dioxide. *Eur. Polym. J., 45*(3), 643-648. doi: DOI 10.1016/j.eurpolymj.2008.11.033

Vaia, R. A., Giannelis,E. P. . (1997). Polymer melt intercalation in organically-modified layered silicates: model predictions and experiment. *Macromolecules, 30*, 8000-8009

Wachsen, O., Reichert, K. H., Kruger, R. P., Much, H., Schulz, G. (1997). Thermal decomposition of biodegradable polyesters .3. studies on the mechanisms of thermal degradation of oligo-l-lactide *Polym. Degrad. Stab., 55*(2), 225-231

Wang, Z.-Y., Li, X. -W., Li, J.-N. (2009). Synthesis of poly(lactic acid)-poly(phenyl phosphate) via direct polycondensation and its characterization. *J Polym Res, 16*, 255–261

Witzke, D. R. (1997). *Introduction to properties, engineering, and prospects of polylactic acid polymer.* Doctor of phylsophy, Michigan state University, Michigan

Yang, K. K., Wang, X. L., Wang, Y. Z. (2007). Progress in nanocomposite of biodegradable polymer. *J. Ind. Eng. Chem., 13*(4), 485-500

Yang, L. X., Chen, X. S., Jing, X.B. (2008). Stabilization of poly(lactic acid) by polycarbodiimide. *Polym. Degrad. Stab., 93*(10), 1923-1929